

IRIS VAN BEUZEKOM

Optimizing Investment Planning of Integrated Multi-Energy Systems

to support urban decision makers
design an energy transition pathway

PhD Thesis

Optimizing Investment Planning of Integrated Multi-Energy Systems

I. van Beuzekom

The research described in this thesis was performed at the Electrical Energy Systems group of the department of Electrical Engineering at Eindhoven University of Technology. The work in this thesis has been sponsored by ITS-ECO BV and EIT InnoEnergy.

Cover design by Studio Ica.

Printed by ADC-Nederland, 's-Hertogenbosch, the Netherlands.

A catalogue record is available from the Eindhoven University of Technology Library.

ISBN: 978-90-386-5600-7

The digital version of this thesis can be downloaded at repository.tue.nl.

Copyright © 2022 by I. van Beuzekom. All Rights Reserved.

Contact: vousiris@gmail.com or connect on LinkedIn

Optimizing Investment Planning of Integrated Multi-Energy Systems

to support urban decision makers
design an energy transition pathway

PROEFSCHRIFT

ter verkrijging van de graad van doctor aan de Technische Universiteit Eindhoven, op gezag van de rector magnificus prof.dr.ir. F.P.T. (Frank) Baaijens, voor een commissie aangewezen door het College voor Promoties, in het openbaar te verdedigen op dinsdag 13 december 2022 om 13:30 uur

door

Iris van Beuzekom

geboren te Rotterdam

Dit proefschrift is goedgekeurd door de promotoren en de samenstelling van de promotiecommissie is als volgt:

Voorzitter: prof.dr. K.A. Williams
Promotor: prof.dr.ir. J.G. (Han) Slootweg
Copromotor: dr.ir. B.M. (Bri-Mathias) Hodge (University of Colorado Boulder)
Leden: prof.dr. F. (Floor) Alkemade
prof.dr. J.A. (Joaquim) Dos Santos Gromicho (Universiteit van Amsterdam)
prof.dr.ir. Z. (Zofia) Lukszo (TU Delft)
prof.dr.ir. M. (Madeleine) Gibescu (Universiteit Utrecht)
prof.dr.ir. P. (Pierre) Pinson PhD (Imperial College London)

Het onderzoek of ontwerp dat in dit proefschrift wordt beschreven is uitgevoerd in overeenstemming met de TU/e Gedragscode Wetenschapsbeoefening.

Summary

Since the United Nations climate change conference in Paris in 2015, it has become clear that urgent action is required to curb greenhouse gas emissions in order to mitigate the worst effects of anthropogenic climate change. Cities especially are facing major challenges, being both the largest contributors to carbon emissions, as well as the most affected by climate change effects. Urban decision makers have accordingly set stringent climate targets, often ahead of national policies. However, it is very challenging to design a pathway from today towards those targets. First, many future visions focus only on the electricity system given that most sustainable energy sources generate electricity, yet the current energy system is largely non-electric, causing a *carrier mismatch*. Second, most of these energy sources are renewable (RES), weather dependent and generate this electricity in a variable manner, not always when energy demand occurs, causing a *temporal mismatch*. Finally, the required energy transition from a mostly fossil to a sustainable energy system is highly uncertain and dependent on local, national, and even international developments.

In this thesis, these three challenges are tackled using a multi-energy systems perspective, combined with a long-term multi-period investment planning approach. To support urban decision makers in designing the transition of their energy system from today to a sustainable future, a framework for the optimization of integrated multi-energy systems is proposed. This *multi-energy framework* includes investments in energy network (*distribution*), conversion, storage, and supply assets and ensures that urban climate goals are reached, and the energy system remains reliable. The resulting optimization problem is formulated as a mixed integer linear program and translates to a novel application of a capacitated facility location network design problem.

To validate and demonstrate the developed approach, an urban case study of the city of Eindhoven is assembled. The case study includes all the en-

ergy networks present in the city: electricity, gas, and heat. It aligns with the stringent climate goals of the city and its corresponding timeline: reaching a 95% CO_2 -emissions reduction by 2050. The case combines multiple different data sets on the city's energy demand development, including residential, commercial, industrial, and transportation demand, asset data and technological developments, and relevant socio-economic parameters. In biannual time steps from today (2018) to 2050, the required investments in the city's energy infrastructure are optimized on and between each demand location.

First, two sets of what-if scenarios are used to test the framework and determine the consequences of uncertainty in climate policy and weather effects. The results confirm the validity of the framework. A more stringent climate policy leads to more expensive solutions, yet with substantially lower cumulative CO_2 -emissions. Additionally, delayed policy action can reduce total expenses while still reaching climate goals, yet causing significantly higher cumulative emissions, which can have considerable consequences for the global temperature increase. This is an important finding and demonstrates the real-world value of the framework for decision makers, as well as the deliberations they engage in to make policy decisions. The variation in inter-annual weather effects causes variability in the results. Similar to the climate policy scenarios, more challenging scenarios require more investments, yet scenarios with a relatively higher RES supply require less investments. The main difference is in the operational response within the energy system to ensure reliability. Heat- and gas-related conversion and storage assets respond to the variable electric supply, confirming the potential of a multi-energy system to absorb these fluctuations. This is another validation of the framework and confirms the importance of incorporating inter-annual weather effects.

However, uncertainty does not just manifest itself in isolated parameters, but in many parameters simultaneously. Hence, an exploratory modeling methodology is incorporated into the framework to test multi-dimensional (*deep*) uncertainty. Demand, technological, and socio-economic developments are varied simultaneously. The exploratory methodology uses Latin Hypercube Sampling to generate a set of experiments, and thereafter a variety of data science techniques including an Extra Trees classifier and agglomerative clustering, to analyze the results and compare them to a base case. As expected, deep uncertainty has a significant impact on the spread of potential solutions, which validates the exploratory methodology approach. This wide view of model sensitivity allows decision makers to explore investment trends and determine effective policy actions to ensure a favorable pathway. For instance, demand uncertainty causes the largest investment variations and confirms the benefit of a policy aimed at accelerating electrification. Nearly every design

requires a combination of conversion assets, again underlining the importance and added value of a multi-energy perspective. Most investments are concentrated at high-demand locations, showing the relevance of incorporating spatial constraints. Finally, most investments occur in the second half of the time frame, at which point the energy transition becomes most challenging and highly developing technologies become more economic.

To conclude, to support urban decision makers designing the transition of their energy system from today towards a sustainable future, this thesis proposes a multi-energy framework, applying a long-term multi-period investment planning approach and incorporating an exploratory modeling methodology to address the uncertainty associated with this endeavor. The framework is effective at providing trajectory solutions despite the significant challenges occurring during the energy transition, and the deep uncertainty surrounding it. The results are consistent and responsive to the changes in uncertain parameters. Besides clear differences between the different tests, there were also many similarities in investment patterns, both of which provide useful knowledge for an urban decision maker and confirm the added value of the framework for energy transition design in urban areas.

Samenvatting

Sinds de klimaatconferentie van de Verenigde Naties in Parijs in 2015 is er geen twijfel meer dat dringend actie nodig is om verdere uitstoot van broeikasgassen versneld te verminderen en zo de ergste gevolgen van klimaatverandering te voorkomen. Vooral steden staan hierin voor grote uitdagingen, omdat ze zowel de grootste bijdrage leveren aan broeikasgasemissies, als de grootste gevolgen ondervinden van klimaatverandering. Zodoende hebben veel stedelijke beleidsmakers strenge klimaatdoelen opgesteld, vaak voorlopig op nationale doelen. Het is echter enorm lastig om een plan te ontwikkelen van vandaag naar die toekomstige doelen. Veel toekomstvisies kijken alleen naar het elektriciteitssysteem, omdat de meeste duurzame energiebronnen elektriciteit genereren. Echter is het huidige energiesysteem grotendeels niet elektrisch, wat zorgt voor een zogenoemde *carrier mismatch*. Daarnaast zijn veel duurzame energiebronnen afhankelijk van weersomstandigheden en fluctueert de elektriciteitsgeneratie daarbij mee, niet altijd op dezelfde manier als de vraag naar energie, wat zorgt voor een *temporal mismatch*. Tot slot is de benodigde transitie van een voornamelijk fossiel naar een duurzaam energiesysteem enorm onzeker en afhankelijk van lokale, nationale, en zelfs internationale ontwikkelingen.

In deze thesis worden deze drie uitdagingen aangepakt door toepassing van een systeemperspectief op alle energiedragers, gecombineerd met een investeringsplanning methode voor lange termijn met meerdere tijdsperioden. Om steden te ondersteunen met het ontwikkelen van een energietransitieplan van vandaag naar een duurzame toekomst wordt een raamwerk voor de optimalisatie van geïntegreerde *multi-energy* systemen voorgesteld. Dit raamwerk bevat investeringsbeslissingen voor energienetwerken, energieconversie-, energieopslag-, en energieopweksystemen en zorgt dat klimaatdoelen behaald worden, terwijl het systeem als geheel in balans blijft. Het resulterende optimalisatieprobleem wordt geformuleerd als *mixed integer linear program* en

vertaalt zich naar een nieuwe toepassing van een *capacitated facility location network design problem*.

Om dit raamwerk te valideren en demonstreren is een case study opgesteld van Eindhoven. Deze case bevat alle energienetwerken aanwezig in de stad, elektriciteit, warmte en gas, en gebruikt de klimaatdoelen van de stad: 95% CO₂-reductie in 2050 ten opzichte van 1990. Verschillende datasets worden gecombineerd, onder andere over de ontwikkelingen van de energievraag in de stad, inclusief woninggebieden, commerciële en industriële gebieden en lokaal transport, technische data en technologische ontwikkelingen, alsook socio-economische ontwikkelingen. In tweejaarlijkse tijdstappen van vandaag tot aan 2050 worden de benodigde investeringen in de energie-infrastructuur van de stad geoptimaliseerd en het energietransitieplan ontworpen.

Het raamwerk is eerst getest op variaties in klimaatbeleid en jaarlijkse weersvariaties. Acht klimaatbeleid scenario's zijn gegenereerd: van een 'business-as-usual' scenario zonder CO₂-emissie reducties, tot een scenario waar de emissies al in 2030 teruggebracht zijn naar nul. Een strenger beleid leidt tot hogere kosten, echter met significant minder cumulatieve CO₂-emissies. Uitgesteld beleid lijkt de kosten te drukken, echter zorgt dit voor enorme toename in de cumulatieve CO₂-emissies wat serieuze gevolgen kan hebben voor de globale temperatuurstijging met mogelijk veel hogere kosten van dien. Dit is een belangrijk resultaat, wat de toegevoegde waarde van het raamwerk toont, alsook de afwegingen die beleidsmakers moeten maken. De scenario's met weersvariaties zijn gebaseerd op historische data en de resulterende variaties in energieopwekking zijn veranderd in amplitude en absolute hoeveelheid. Wederom leiden de uitdagendere scenario's tot hogere kosten. Echter tonen de resultaten nu veel meer respons binnen de operatie van het energiesysteem. De weersvariaties leiden tot variaties in de opwek van elektriciteit, waarop warmte- en gas-gedreven conversie- en opslagsystemen reageren. Dit bevestigt de potentie van een multi-energy systeem om weersfluctuaties op te vangen, alsook het belang van het meenemen van weerseffecten op deze lange termijn.

Overigens manifesteert onzekerheid zich meestal niet in geïsoleerde parameters, maar in meerdere parameters tegelijk. Zeker tijdens de energietransitie is er sprake van zogenoemde diepe onzekerheid. Dit is aan de orde wanneer meerdere parameters die invloed hebben op het energiesysteem, tegelijkertijd onzeker zijn en experts het niet eens worden over de mate van deze onzekerheid. Om deze reden is een *exploratory modeling* methode toegevoegd aan het raamwerk om dit te onderzoeken. In de case worden ditmaal de ontwikkelingen in vraag naar energie, alsook de technologische en socio-economische ontwikkelingen tegelijk gevarieerd. Latin Hypercube Sampling

wordt toegepast om een set van experimenten te genereren waarbij de distributie van de onzekerheid onbekend is. Vervolgens worden verschillende data science-technieken toegepast, waaronder een *Extra Trees classifier* en een agglomeratief clusteralgoritme, om de resultaten te analyseren en te vergelijken met een base case zonder onzekerheid.

Zoals verwacht heeft deze diepe onzekerheid een enorm effect op de spreiding van de mogelijke oplossingen, wat direct een validatie is van de exploratory modeling methode. Deze brede kijk op de gevoeligheid van een model geeft beleidmakers de mogelijkheid om investeringstrends te ontdekken en effectief beleid te bepalen om bepaalde toekomstbeelden mogelijk te maken. Zo creëert bijvoorbeeld de onzekerheid in de vraag naar energie de grootste fluctuaties in investeringen, waarbij de duurste ontwerpen diegenen zijn met een hoge gasvraag in 2050. Dit toont de waarde van beleid gericht op versnelde elektrificatie en hogere energie-efficiëntie. Bijna elk ontwerp vergt een combinatie van energieconversiesystemen, wat wederom het voordeel en belang van een multi-energy perspectief benadrukt. De meeste investeringen concentreren zich op locaties met de hoogste vraag naar energie. Dit toont hoe relevant het is om geografische aspecten mee te nemen. Tot slot worden de meeste investeringen gedaan in de tweede helft van het tijdspad. Op dat moment zijn de uitdagingen van de energietransitie het grootst en worden bovendien snel ontwikkelende technologieën economisch steeds interessanter.

Ter conclusie, om stedelijke beleidmakers te ondersteunen in het ontwikkelen van energietransitieplannen van vandaag naar een duurzame toekomst, stelt deze thesis een multi-energy raamwerk voor. Dit vertaalt zich naar een optimalisatiemodel voor investeringsplannen op lange termijn met meerdere tijdstappen, inclusief een exploratory modeling methode om de onzekerheid op zulke termijnen mee te nemen. Het raamwerk kan effectief ontwerpen maken van energietransitieplannen, ondanks de enorme uitdagingen en diepe onzekerheid die hierbij komen kijken. De resultaten zijn consistent en reageren als verwacht op veranderingen in onzekere parameters. Naast duidelijke verschillen bij de verschillende tests op de stedelijke case, zijn er ook vele overeenkomsten in de investeringspatronen. Beide soorten resultaten zijn nuttig voor een stedelijke beleidmaker en bevestigen de toegevoegde waarde van het raamwerk voor het ontwerpen van energietransitieplannen in stedelijke gebieden.

Contents

Summary	v
Samenvatting	ix
List of Figures	xvii
List of Tables	xxi
1 Introduction	1
1.1 Background and motivation	1
1.2 Research gaps	2
1.3 Research questions and approach	3
1.4 Research scope	5
1.4.1 In scope	5
1.4.2 Out of scope	6
1.5 Thesis outline	7
1.6 Conclusion	8
2 Developments in the energy transition	9
2.1 Introduction	9
2.2 Challenges of the energy transition	10
2.3 Multi-energy systems	12
2.3.1 Developments of multi-energy systems	12
2.3.2 Fully integrated perspective	14
2.4 Long-term multi-period planning	15

2.5	Mathematical complexity	16
2.5.1	Facility location problem	17
2.5.2	Network design problem	17
2.5.3	Combined FLND problem	18
2.6	Handling uncertainty	18
2.6.1	Sensitivity analysis in energy models	19
2.6.2	Exploratory modeling approach	20
2.7	Urban case study	22
2.8	Conclusion	23
3	Formulation of the multi-energy framework	25
3.1	Introduction	25
3.2	Optimization model	25
3.2.1	Model notation	27
3.2.2	Model formulation	30
3.3	Uncertainty analysis	34
3.3.1	Uncertainty characterization	35
3.3.2	Sampling	36
3.3.3	Data processing & result analysis	36
3.4	Computational approach	40
3.4.1	Solving the MILP	41
3.4.2	Programming details	44
3.5	Conclusion	45
4	Urban case study based on a large Dutch city	47
4.1	Introduction	47
4.2	Data	48
4.2.1	Demand-side	48
4.2.2	Supply-side	50
4.2.3	Pathway effects	51
4.3	Case application and assumptions	52
4.3.1	General	52
4.3.2	Network assets	56
4.3.3	Conversion assets	56
4.3.4	Supply assets	57
4.3.5	Storage assets	58
4.3.6	Complexity	58
4.4	Conclusion	59

5 Application of the framework to climate policy & weather variation scenarios	61
5.1 Introduction	61
5.2 Climate policy scenarios	62
5.2.1 Scenario setup	63
5.2.2 Results	64
5.2.3 Main findings	71
5.3 Weather variation scenarios	71
5.3.1 Scenario setup	72
5.3.2 Results	74
5.3.3 Main findings	79
5.4 Conclusion	80
6 Application of the framework to deep uncertainty	83
6.1 Introduction	83
6.2 Uncertainty characterization and sampling	84
6.2.1 Energy demand	85
6.2.2 Social discount rate	87
6.2.3 Technological development rate	87
6.3 Experiment setup	89
6.4 Results	90
6.4.1 Base case results	90
6.4.2 Global findings	92
6.4.3 Individual uncertainty	95
6.4.4 Design trade-offs	97
6.4.5 Design clusters	100
6.4.6 Main findings	107
6.5 Conclusion	108
7 Conclusions	111
7.1 Introduction	111
7.2 Conclusions	112
7.3 Contributions	114
7.4 Recommendations	115
7.4.1 Scientific research	116
7.4.2 Practical implementations	117
7.4.3 Recommendation note	118

8 Appendix	119
8.1 Scenario data	119
8.1.1 Climate policy scenarios	120
8.1.2 Weather scenarios	121
8.2 Exploratory data & results	125
8.2.1 Uncertainty characterization	125
8.2.2 Experiment settings	129
8.2.3 Additional results	129
8.3 Code	136
Acknowledgments	173
Curriculum Vitae	177

List of Figures

1.1	Synopsis of the energy transition from today to a sustainable future.	1
2.1	Challenges of the energy transition	10
2.2	Example of an energy hub and energy interconnectors, adapted from [39]	13
2.3	Integrated multi-energy system - 9 node example	15
2.4	Result example of different planning approaches, adapted from [68]	16
2.5	Future scenario types, adapted from [96]	19
3.1	Graphic representation of the optimization framework for integrated urban energy systems, including input data, objective function, constraints, and output data, adapted from [102] . .	26
3.2	Exploratory modeling methodology visualisation, including demand development D , social discount rate δ , and technological development rates ϕ_x	35
3.3	Latin Hypercube Sampling with probability density functions of x_1 and x_2 on the left, and their cumulative probability with resulting samples $[N_1,..,N_4]$ on the right.	37
3.4	Patient Rule Induction Method (PRIM) algorithm visualization, adapted from [108]	39
3.5	Optimization framework modeling decisions within and in between energy systems, and between time periods	41
3.6	Gurobi MIP algorithm building blocks, adapted from [137] . .	43

3.7	Solution progress of a typical experiment run	44
4.1	City parts of Eindhoven with multi-energy network projections	48
4.2	Eindhoven energy demand by sector and energy supply by source in PJ in 2011, from [122]	49
4.3	Energy savings in Eindhoven in PJ by sector in 2040, from [122]	51
4.4	Eindhoven topology of its three carrier energy system shaping the 21-node case study - including potential asset investments .	54
5.1	What-if scenarios - demonstrating uncertainty in long-term cli- mate policy and inter-annual weather variations, adapted from [96]	62
5.2	Climate policy scenarios 0-8 with relative carbon emissions from 2018 to 2050	63
5.3	Climate policy results - Total investment costs in MEur (green line) and number of investments per asset (stacked bars) for Scenario 1-8 in comparison to Scenario 0	66
5.4	Climate policy BAU Scenario 0 - Geographical results showing the assets ^a constructed in the electricity, heat, and gas systems in parallel ^b	67
5.5	Climate policy Scenario 4 - Energy demand (stacked bars), sup- ply, conversion from and to (lines), and storage (columns) in PJ from 2018 to 2050	68
5.6	Climate policy Scenario 6 - Energy demand (stacked bars), sup- ply, conversion from and to (lines), and storage (columns) in PJ from 2018 to 2050	70
5.7	Weather variation scenarios 0-8 with relative capacity factors for PV ^a and Wind supply from 2018 to 2050	73
5.8	Weather variation results - Total investment costs in MEur (green line) and number of investments per asset (stacked bars) for Scenario 1-8 in comparison to Scenario 0	76
5.9	Weather variation Scenario 4 - Energy demand (stacked bars), supply, conversion from and to (lines), and storage (columns) in PJ from 2018 to 2050	77
5.10	Weather variation Scenario 0 compared to Scenario 5 - use of Combined Heat and Power (CHP) and Heat Pump (HP) conver- sion in PJ from 2018 to 2050	78
5.11	Weather variation Scenario 8 - Energy demand (stacked bars), supply, conversion from and to (lines), and storage (columns) in PJ from 2018 to 2050	79

6.1	Unframed scenario - exploring uncertainty in demand development, social discount rate and technological development simultaneously, adapted from [96]	84
6.2	Exploratory modeling methodology visualisation, including demand development D , social discount rate δ , and technological development rates ϕ_x	85
6.3	Samples for all 800 experiments for each demand scenario	87
6.4	Sample distribution for all 800 experiments for each uncertain real parameter: the social discount rate δ (<i>dark blue</i>), the technological development rates for P2G conversion ϕ_{m_3} (<i>light green</i>), PV supply ϕ_{s_2} (<i>yellow</i>), electricity storage ϕ_{w_1} (<i>light blue</i>), and wind supply ϕ_{s_3} (<i>dark green</i>).	89
6.5	Deterministic results showing the electricity (<i>blue</i>), gas (<i>green</i>), and heat (<i>red</i>) systems in parallel. All assets are numbered according to their installed capacity. Conversion assets are shown in the system that they deliver to, so CHP conversion assets are shown in both the electricity and the heat system. All assets without a label were built at t_0 . Black-lined labels show additions per time period.	91
6.6	Lineplot of the cumulative capacity for all electricity network investments per experiment, the result and probability density for all 800 experiment	94
6.7	Lineplot of the cumulative capacity for all Power-to-Gas conversion investments per experiment, the result and probability density for all 800 experiments	94
6.8	Lineplot of the cumulative capacity for all wind supply investments per experiment, the result and probability density for all 800 experiments	95
6.9	Lineplot of the cumulative capacity for all gas storage investments per experiment, the result and probability density for all 800 experiments	95
6.10	Sensitivity of the result values to all 6 uncertain parameters using the feature score in % (yellow = high sensitivity, dark blue = low sensitivity)	96
6.11	Boxplot portraying the distribution and shape of the cumulative investment capacities for each asset type for all 800 experiments from 2018-2050	98
6.12	Correlation Matrix Heatmap of result values	99

6.13 Dendrogram showing the hierarchical clustering of the cosine distance matrix, with 800 experiment outcomes arranged in 11 clusters with cosine distance value threshold at 0.6	101
6.14 The median number of investments aggregate to asset type for all non-clustered experiments and each cluster	103
6.15 The median number of investments aggregated to location or significant edge (≥ 2 investments) for all non-clustered experiments and each cluster	105
6.16 The median number of investments aggregated to time period for all non-clustered experiments and each cluster	106
8.1 Demand Scenario 1	126
8.2 Demand Scenario 6	127
8.3 Demand Scenario 11	128
8.4 Lineplot & result density of the cumulative cost & capacity of all electricity network investments made from 2018-2050 per experiment	130
8.5 Lineplot & result density of the cumulative cost & capacity of all gas network investments made from 2018-2050 per experiment	131
8.6 Lineplot & result density of the cumulative cost & capacity of all heat network investments made from 2018-2050 per experiment	131
8.7 Lineplot & result density of the cumulative cost & capacity of all CHP conversion investments made from 2018-2050 per experiment	132
8.8 Lineplot & result density of the cumulative cost & capacity of all HP conversion investments made from 2018-2050 per experiment	132
8.9 Lineplot & result density of the cumulative cost & capacity of all P2G conversion investments made from 2018-2050 per experiment	133
8.10 Lineplot & result density of the cumulative cost & capacity of all PV supply investments made from 2018-2050 per experiment .	133
8.11 Lineplot & result density of the cumulative cost & capacity of all wind supply investments made from 2018-2050 per experiment	134
8.12 Lineplot & result density of the cumulative cost & capacity of all gas storage investments made from 2018-2050 per experiment	134
8.13 A combination of all pair plots between each outcome of interest showing the result values of all 800 experiments	135

List of Tables

3.1	Indices, sets, and other sub/superscripts	27
3.2	Parameters	28
3.3	Decision variables	29
4.1	Demand distribution per carrier e and per sector for each Eindhoven city part L [in %]	50
4.2	Asset investment input data including capital cost C , energy (and power) capacity Γ , efficiency η and relative annual operating time ρ	52
4.3	Pathway effect parameter input data	53
4.4	Demonstration cases - set definitions	55
5.1	Climate policy results - Main quantitative results per scenario in number of investments I , total installed capacity Γ in PJ, total costs in MEur and cost difference Δ with BAU Scenario 0	65
5.2	Weather variation results - Main quantitative results per climate policy scenario in number of investments I , total installed capacity Γ in PJ, total costs in MEur and cost difference Δ with Scenario 0	75
6.1	Uncertainty ranges for 12 demand development time-series compared to the current situation, including final demand value D , demand mix, and curve	86
6.2	Uncertainty ranges for social discount and technological development rates	88

6.3	Quantitative results of the base case compared to all 800 experiments	93
6.4	Design cluster characteristics - ordered by number of experiments and showing the average number of investments I , installed energy capacity Γ in PJ, and the main uncertainty drivers	102
8.1	Climate policy Scenarios 0-8 - gas supply from 2018 to 2050	120
8.2	Average Dutch national capacity factors for photovoltaic (PV) and on- and offshore wind energy from [149], [150]	122
8.3	Weather variation Scenarios 0-8 - relative capacity factors for PV from 2018 to 2050	123
8.4	Weather variation Scenarios 0-8 - relative capacity factors for wind from 2018 to 2050	124
8.5	Demand Scenario 1	126
8.6	Demand Scenario 6	127
8.7	Demand Scenario 11	128
8.8	Exploratory approach - experiment settings	129

Chapter 1

Introduction

1.1 Background and motivation

In 2015 at the United Nations climate change conference in Paris, COP15, the governments of 195 countries agreed that stronger and more ambitious climate action was urgently required [1]. Greenhouse gas (GHG) emission reductions need to be accelerated such that global temperature rise remains below 1.5 degrees Celsius above pre-industrial levels [2]. The majority of anthropogenic GHG emissions originate in the energy system [3], hence decarbonizing it is very important and requires large-scale implementation of renewable energy sources (RES).

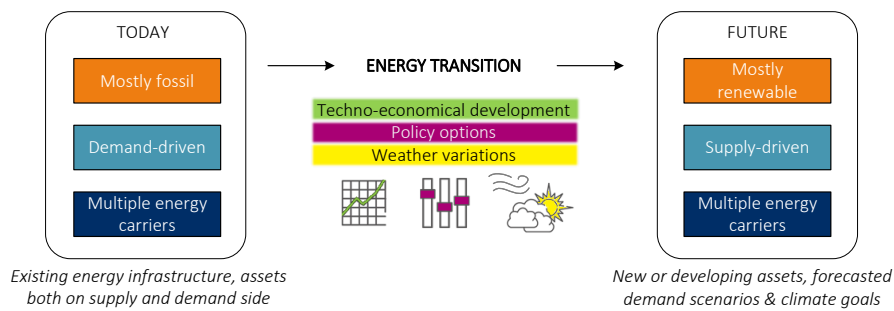


Figure 1.1: Synopsis of the energy transition from today to a sustainable future.

Yet such an energy transition from a mostly fossil to a mostly renewable energy system is also incredibly challenging (see Figure 1.1). The current system is based on a myriad of existing, centralized infrastructure centrally designed around a relatively controllable and predictable energy supply. This needs to move towards a far more complex, uncertain, and variable future, containing multiple, shifting energy carriers, while influenced by techno-economic developments, climate policy, and weather variations, all of which have impacts on different spatio-temporal levels.

This chapter briefly discusses the research gaps found in this field (1.2), which are further extended in Chapter 2. Section 1.3 formulates the research questions and outlines the approach used to answer them. Section 1.4 defines the research scope of this thesis, including what is outside its boundaries. Next, Section 1.5 provides the outline of this thesis. The final section summarizes and concludes on the main points of this introductory chapter (1.6).

1.2 Research gaps

Most literature on climate action focuses on a single energy sector, which is often the power sector as most RES like wind turbines and photovoltaic (PV) panels directly supply electricity. Yet less than 25% of the world's final energy demand is currently electric [4] and most demand scenarios project this to remain at 50% or below in the 2050 time-frame [5]. It is therefore imperative to look at solutions regarding the entire energy system in order to reach the climate goals of 80%-100% CO_2 reduction by 2050 [6]. Recently, the integration of different energy systems has been proposed as the evolving energy paradigm, as it offers better perspectives for achieving a sustainable energy supply and supporting the energy transition than traditional mono-energy system approaches [7]. Such integrated multi-energy systems (MES) consider all relevant energy carriers (e.g. electricity, heat, fuels) to create increased degrees of freedom [8] and the strengths and weaknesses of each carrier can be leveraged or compensated. However, most MES research apply ex ante simplification, either by analyzing or optimizing the systems separately and connecting them iteratively [9], by considering only one additional energy carrier, often gas [10], or by ignoring network constraints [11]. Hence, a research gap remains in the application of a fully integrated approach to leverage the potential of all relevant energy carriers.

Temporally, most literature either looks at short-term operational challenges or at long-term future scenarios. The former includes creating new operational tools or techniques to deal with potential effects of large-scale RES

implementation and demand electrification, e.g. grid ancillary services [12], demand side management [13], or virtual power plants [14]. Such research is relevant, but it does not provide an approach on how to reach long-term climate goals, which is the focus of this thesis. The latter creates the ‘dot on the horizon’ that needs to be reached by a certain year in order to curb climate change [15]. Yet there is a research gap on how to design the pathway from today towards these future scenarios. A multi-period setup allows the explicit inclusion of pathway effects, like techno-economic developments, policy options, and weather variations.

Spatially, most research on climate action focuses on either a large scale, e.g. national level [16], or a small scale, e.g. building level [17]. Yet at the urban scale, cities play a large role in the implementation of strong climate actions given their increasing population density and resource intensity [18]. Furthermore, many cities are already dealing with the effects of climate change, and over 90% are at risk of flooding from rising sea levels and powerful storms [19]. This leads to a strong motivation to act; often ahead of national policies [20]. However, urban energy systems are surprisingly under-studied in the literature and thus ripe for developing actionable policies that can have a clear impact.

1.3 Research questions and approach

To effectively address the challenges of the energy transition and relevant research gaps, this thesis simultaneously considers an integrated multi-energy perspective to optimally combine energy carriers and reach stringent climate goals, a long-term multi-period investment planning perspective to effectively help decision makers design and optimize their energy transition pathway, and an urban perspective to create actionable policies with a clear impact. This leads to the main research objective:

to support urban decision makers design a pathway for their energy transition such that climate goals are reached in the most cost-efficient manner, while assuring a reliable energy system

To design an investment pathway towards these climate goals, multiple time periods need to be included, answering the question of what, when, and where to invest. Doing so in the most cost-efficient manner fits the application of an investment planning optimization model that minimizes the societal

costs and includes other relevant constraints, for example to assure the energy system remains reliable throughout the transition. In long-term planning models there is also a significant level of uncertainty to be taken into account, which is compounded by the uncertainty of the energy transition itself. Integrating all these parts into one model adds considerable complexity, and difficulties for solving it, especially when including uncertainty.

To demonstrate such an approach, it is useful to apply it to a case study. This can be used to test the performance of the approach, as well as its practical applicability. The former means it should respond logically to adjustments in different inputs, as expected when modeling energy system behavior. The latter means it should provide insightful results aimed at tackling whatever challenges the energy transition brings, including uncertainty. To support this research approach, several sub-questions have been formulated:

1. What are current developments in energy systems and the main challenges of the energy transition? [Chapter 2]
2. Which approaches are used to support decision makers in dealing with these challenges? [Chapter 2]
3. How to build an investment model that combines a multi-energy perspective with a long-term, multi period setup into the design of an energy transition pathway? [Chapter 3]
4. How to include uncertainty considerations into such an investment model? [Chapter 3]
5. What is required for a comprehensive multi-energy case study to test the proposed framework both in model behavior and practical applicability? [Chapter 4]
6. How can climate policy and long-term weather variations affect pathway designs for an urban energy system? [Chapter 5]
7. What does an investment strategy for an urban energy system look like given deep uncertainty? [Chapter 6]

1.4 Research scope

This section presents the scope of this thesis, including specific elements that are within, as well as outside the scope of this work. These scope decisions are further substantiated in Chapter 2.

1.4.1 In scope

The proposed multi-energy framework can be applied to many different temporal or geographical scales. In this research, we focus on long-term, multi-period planning for an urban scale using multiple energy carriers. Specifically, the following elements are included in the scope:

Integrated multi-energy systems - including two or more energy systems. The mathematical formulation of the framework is given for three energy systems. Each of these systems can be fully integrated into each other, i.e. leading to a three dimensional network expansion problem.

Long-term, multi-period planning - in order to generate designs for the energy transition and ensure long-term climate goals are reached, a long-term perspective is required. In addition, to appropriately incorporate pathway effects during such a long-term, multiple periods are modeled. This allows inclusion of the social discount rate, technological development factors, and other supply factors, e.g. policy or long-term weather variations.

Green- and brownfield planning - the framework is constructed such that both *greenfield*, and *brownfield* planning are possible. Only location and demand development data are required as input for the optimization model. In greenfield planning, no data is yet known about current energy systems, or a completely new energy system is designed. Brownfield planning includes data on the current energy system, such as current assets, and often contains more investment constraints based on local data.

Medium-voltage equivalent networks - the urban focus of this thesis includes a focus on medium-voltage (MV) equivalent networks, which also refers to medium pressure gas networks and district heating (DH) networks. This is where most conversion, supply, and storage assets are expected to be connected. Such assets can also be aggregated from a low-voltage (LV) equivalent network to an MV/LV node connection.

Case study development - given the lack of available multi-energy case studies, the development of an appropriate case is part of the scope. It is based on a high-level study of the Eindhoven municipality, yet many additions and adaptations were required to make it fitting for the energy transition chal-

lenges as defined in this thesis. In addition, both the what-if scenario sets, as well as the exploratory scenario sets were developed within this research.

1.4.2 Out of scope

The following elements are outside the scope of this thesis:

Detailed single networks - multiple energy networks are included into the scope of this work, resulting in significant modeling complexity. To manage this, all are modeled in the same manner, relying on the overarching characteristics of each energy carrier and including a linear approximation of transportation losses and conversion losses.

High- or low-voltage equivalent networks - with a focus on multiple energy systems at an MV-equivalent level, detailed analysis of high- and low-voltage (HV and LV) equivalent networks are out of scope, which includes high and low gas pressure networks and distribution from a DH network to an end-user. Information on the HV-equivalent network is used to determine feed-in points to the MV-equivalent network. Additionally, demand information from LV-equivalent networks is aggregated to determine demand at MV-equivalent network locations.

Short- or medium term operations - This work focuses on long-term planning of infrastructural investments and its consequences for energy system designs to enable the energy transition (up to 2050). Though operational energy losses are included, any other short- and medium term planning and operational (cost) considerations are outside of the scope.

Dynamic energy system behavior - The multi-energy framework assumes steady-state behavior within the time period, hence implications for energy system stability and power quality are not included.

Optimization algorithm development - given the complexity of the optimization model described in this thesis, many mathematical and computational difficulties arose. Yet, developing optimization algorithms is not part of this thesis. Instead, this work uses the bespoke, open-source optimization algorithm Gurobi, and constructed a case study with reduced complexity to demonstrate the framework.

Demand side management - Although consumers can shift their energy consumption in time, and this is frequently modeled in power systems to manage the power balance, it is not yet clear how this affects a multi-energy system. To conduct conservative planning and ensure reliable energy system design, demand side management is not considered.

1.5 Thesis outline

This thesis is divided into seven chapters, with the remaining chapters organized as follows:

Chapter 2 discusses relevant developments in the energy transition. First, three main challenges of the energy transition that form the basis of this thesis are defined. Then the different topics addressed in this thesis are highlighted: multi-energy systems, long-term multi-period planning, the mathematical complexity of the resulting problem, how to incorporate uncertainty, and the urban case study. It includes some background for each topic, which relevant research was performed previously, and which research gaps remain. Finally, it concludes with how this research aims to address these gaps.

Chapter 3 describes the framework for optimal long-term, multi-period investment planning of integrated urban multi-energy systems. It includes all model notations and the mathematical formulation. Next, this chapter describes the exploratory approach used for uncertainty analysis, which completes the *multi-energy framework*. Finally, the computational approach is described, which includes how the model is solved and which software and hardware are used.

Chapter 4 contains the case description for the extensive, multi-energy urban case study that is used to demonstrate the multi-energy framework framework. It is based on input from the municipality of Eindhoven, complemented by Dutch national data, European technological databases, and various other inputs. On the demand-side, residential, commercial, industrial, and local transport developments are included. On the supply side, assets for supply, distribution, conversion, and storage are included. The chapter further highlights how these data sources are translated to the multi-energy framework and the case study.

Chapter 5 presents the first two applications of the framework solving the first two challenges of the energy transition relating to different mismatches in demand and supply. Two distinct sets of what-if scenarios are used to provide a high-level overview of the consequences of two particular uncertainties: declining fossil gas supply, and inter-annual weather variations. The first is influenced by policy makers and creates significant consequences for the total cost of the system designs. The second is very relevant especially for the amount of wind energy generated, which in turn has increasing consequences

as investments in renewables increase. The framework shows a broad range of feasible solutions for each of the challenges.

Chapter 6 provides the results for solving the final challenge of the energy transition as defined in this thesis, which is handling the uncertainty present in any future energy model compounded by the uncertainty surrounding the energy transition itself (*deep uncertainty*). Using an exploratory approach, multiple uncertainties are varied simultaneously to generate a large set of experiments. The results are compared to a base case at a global level. Then the influence of each individual uncertainty on the resulting designs is determined, followed by an analysis of specific design trade-offs. Finally, the results are clustered to determine similar designs when it comes to asset type, location, and time period. This uncertainty analysis provides a wide view of model sensitivity and allows decision-makers to determine robust and effective investments, trade-offs between different investments, and tipping points in the energy system design.

Chapter 7 presents the overall conclusions of the added value of the multi-energy framework. It also gives specific conclusions for each of the energy transition challenges tackled in this thesis. It summarizes the contributions of this thesis and it provides recommendations for future research both for additional practical implementations, as well as to further scientific research in different fields.

Each chapter starts with an introduction to the topic and gives an outline of the chapter. At the end of each chapter, closing remarks include a brief summary and preliminary conclusions.

1.6 Conclusion

In this chapter, the motivation for the research in this thesis was introduced, followed by relevant research gaps. This led to a research objective, several research questions and an approach on how to answer these questions. The research scope defined the outline of the research. Finally, the outline of the thesis was given with a brief description of each chapter. In the next chapter, the developments in the energy transition and thus the background of this thesis are examined more in-depth.

Chapter 2

Developments in the energy transition

2.1 Introduction

This chapter explores relevant developments in the energy transition and specifically what challenges arise on the path towards stringent climate goals. Three main challenges are identified, which together with the research gaps identified in Chapter 1, compose the foundation of this thesis. In order to tackle these challenges and support urban decision makers design an energy transition pathway, an energy system model needs to meet various requirements. First is the need to apply integrated multi-energy systems to reach stringent climate goals. Second is the application of long-term, multi-period investment planning, which allows for the inclusion of critical pathway effects. Both of these model requirements incur significant mathematical complexity, which has consequences for its application and among other things, the inclusion of uncertainty, all of which is treated in this chapter.

The chapter starts with a description of the challenges of the energy transition, and how this thesis aims to tackle these (2.2). Then each of the parts of the solution are discussed. First, and foremost, is the use of a multi-energy systems perspective (2.3). This is complemented by the application of a long-term, multi-period investment planning perspective (2.4). The proposed multi-energy, multi-period framework [21] leads to significant mathematical complexity, and a novel application of the combined facility location network design problem, which is detailed in Section 2.5. This affects how the final

challenge of the energy transition can be tackled, which is how to incorporate the uncertainty present in long-term planning of energy models [22] (2.6). For testing purposes and to provide a demonstration of the practical relevance of the framework, a multi-energy case study is specifically created (2.7). Each section contains brief introductions on the subject matter, discusses relevant literature and specifies how this work fills existing research gaps. The rest of this chapter forms the basis of the justification for the decisions that were made in the rest of the thesis. Section 2.8 summarizes and concludes this chapter.

2.2 Challenges of the energy transition

In order to achieve stringent greenhouse gas emission reductions, a transition of the entire energy system from fossil to renewable resources needs to be implemented. Such an energy transition brings several challenges, as depicted in Figure 2.1 (extended from Figure 1.1 in Chapter 1).

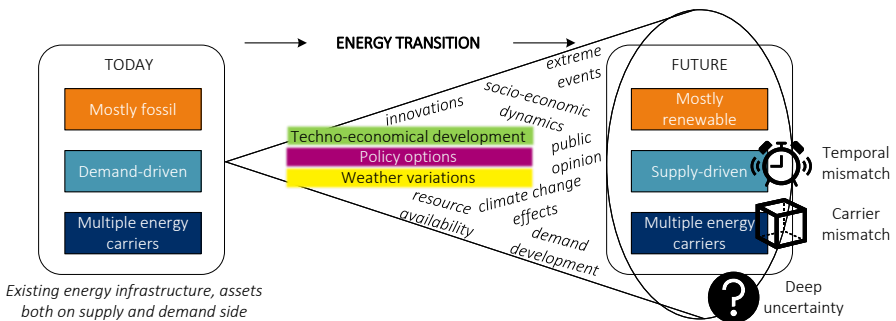


Figure 2.1: Challenges of the energy transition

Most renewables generate variable electric energy, yet most demand is currently not electric. At the moment, the world's energy demand is less than 25% electric [4], and even in 2050, most projections estimate a maximum of 50% electric demand [23] [5]. This creates a *carrier mismatch* between the energy carrier type that is supplied and the one that is demanded, which is defined as the first energy transition challenge in this thesis.

In addition, energy demand does not always manifest at the same time as supply, which creates a *temporal mismatch*. This mismatch is extensively studied at shorter terms, e.g. assessing diurnal storage needs in systems with

high PV penetration [24], applying probabilistic unit commitment with demand response in a high wind power system [25], and using a combination of wind and solar resources to meet electrical loads [26]. Some studies include medium term (seasonal) mismatches and conclude these are harder to solve than short-term mismatches [27], and are exacerbated in the long-term. There is little focus on climate variability, or inter-annual weather variations, which are consistently underestimated in long-term energy models [28], even though such variations are very relevant especially when a majority of the future, sustainable energy supply is weather dependent [29] [30]. The long-term temporal mismatch is defined as the second energy transition challenge.

Finally, the long-term development of any energy system and specifically those in transition is influenced by a combination of factors that are uncertain, e.g. socio-economic dynamics, technological innovations, and resource availability [31]. The projections of these developments vary widely among different studies [32], which is why the long-term development of an energy system is said to be subject to *deep uncertainty* [33]. Deep uncertainty exists when analysts or decision makers don't know or don't agree on which models relate key forces that shape the future, the probability distributions of parameters in these models, and/or how to value the model outcomes [34]. Handling such deep uncertainty is one of the main challenges in constructing useful energy system models for decision makers [35], and forms the third energy transition challenge in this thesis.

To effectively address the first two challenges, this thesis proposes a novel optimization framework for long-term, multi-period investment planning of integrated urban energy systems. The framework includes investment decisions on energy distribution networks, energy conversion, energy supply, and energy storage assets, ensuring each demand carrier type is met at each location and during each time period. It can start with a blank slate (*greenfield*), or incorporate existing assets and local constraints, i.e. a *brownfield* situation, [36]. Moreover, it accounts for pathway effects affecting the investment decisions, including economic parameters like a social discount rate, technological development factors improving cost-effectiveness of relevant technologies, climate policies, and long-term weather variations.

In mathematical terms, the resulting optimization problem is formulated as a multi-period, mixed-integer linear program (MILP), combining a capacitated facility location problem with a multi-dimensional, capacitated network design problem [37]. This is a significantly complex problem [38] and has consequences on how to tackle the third energy transition challenge of deep uncertainty.

2.3 Multi-energy systems

First and foremost in this thesis is the application of a multi-energy perspective to solve the challenges of the energy transition. The world needs to reduce nearly all its carbon emissions by 2050 in order to remain below 1.5° Celsius warming [2]. Most of these originate in the energy sector [3], which is shaped by multiple, different energy carriers, like gaseous and liquid fuels, electricity, heat, etc. Yet most literature focuses on a single energy sector, which is often the power system as most RES directly supply electricity. However, 75% of the world's final energy demand is currently not electric and even with significant electrification efforts, it is projected to remain at 50% in the 2050 time-frame [23] [5]. In order to reach the climate goals of 80%-100% CO_2 reduction by 2050 [6], it is imperative to look at solutions regarding the entire energy system, including all relevant energy carriers. Section 2.3.1 provides an overview of multi-energy system literature and lists the limitations of the approaches used. Section 2.3.2 specifies the motivation for the solution applied in this thesis.

2.3.1 Developments of multi-energy systems

The concept of a multi-energy system was first introduced in 2007 [39]. These researchers tried to answer the question: "What should energy systems look like in 30-50 years?" To answer this question they employed a greenfield approach, i.e. unrestricted by existing systems to determine 'real optima', and proposed two concepts: transformation, conversion, and storage of various forms of energy in centralized units called *energy hubs*, and combined transportation of different energy carriers over longer distances in single transmission devices called *energy interconnectors*. Figure 2.2 shows an energy hub and interconnector configuration. This particular hub has interconnections with electricity, natural gas, district heat, and wood chip inputs. It uses a transformer, a micro-turbine, a heat exchanger, and a furnace to convert these inputs to electricity, heating, and cooling outputs. It can also store electricity using a battery, and heat using a hot water storage system, providing temporal flexibility to adapt supply to demand.

Most energy hub follow-up research focused on the operational, short-term side of energy systems: reviewing distributed multi-generation systems [40], expanding the energy hub framework to include optimal energy hub dispatch, optimal multiple-energy carrier power flow, and reliability assessment of energy hubs [41], further improving optimal dispatch for multi-energy systems

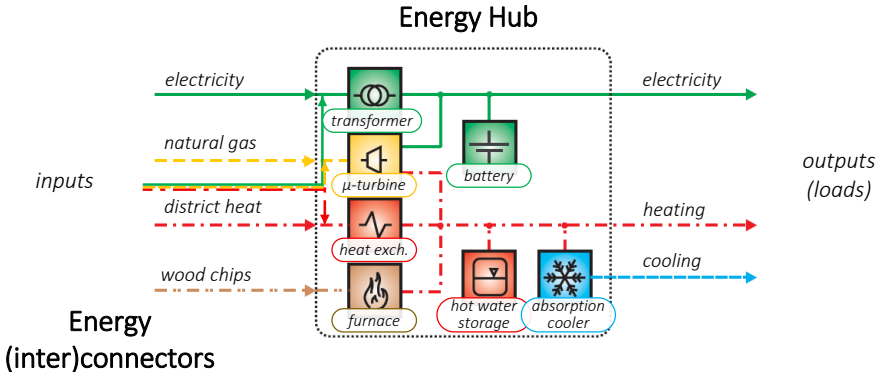


Figure 2.2: Example of an energy hub and energy interconnectors, adapted from [39]

using a piece-wise linear approximation of energy hub converters [42], using integrated demand response to make smart energy hubs [43], developing standardized matrix modeling of MES to facilitate computerized modeling [44], integrating preventive maintenance with energy hub scheduling [45]. Some research included seasonal views such as Gabrielli et al. [46], who determined the optimal design of MES with seasonal storage, and Rahgozar et al. [47] who focused on the resilience energy hubs can offer, including demand response and energy storage systems.

In the years following the energy hub activities, more researchers agreed that the integration of different energy systems offers better perspectives for achieving a sustainable energy supply and supporting the energy transition than traditional mono-energy system approaches [7]. More general than the energy hub theory, multi-energy systems (MES) consider all relevant energy carriers to create increased degrees of freedom and the strengths and weaknesses of each carrier can be activated or compensated [8]. For example, electricity is quite flexible in its end-use applications and easily produced sustainably, but unless there is a pumped hydro storage system nearby, it is difficult to store in the long-term and on a large scale [48]. Heat is more easily stored, especially seasonally [49], but is mostly limited to ‘low-grade’ energy applications [50]; although notable exceptions are under development [51] [52]. Fuels are easiest to store, especially long-term [53], but as of yet difficult to produce renewably and economically in large quantities [54]. In other words, short-term carriers can be converted into long(er) term carriers and carriers can be adjusted based on the required energy service. Especially for a system

in transition, planning an urban energy system in an integrated manner can smooth the path from mostly fossil to mostly renewable.

However, most MES research still applies ex ante simplification, not by just considering a single energy sector, but by analyzing or optimizing the systems separately and connecting them iteratively at one or a handful of physical [9] or virtual locations (e.g. markets) [55], by considering only one additional energy carrier beyond electricity, often natural gas [56], [46], [10], sometimes hydrogen [57], or by focusing only on operational challenges [58], [59]. In addition, most research does not consider network design decisions, or of a maximum of two networks [60] [61]. When more than two networks were considered, only one or a few energy hubs were considered [62], [44], [63]. Previous research has shown that existing multi-energy models are not capable of optimizing the relevant geographical and temporal aspects of all carriers [11]. Most models like EnergyPLAN, DER-CAM, or LEAP, either do not model energy networks at all, or do not consider capacity constraints, or like Balmorel, eTransport, and TIMES, geographical aspects are not incorporated.

2.3.2 Fully integrated perspective

In order to capture the complete potential of multiple energy carriers, this thesis emphasizes the application of an *integrated* multi-energy system perspective. This translates to the ability to fully couple each energy system in each location, creating a whole network of energy hubs if required. This perspective has several consequences for the investment optimization framework. Figure 2.3 illustrates a simple example of an energy system with three energy carriers and three locations. Different assets can be constructed. In this example, for each carrier there is a network option, a supply option, a storage option, and conversion options to and from each carrier. This is a temporally static depiction, visualized using nine nodes. This setup allows incorporation of geographical factors, including network constraints, which are relevant in network planning. The operational behavior and constraints of each asset are included to ensure sufficient energy supply at operational time scales.

This is a basic, theoretical example showing all potential assets for three energy carriers. In practice, supply assets might not exist for all carriers, multiple carriers might be supplied by a single asset, some carriers might not be convertible to others, or some carriers might be convertible to multiple other carriers. For example, a Combined Heat and Power system uses gas to generate both electricity and heat [64].

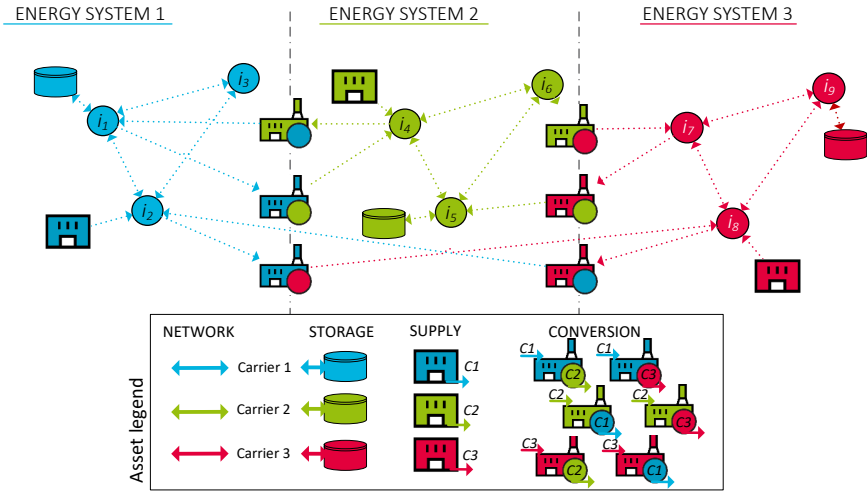


Figure 2.3: Integrated multi-energy system - 9 node example

2.4 Long-term multi-period planning

Most literature with a long-term perspective focuses on the ‘dot on the horizon’ that needs to be reached by a certain year in order to remain under 1.5°C warming, e.g. discussing which energy mixes are required (% renewables) [15], how demand can be electrified [65], or the future role of nuclear [66]. Yet there is a research gap on how to design the (multi-period) pathway from today towards these future scenarios in a multi-energy setting [46], which, besides accelerating the energy transition, can also lead to significant cost savings [67].

Moreover, in those studies that do consider long-term, multi-period planning, often a single-year static projection is used, instead of a forward-looking approach that accounts for the time value of staged investments. This can lead to incomplete or inaccurate analyses, while including it leads to much more cost-efficient solutions, as [68] demonstrated for a microgrid (see Figure 2.4). Most studies do so using net present value calculations using a certain discount rate [69].

In addition, multi-period planning allows for the explicit inclusion of other *pathway effects* besides (socio-)economic ones, like technological developments, policy options, and weather variations. All of these effects can have significant

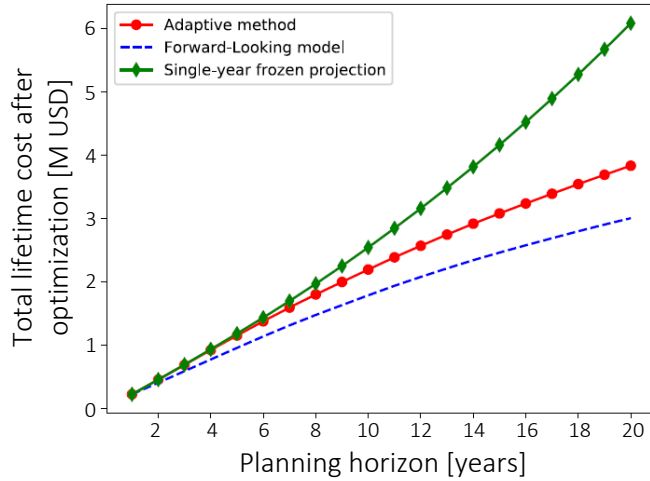


Figure 2.4: Result example of different planning approaches, adapted from [68]

consequences for effective energy transition pathways, and yet are often underestimated or disregarded [70] [28] [71].

2.5 Mathematical complexity

The proposed framework for multi-energy design investment planning is formulated as a mixed-integer linear optimization problem (MILP). It makes *integer* decisions on how many of which assets to construct, when and where. Yet it also ensures demand is always met at each location, and during each time period, which affects the *linear* energy flows in the system. In more specific mathematical terms, the framework combines a *capacitated* facility location problem with a multi-dimensional, *capacitated* network design problem.

Most of the relevant literature focuses on just one of these problems, or when combined, it is under the assumption that both the facilities and the network connections are *uncapacitated*. Uncapacitated problems are generally referred to as 'simple' versions of the original problem, as a decision maker can determine the size of each facility without any budgetary, technological, or physical restrictions [72]. In this section, the separate mathematical problems are described first, and then the combined problem is treated.

2.5.1 Facility location problem

The facility location problem (FLP) is a classic optimization problem. The goal is to determine the optimal location of a set of facilities, e.g. warehouses or factories, given certain facility costs, geographical demands, and transportation distances to a set of customers [73]. It is often formulated as an integer problem, with a fixed set of facility and customer locations, where binary variables are used to determine which facilities should be open or closed, and whether they can supply a certain customer [74]. The *unconstrained FLP* is already NP-hard [75].

In the multi-energy framework, multiple facilities exist: conversion, supply, and storage assets. Each of these can technically supply energy to a customer, directly from a supply asset, or indirectly through a conversion process or through storage. In addition, besides merely considering whether to open a facility, the framework also determines the capacity of said facility. This makes it a *capacitated FLP* and increases the complexity.

In this thesis the capacitated FLP is considered, along with additional complexities. First is the multi-period perspective, which means the FLP is solved for each time period, and energy 'supply' can travel through time while in storage. Second, in a classic FLP, it is assumed that the underlying network already exists. Although this is a possibility if the modeling framework is applied in a brownfield situation, with previously existing network connections; there is always the possibility of expanding or upgrading the network. For example, in some cases gas networks might be decommissioned and replaced by heat or electricity networks. If the framework is applied to a greenfield situation, or if data on the network topology is unavailable, the entire network needs to be fully designed as well.

2.5.2 Network design problem

That leads to another optimization problem: the network design problem (NDP), which is in fact NP-complete [76]. It is also called topology design, and is often combined with a network flow problem (NDFP). The objective is to minimize the total cost of the system, generally defined as the sum of design costs and the transportation (or energy distribution) costs, while fulfilling all demands in the system. In addition to a variable cost for transporting a certain flow, a fixed cost for using an edge can be imposed. Because these design variables involve choices from a discrete set of values, and the flow balancing problem is generally linear, the NDFP can be modeled as a mixed integer linear program [77]. This problem, also known as a network loading problem, is

strongly NP-hard even with just two facilities [78].

In the multi-energy framework, the different energy networks need to be designed and all energy flows need to be balanced, so indeed it is a network design and flow problem (NDFP). In an energy system, networks are always limited by their capacity, so this problem is also *capacitated*. Though energy flow is nonlinear, the losses in an urban area are limited and thus the effect of linearizing losses is minimal [79]. Especially considering the complexity of the problem and the additional computation a nonlinear mixed integer problem (MINLP) would incur, linearized losses are applied.

2.5.3 Combined FLND problem

The combined facility location network design problem (FLNDP) was first introduced in uncapacitated form [80], where the authors identified that in some cases it is more beneficial to change the underlying network than to place new facilities. In the following years, much research remained focused on the uncapacitated form, e.g. adding a budget constraint [81], minimizing travel time [82]. Subsequent publications either made a capacitated network design [83], [84] and [85], or a capacitated facility location [86], [87], yet never both, and never in a multi-period problem. In short, the combination of a fully capacitated FLNDP (CFLNDP) is a novel application and implies significant, additional mathematical complexity. Even using a single time period and just two energy carriers, the CFLNDP is strongly NP-hard [38].

2.6 Handling uncertainty

As introduced in Section 2.2, handling the *deep uncertainty* present in long-term planning of energy transition designs is the third major challenge treated in this thesis. An ideal solution would be to incorporate uncertainties directly into the optimization framework, either using robust optimization or stochastic programming techniques. However, the very definition of deep uncertainty is that it is hard to quantify such that it can be applied in stochastic models, as the distribution of the uncertain parameters is unknown. Moreover, endogenously incorporating multiple uncertainties would create combinatorial growth in the number of variables, and thus in the computational complexity [31]. Given that the framework already combines two NP-hard problems, the uncertainties are analyzed through a sensitivity analysis.

2.6.1 Sensitivity analysis in energy models

In the field of energy models, much sensitivity analysis research has been performed at a smaller geographical scale: using a rolling-horizon approach for microgrids [68], combined with global sensitivity analysis for distributed energy systems (DES) [88], using a multi-modal perspective for DES [89], and using robust optimization for a building energy system [90]. Similar studies were also performed at a much larger scale: using a multi-scale representation of uncertainties for a US state [91], using a Sankey-diagram style to represent the energy system and stochastic optimization using event trees to include uncertainties mostly for a national scale [92], using near-optimal in conjunction with cost-optimal scenarios and Monte Carlo sampling for the UK energy system [93], and using the WorldScale tool to analyze the effect of different climate policies at a European scale [94]. Most of these approaches consider a different scale than urban, either a smaller scale like DES, microgrids, or a single building, or a much larger scale, like a state/province or country/region. Also, most research focuses on the power system, or when multiple carriers are considered, their networks are not [95].

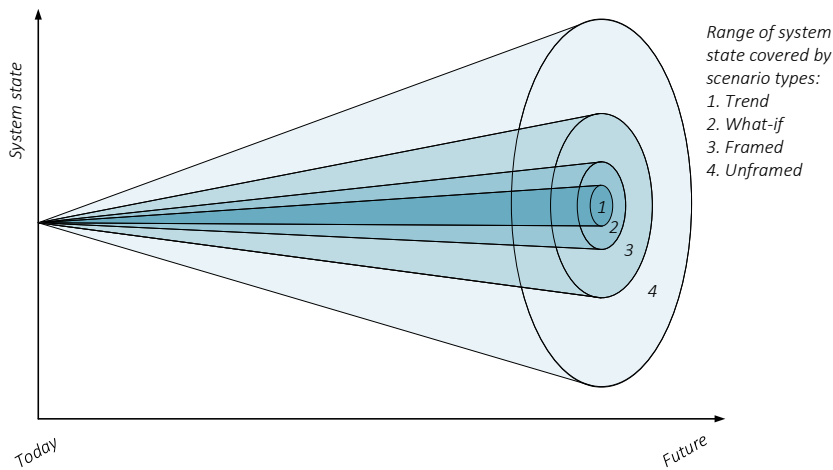


Figure 2.5: Future scenario types, adapted from [96]

In addition, most sensitivity analyses handle uncertainty using a variety of 'what-if' scenarios (see Figure 2.5, type 2) varying only one uncertain pa-

rameter at a time; often for demonstrative purposes [96]. Such an analysis provides information about the quality of the energy model under consideration and it provides first insights into the consequences of varying a single uncertain parameter. Hence, this is also the first analysis to be performed for the multi-energy framework as proposed in this thesis. Chapter 5 provides results for two different uncertain parameters.

2.6.2 Exploratory modeling approach

This takes a step beyond just analyzing a trend (Figure 2.5, type 1), yet such forecasts can still lead to a restricted understanding of future dynamics which can result in energy system designs with limited robustness [97]. Exploratory modeling aims to improve such robustness through a large series of computational experiments to explore the implications of varying multiple parameters simultaneously [98]. These experiments, or scenarios, can be generated in a framed (type 3) or unframed manner (type 4). Framed scenarios are generally produced by placing two uncertain factors in a 2x2 matrix, where each combination forms a scenario [96]. Given the complex nature of the energy transition, unframed scenarios are preferred, as these allow for exploring a wider range of possible futures with the least amount of bias. In Chapter 6, an unframed system state is resembled by determining a large range per parameter and combining them using a (near-)random sampling method.

Latin Hypercube Sampling (LHS) is applied to systematically explore the multi-dimensional range of parameters [99]. LHS is preferred over Monte-Carlo sampling because it systematically spreads sample points across all possible values, using *stratified* sampling without replacement, instead of taking random samples. It combines many of the desirable features of both random and stratified sampling. It produces more stable results than random sampling, and does so more efficiently. It is easier to implement than stratified sampling, especially for high dimension problems, since it is not necessary to determine strata, strata probabilities, or even uncertain parameter distributions. Consequently, the unframed system state is explored more thoroughly in reduced computation time [100].

For an effective application of the uncertainty analysis, relevant uncertain parameters need to be selected and specified. This is not an easy task given the wide variety of techno-economic assumptions across energy models [101]. Specifically for DES, [102] performed an extensive review. Researchers have also developed methods to quantify uncertainty in specific subparts of energy system models like photovoltaic (PV) module prices [103], nuclear reactor operation [104], or gas turbine operation [105]. In this work, a combination

of top-down and bottom-up analysis is performed. The bottom-up approach involves analyzing model parameters to identify those that are subject to external uncertainty. Then, a top-down approach is employed to determine uncertain parameters in several long-term energy models and scenario planning studies [106], or as so defined by the relevant (urban) decision makers. Subsequently, both approaches are combined and overlapping uncertainties selected for further specification. Assigning an appropriate uncertainty range of the model parameters is based on gathered data sets from technology providers, literature, case studies, and expert judgement [107].

After the uncertainty specification and LHS sampling, a set of experiments is generated to run through the optimization model, resulting in distinct energy transition designs. To distinguish investment patterns and relate these to the underlying uncertainties, a combination of data science techniques is employed. First, an Extra Trees classifier is used to determine the individual influence of each uncertain parameter on the results. This technique is employed because, compared to Sobol indices and linear regression, it requires relatively limited computational resources, does not assume linearity and lacks a restrictive assumption for unimodal symmetry [108]. Second, a correlation analysis is performed to determine design trade-offs. This is combined with a Patient Rule Induction Method (PRIM) partitioning technique [109] to find the underlying uncertainty ranges or tipping points. PRIM is the most frequently employed algorithm for scenario discovery [108]. It was adjusted to allow for non-binary variables [110].

Finally, all the results are also clustered to distinguish broad investment patterns. This is done using a cosine distance measure, to which we apply an *hierarchical, agglomerative* clustering algorithm with a *complete linkage* criterion. The cosine distance is preferred over other distance metrics like the *Euclidian* or *Manhattan* distance. It is well suited for high-dimensional and sparse vectors, while the other metrics are more applicable when vector magnitude is more relevant [111]. This creates a larger focus on the investment pattern, as opposed to the number of investments. For decision support, it is more interesting whether there were investments at all in a certain asset, at a certain location, or during a certain time period, this better aligns with the result focus. Hierarchical is selected as opposed to non-hierarchical clustering, because it systematically evaluates all potential clusters, which leads to higher in-cluster design similarity [112]. An agglomerative approach is selected, as opposed to divisive, because it is less sensitive to the clustering initialization [113]. Third, complete linkage is selected as opposed to single or average linkage, to ensure compact clusters with high in-cluster design similarity [114]. To quantitatively evaluate the characteristics of each cluster, a Classification and

Regression Tree (CART) [115] is applied. This is combined with a qualitative analysis of the patterns of the investment design aspects: asset type, location, and time period.

More details on the exploratory methodology for uncertainty analysis and especially the programming modules used, can be found in [116], [106], [117]. Chapter 3, Section 3.3.1 further explains the application of these techniques.

2.7 Urban case study

In order to test the multi-energy framework, a fitting case study is required. Preferably one for which both model behavior as well as the practical applicability can be tested. Given the heterogeneous nature of different energy carriers and related assets, many different data sets need to be analyzed, processed and combined. For example, varying asset maturity levels requires different processing attention. While some assets are in their final technological development stages (or the highest Technology Readiness Level (TRL) [118]), other assets have just reached the pilot stage. This means the sheer number of options for the former assets is enormous, requiring careful asset selection. For the latter asset type however, it is much more important to find realistic development potentials. Consequently, combinations had to be made between historical data and relevant forecasts, economic input and technological projections [119], and local and national data with European and global data [120]. The assembly of such an integrated multi-energy case study sharply contrasts with standard, single-network cases like the IEEE 33-bus distribution system [121], which is readily available for research in power systems. Such standard test systems do not (yet) exist for multi-energy research.

Hence, to demonstrate the proposed framework, an extensive, multi-energy case study is assembled based on the city of Eindhoven, the Netherlands, combining all relevant energy infrastructures: electricity, gas, and heat. It assumes a strict climate policy, reducing fossil fuel supply to zero in 2050. On the demand side, it includes demand development projections from residential, commercial, and industrial sectors, as well as local transportation demand. These are partially provided by the municipality [122], and complemented by national statistics and forecasts [123]. On the supply side, historical gas supply is slowly phased out and two types of renewable supply are possible: photovoltaic (PV) and wind energy. Energy can be distributed through the three different networks, and each carrier can be stored. Three conversion assets, Combined Heat & Power (CHP), Heat Pumps (HP), and Power-to-Gas

(P2G), can be constructed to integrate the different energy systems. The entire case description can be found in Chapter 4.

2.8 Conclusion

In this chapter, the three challenges that this thesis focuses on are derived from the developments of the energy transition: the *carrier mismatch*, the *temporal mismatch*, and the *deep uncertainty*. Solving these challenges requires an approach with different elements. First is the application of an integrated multi-energy system perspective, to ensure efficient and robust energy transition designs. Second is the application of long-term, and specifically multi-period investment planning to allow for the inclusion of pathway effects. These aspects also cause significant mathematical complexity, and translate to a novel application of the capacitated facility location network design problem. This has consequences for how to handle the challenge of deep uncertainty, which is tackled using an exploratory modeling approach. Finally, the entire framework is tested and demonstrated on a multi-energy, urban case study. This thesis aims to contribute towards supporting urban decision makers using the proposed *multi-energy framework* (Chapter 3), with the assembled case study (Chapter 4), and in both applications of this case to the framework, in Chapters 5 and 6.

Chapter 3

Formulation of the multi-energy framework

3.1 Introduction

In order to help urban decision makers design their energy transition pathway, this thesis proposes a long-term, multi-period investment planning framework for multiple energy systems. The first section (3.2) describes the core of the framework: the optimization model. Using this model, and input from any city, a multi-energy transition design is generated; determining which investments to make, when, and where. Yet long-term planning of energy systems, especially those in transition, is deeply uncertain. Hence, Section 3.3 describes how a specific uncertainty analysis is added to the framework. Then the computational approach for solving the optimization model and uncertainty analysis is given in Section 3.4. Finally, this chapter is concluded in Section 3.5.

3.2 Optimization model

The optimization model is developed as a mixed-integer linear program which determines when, where, and which investments are required. This section starts with the model notation, followed by a detailed model formulation. Figure 3.1 shows a graphic representation of the optimization framework. It includes the different types of input data, the objective function, the different constraints, and the output data.

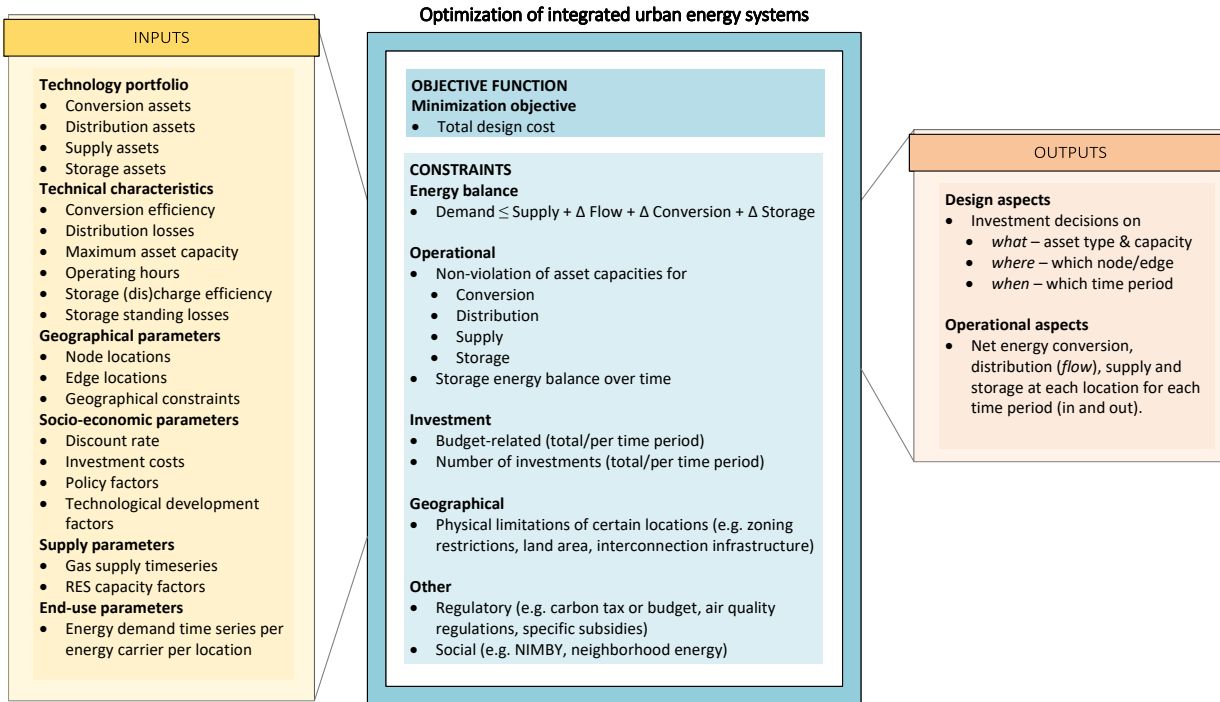


Figure 3.1: Graphic representation of the optimization framework for integrated urban energy systems, including input data, objective function, constraints, and output data, adapted from [102]

3.2.1 Model notation

Table 3.1: Indices, sets, and other sub/superscripts

Indices		Sets	
d	Energy distribution assets	DA	Distribution assets
e	Energy carrier types	E	Energy carriers
l	Locations	I	Investments
m	Energy conversion assets	MA	Conversion assets
s	Energy supply assets	SA	Supply assets
t	Time periods	T	Time periods
u	Edges	U	Edges
i	Nodes	V	Nodes
w	Energy storage assets	WA	Storage assets

Sub- and superscripts			
min	lower limit	max	upper limit
sl	Standing losses		

Indices and sets

The model can distinguish a whole range of energy carriers e , which can be transported using corresponding distribution network assets d , stored with energy storage assets w , and supplied by different supply assets s . These carriers can also be converted from one to another using conversion assets m . Table 3.1 contains all the indices, sets, as well as other sub- and superscripts used in the model.

Also note that the set of locations is different from the set of nodes. $i \in V$ denotes the set of nodes, and $l \in L$ denotes the set of locations, where $|V| = |E||L|$. Each location contains a number of nodes equal to the number of energy carriers modeled.

Parameters

Table 3.2 contains all the parameters in alphabetical order.

Table 3.2: Parameters

Parameters	
C_{dut}	Capital cost of en. distr. asset d on edge u in time period t
C_{mlt}	Capital cost of en. conv. asset m at location l in time period t
C_{slt}	Capital cost of en. sup. asset s at l in t
C_{wlt}	Capital cost of en. stor. asset w at l in t
D_{elt}	Demand per energy carrier e at l in t
δ	Social discount rate
Γ_d	Capacity of energy distribution asset d
Γ_m	Capacity of energy conversion asset m
Γ_s	Capacity of energy supply asset s
Γ_w	Capacity of energy storage asset w
η_{du}	Transportation efficiency of energy distribution asset d on edge u
$\eta_{m,e \rightarrow e'}$	Conversion efficiency of m of one energy carrier e to another e'
η_{st}^{CF}	Capacity factor of energy supply asset s at time period t
η_s^{CFavg}	Average capacity factor of energy supply asset s
η_w^+	Efficiency of <i>charging</i> energy storage asset w
η_w^-	Efficiency of <i>discharging</i> energy storage asset w
η_w^{sl}	Standing losses of energy storage asset w
O_{dut}^{fix}	Fixed operational cost of en. distr. asset d at u in t
O_{dut}^{var}	Variable operational cost of d at u in t
O_{mlt}^{fix}	Fixed operational cost of en. conv. asset m at l in t
O_{mlt}^{var}	Variable operational cost of en. conv. asset m at l in t
O_{slt}^{fix}	Fixed operational cost of en. sup. asset s at l in t
O_{slt}^{var}	Variable operational cost of en. sup. asset s at l in t
O_{wlt}^{fix}	Fixed operational cost of en. stor. asset w at l in t
O_{wlt}^{var}	Variable operational cost of en. stor. asset w at l in t
ϕ_m	Technological development rate of energy conversion asset m
ϕ_d	Technological development rate of energy distribution asset d
ϕ_s	Technological development rate of energy supply asset s
ϕ_w	Technological development rate of energy storage asset w
Π_{st}	Policy factor for supply asset s at time period t
ρ_d	Relative operating time of energy distribution asset d
ρ_m	Relative operating time of energy conversion asset m
ρ_s	Relative operating time of energy supply asset s
ρ_w	Relative operating time of energy storage asset w
σ_{st}	External factor for supply asset s at time period t

Decision variables

Table 3.3 contains the decision variables. Note that in some cases, certain decision variables can be parameterized. For example, if scenarios are simulated where one or more types of energy supply are forced to decrease, then the variable energy supply $S_{e1,lt}$ can instead be defined as parameter $E_{1,lt}$, varying per location and time period.

Table 3.3: Decision variables

Decision variables	
B_{dut}	Integer variable that represents the number of energy distribution asset d investments at edge u and in time period t
B_{mlt}	Integer variable that represents the number of energy conversion asset m investments in at location l and in time period t
B_{slt}	Integer variable that represents the number of energy supply asset s investments in at location l and in time period t
B_{wlt}	Integer variable that represents the number of energy storage asset w investments in at location l and in time period t
F_{eut}	Energy flow of energy carrier e over edge u and in time period t
M_{elt}	Energy conversion of energy carrier e at location l and in time period t
S_{elt}	Energy supply of energy carrier e at location l and in time period t
W_{elt}^{start}	Energy stored of energy carrier e at location l at the start of time period t
W_{elt}^{end}	Energy stored of energy carrier e at location l at the end of time period t
W_{elt}^+	Energy storage (<i>charge/injection</i>) of energy carrier e at location l and in time period t
W_{elt}^-	Energy withdrawal (<i>discharge</i>) of energy carrier e at location l and in time period t
\dot{W}_{elt}^+	Energy storage (<i>charge/injection</i>) rate of energy carrier e at location l and in time period t
\dot{W}_{elt}^-	Energy withdrawal (<i>discharge</i>) rate of energy carrier e at location l and in time period t

3.2.2 Model formulation

The proposed long-term, multi-period investment planning model for integrated urban energy systems is formulated as follows. First, the objective function 3.1 minimizes the total investment costs C and expected fixed and variable operational costs O of the energy system design over the entire planned time period:

$$\begin{aligned} \min \sum_{t \in T} \sum_{e \in E} \{ & \sum_{u \in U} \sum_{d \in DA} (B_{dut}(C_{dut} + O_{dut}^{fix}) + O_{dut}^{var} F_{eut}) + \\ & \sum_{m \in MA} (B_{mlt}(C_{mlt} + O_{mlt}^{fix}) + O_{mlt}^{var} M_{elt}) + \\ & \sum_{l \in L} (\sum_{s \in SA} (B_{slt}(C_{slt} + O_{slt}^{fix}) + O_{slt}^{var} S_{elt}) + \\ & \sum_{w \in WA} (B_{wlt}(C_{wlt} + O_{wlt}^{fix}) + O_{wlt}^{var} W_{elt})) \} \\ & B \in 0, 1, \dots, N \quad (3.1) \end{aligned}$$

where B is the number of asset investments, F the energy distribution (flow), M the energy conversion, S the energy supply, and W the energy storage. The energy system design covers investments for each time period t , for each energy carrier e , at each edge u or location l , for each distribution d , conversion m , supply s , and storage asset w . The main energy balancing constraint is given by:

$$s.t. D_{elt} \leq S_{elt} + \Delta F_{elt} + \Delta M_{elt} + \Delta W_{elt} \quad \forall e \in E, l \in L, t \in T \quad (3.2)$$

which ensures that demand D of each energy carrier e is met at each location l and in each time period t using energy supply S , and the net (Δ) amount of distribution F , conversion M , and storage W . The main constraint for the net amount of distribution is:

$$\Delta F_{elt} = \sum_{d \in DA} (\sum_{u \in U_l^{in}} F_{eut} \eta_{du} - \sum_{u \in U_l^{out}} F_{eut}), \quad \forall e \in E, l \in L, t \in T \quad (3.3)$$

where edge u is undirected, so energy from each energy carrier e , edge u , and time period t can both flow away, and into the location l . In the latter

case, energy losses are calculated using a linearized loss factor $\eta_{d,u}$. Note that the net flow variable for the energy balance constraint is calculated for each location to relate to the other balancing variables, while the remaining flow variables relate to the edges, which is where the flow actually occurs. Next is the main conversion constraint, depicted here for three energy carriers e_1 , e_2 , and e_3 :

$$\Delta M_{elt} = \Delta M_{e_1 lt} + \Delta M_{e_2 lt} + \Delta M_{e_3 lt}, \forall e \in E, l \in L, t \in T \quad (3.4)$$

$$\Delta M_{elt} = \sum_{m \in MA} \sum_{e \in E} (M_{melt} (-1 + \sum_{e' \in E} \eta_{m,e' \rightarrow e, e' \neq e})), \forall e \in E, l \in L, t \in T \quad (3.5)$$

with Constraint 3.5 being the generalized conversion constraint for an unlimited number of energy carriers e and conversion assets m . At each location l , during each time period t , each energy carrier e can be consumed for conversion or generated with a certain conversion efficiency $\eta_{m,e' \rightarrow e, e' \neq e}$ from any other carrier e' . Applying this formula to three energy carriers leads to the following conversion (or *coupling*) matrix:

$$M = \begin{pmatrix} e_1 & e_2 & e_3 \\ e_1 & 1 & \eta_{m,e_1 \rightarrow e_2} & \eta_{m,e_1 \rightarrow e_3} \\ e_2 & \eta_{m,e_2 \rightarrow e_1} & 1 & \eta_{m,e_2 \rightarrow e_3} \\ e_3 & \eta_{m,e_3 \rightarrow e_1} & \eta_{m,e_3 \rightarrow e_2} & 1 \end{pmatrix}$$

These matrices can also be generated for each individual carrier, then related to the number of conversion methods. The following equations form the net storage value, the final part of the main energy balance equation 3.2:

$$W_{elt}^{start} = \sum_{w \in WA} W_{welt-1}^{end} (1 - \eta_w^{sl}), \forall e \in E, l \in L, t > 0 \in T \quad (3.6)$$

$$W_{elt}^{end} = W_{elt}^{start} + \Delta W_{elt}, \forall w \in WA, e \in E, l \in L, t \in T \quad (3.7)$$

$$\Delta W_{elt} = \sum_{w \in WA} W_{welt}^+ \eta_w^+ - \sum_{w \in WA} W_{welt}^- \eta_w^-, \forall w \in WA, e \in E, l \in L, t \in T \quad (3.8)$$

with 3.6 as the main storage constraint, which explicitly links time periods. The energy storage level at the start of a time period W_{elt}^{start} is based on the storage level at the end of the previous time period for each storage type w , as it has to be adjusted for standing losses η_w^{sl} . Note that the sum of all W_{welt-1}^{end} by storage type, leads to W_{elt-1}^{end} . Equations 3.7 and 3.8 depict how storage levels can be adjusted within a time period: for each energy carrier e , at each location l , and each time period t , considering storage (*charging* or *injection*)

and withdrawal (*discharging*) losses, η_w^+ and η_w^- respectively. Together these are referred to as *round-trip efficiency*.

As the proposed model is a long-term investment optimization framework, it also involves techno-economic development of all infrastructure considered in the energy transition design. The following constraints depict those developments:

$$C_{dut} = C_{du0}(1 + \phi_d)^{t_0 - t} / (1 + \delta)^{t - t_0}, \quad \forall d \in DA, u \in U, t \in T \quad (3.9)$$

$$C_{mlt} = C_{ml0}(1 + \phi_m)^{t_0 - t} / (1 + \delta)^{t - t_0}, \quad \forall m \in MA, l \in L, t \in T \quad (3.10)$$

$$C_{slt} = C_{sl0}(1 + \phi_s)^{t_0 - t} / (1 + \delta)^{t - t_0}, \quad \forall s \in SA, l \in L, t \in T \quad (3.11)$$

$$C_{wlt} = C_{wl0}(1 + \phi_w)^{t_0 - t} / (1 + \delta)^{t - t_0}, \quad \forall w \in WA, l \in L, t \in T \quad (3.12)$$

where future investment costs C for each distribution d , conversion m , supply s , and storage asset w are discounted by the *social discount rate* δ , and their respective technological development factors ϕ , at each edge u or location l , for each time period t . Even though the aim is to model investment decisions, it is not to maximize the return for an investor, but to evaluate the total energy system costs under different (policy-driven) circumstances; which is a social perspective [124] fitting as the design is constructed from the perspective of a (municipal) government, a district system operator or both. In addition, as targeted technological development is deemed crucial to accelerate the energy transition [125], technological learning curves are incorporated into ϕ_x .

The next step is to define the bounds on the different assets and the possible energy distribution, conversion, supply, and storage for each of them. All these constraints also link time periods, as all energy capacities are cumulative. If a certain capacity was already present at a location l or on an edge u , it remains available into the following time period. First are the constraints pertaining to the maximum flow on an edge u :

$$0 \leq F_{eut} \leq \sum_{d \in DA_e} F_{deut}^{max}, \quad \forall e \in E, u \in U, t \in T \quad (3.13)$$

$$F_{deut}^{max} = \sum_{v=0}^t B_{dlv} \Gamma_d \rho_d, \quad \forall d \in DA, e \in E, u \in U, t \in T \quad (3.14)$$

where DA_e is defined as the subset of distribution types of energy type e . Then for each energy distribution asset d invested in B_{dut} , the maximum flow possible F_{deut}^{max} for the relating energy carrier e increases with Γ_d and is limited

by the relative operating time ρ_d . Note that the edges are undirected, meaning there is no distinction between the construction of an edge in one direction ($u \in U_l^{in}$) or the other ($u \in U_l^{out}$), as energy can flow in both directions. The maximum energy conversion is given by:

$$0 \leq M_{elt} \leq \sum_{m \in MA_e} M_{melt}^{max}, \quad \forall e \in E, l \in L, t \in T \quad (3.15)$$

$$M_{melt}^{max} = \sum_{v=0}^t B_{mlv} \Gamma_m \rho_m, \quad \forall m \in MA, e \in E, l \in L, t \in T \quad (3.16)$$

where MA_e is defined as the subset of conversion types of energy type e . Then for each energy conversion asset invested in B_{mlt} up to and including the current time period t , the maximum conversion capacity M_{melt}^{max} is increased by Γ_m and limited by the relative operating time ρ_m . The maximum possible energy that can be supplied is defined by:

$$0 \leq S_{elt} \leq \sum_{s \in SA_e} S_{sel}^{max}, \quad \forall e \in E, l \in L, t \in T \quad (3.17)$$

$$S_{sel}^{max} = \sigma_{st} \sum_{v=0}^t B_{slv} \Gamma_s \rho_s, \quad \forall s \in SA, e \in E, l \in L, t \in T \quad (3.18)$$

$$\sigma_{st} = \Pi_{st} \eta_{st}^{CF} / \eta_s^{CFavg}, \quad \forall s \in SA, t \in T \quad (3.19)$$

where SA_e is defined as the subset of supply types of energy type e . The maximum supply capacity S_{sel}^{max} can be increased by investing in energy supply assets B_{slt} with capacity Γ_s , limited by operating time ρ_s . However, S_{sel}^{max} is affected by an external factor σ_{st} , which is defined in Constraint 3.19. This includes both a policy factor Π_{st} , which can for example be used to limit certain (fossil) energy carriers, and weather variations impacting the capacity factor η_{st}^{CF} of certain supply assets, which are normalized using their average capacity factor η_s^{CFavg} . Finally, the maximum energy storage capacities are given by:

$$0 \leq W_{elt}^{end} \leq \sum_{w \in WA_e} W_{welt}^{max}, \quad \forall e \in E, l \in L, t \in T \quad (3.20)$$

$$0 \leq W_{elt}^+ \leq \sum_{w \in WA_e} (W_{welt}^{max} - W_{welt}^{start}), \quad \forall e \in E, l \in L, t \in T \quad (3.21)$$

$$0 \leq W_{elt}^- \leq \sum_{w \in WA_e} W_{welt}^{start}, \quad \forall e \in E, l \in L, t \in T \quad (3.22)$$

$$W_{welt}^{max} = \sum_{v=0}^t B_{wlv} \Gamma_w \rho_w, \quad \forall w \in WA, e \in E, l \in L, t \in T \quad (3.23)$$

where WA_e is the subset of storage types of energy type e . The storage level at the end of a time period is restricted by the maximum storage levels W_{welt}^{max} . Yet the amount that can be (dis)charged $W_{elt}^{+/-}$ is also, or even entirely, restricted by whatever was already present in this particular asset W_{welt}^{start} . These amounts can be increased by investing in storage assets B_{wlt} with a storage capacity Γ_w , limited by an operating time ρ_w . Note that some storage assets also require minimum values, in that case, the 0 is replaced by a W_{welt}^{min} .

Finally, the domain of the variables used need to be defined:

$$B_{ut}^d \leq N, B_{dut} \in \mathbb{Z}^+, \quad \forall d \in DA, u \in U, t \in T \quad (3.24)$$

$$B_{lt}^m \leq N, B_{mlt} \in \mathbb{Z}^+, \quad \forall m \in MA, l \in L, t \in T \quad (3.25)$$

$$B_{lt}^s \leq N, B_{slt} \in \mathbb{Z}^+, \quad \forall s \in SA, l \in L, t \in T \quad (3.26)$$

$$B_{lt}^w \leq N, B_{wlt} \in \mathbb{Z}^+, \quad \forall w \in WA, l \in L, t \in T \quad (3.27)$$

$$F_{eut} \in \mathbb{R}^+, \quad \forall e \in E, u \in U, t \in T \quad (3.28)$$

$$M_{elt}, S_{elt}, W_{elt}^{start}, W_{elt}^{end}, W_{elt}^+, W_{elt}^- \in \mathbb{R}^+, \quad \forall e \in E, l \in L, t \in T \quad (3.29)$$

where equations 3.24 through 3.27 define the domain of the investment variables B . They are limited by N number of investments per time period t . Also, the variables are restricted to being integer valued and non-negative. Lastly, Equations 3.28 and 3.29 define the domain of the remaining variables for distribution F , conversion M , supply S , and storage W ; these are all non-negative, real numbers.

3.3 Uncertainty analysis

The previous section describes the deterministic setup of the optimization model. Yet long-term future planning is deeply uncertain and should be in-

corporated into the overall multi-energy framework. The model is applied to two different sets of what-if scenarios (Chapter 5), testing a whole range of uncertainty within two different parameters. Yet these give a limited view of the effect of uncertainties. Ideally, it is be included in a stochastic manner; either via stochastic or robust optimization. Yet given the complexity of the framework, as described in Chapter 2 and further detailed in the next section, this is not feasible. Instead, exploratory modeling is used, which can be viewed as an extensive uncertainty and sensitivity analysis.

This section explains the proposed methodology that is applied, using the steps as depicted in Figure 6.2. First, relevant uncertainties are selected and their range and distributions are characterized. Then a large number of computational experiments is generated, each containing a unique sample of the uncertain parameter values. These and the original base-case are fed into the optimization model as described in the previous section. Each experiment result contains the total costs of the design, all investment decisions of *what* was built, *where*, and *when* and the resulting energy balance for each time period. To further compare the results quantitatively, different data processing techniques are applied to determine the influence of the uncertainties on the results.

3.3.1 Uncertainty characterization

In this part, the focus is on parametric (external) uncertainties, which refers to imperfect knowledge of input parameter values, as opposed to structural (internal) uncertainties, which refers to the uncertainty of the mathematical relations describing the energy system in the model [32]. Structural uncertainties

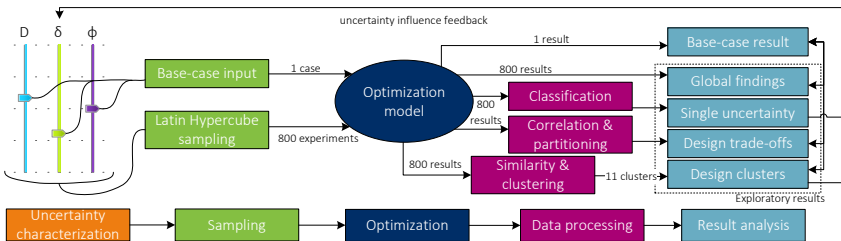


Figure 3.2: Exploratory modeling methodology visualisation, including demand development D , social discount rate δ , and technological development rates ϕ_x

are tested and analyzed in Chapter 5. Parametric uncertainties create the main variation in long-term energy system developments [102]. The multi-energy framework contains social, economic, technological, and environmental parameters (see Figure 3.1). In each of these categories, uncertainty is present in different ways. Social parameters include energy demand development D and policy Π . Economic parameters are asset capital and operational costs C and O , and the discount rate δ . The technological parameters are: asset capacity Γ , efficiency η , and technological development rate ϕ . Different environmental factors can be included, an example is given in the external factor for supply (Equation 3.19), σ , which includes inter-annual weather variations.

In order to select relevant uncertainties, input from the case study is combined with national and international long-term energy models [126], [127], [128], and a diverse set of scenario planning studies [32] [129] [49] [130] [131] [132]. Subsequently, the selected uncertainties are characterized using input from the case study and its relevant stakeholders, complemented with relevant literature and local, national, and international databases.

3.3.2 Sampling

To systematically sample and explore the provided input space of all uncertain parameters, Latin Hypercube Sampling (LHS) is used [99]. As explained in the previous chapter, it combines the best of random and stratified sampling, efficiently exploring the unframed system state (Figure 2.5) [100]. A sample size N from k uncertain parameters is generated by dividing the range of each uncertainty x_k into $1/N$ intervals of equal probability, and then taking a sample from each of those intervals and randomly combining the samples. Figure 3.3 provides an example where $N = 4$ and $k = 2$, showing the density functions of variables x_1 and x_2 and the resulting samples $[N_1, \dots, N_4]$.

Generally, a large enough sample size is needed to explore all uncertain parameters. In LHS, a rule of thumb is to use at least 100 experiments per parameter, so $N \leq 100k$. In the end, a cube with N^k cells is created which covers the sample space.

3.3.3 Data processing & result analysis

The next steps of the exploratory methodology involve processing the data and analyzing the results, which occur jointly and as such are described together. Before any of the exploratory results are processed, the deterministic results of the base case are given to provide a benchmark for interpreting the rest of

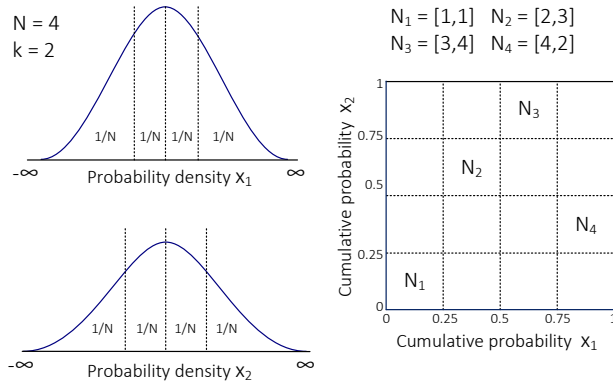


Figure 3.3: Latin Hypercube Sampling with probability density functions of x_1 and x_2 on the left, and their cumulative probability with resulting samples $[N_1,..,N_4]$ on the right.

the results. The base case is described in Chapter 4 and its results are given in section 6.4.1. After the base case, the experiment outcomes are analyzed globally on the three system design aspects. Then a classification is made to determine the sensitivity of the results to each uncertain parameter individually. Third, a correlation analysis is used to determine design trade-offs, or (negative) correlations, and specific tipping points between these trade-offs are found using a partitioning technique. Finally, broad investment patterns are determined using a clustering approach.

Global findings

Globally, information for all three system design aspects is given per experiment outcome: how many of which assets are built (*type*), where (*location/edge*), and when (*time period*). In other words, all integer decisions are included. Given that there are both network investments, as well as non-network investments, which each relate to different asset types, each experiment outcome is shaped as a concatenated vector of both investment types. With XA^U representing the network investments and XA^L the non-network investments; each experiment outcome will have a vector sized $[XA^U UT] + [XA^L LT]$, which is called the result vector $[RV]$. All results are a matrix of size $[N, RV]$.

With this information, aggregations can be made on each different design aspect, creating different result matrices for the asset types $[N, X]$, the locations $[N, L]$ and edges $[N, U]$ and the time periods $[N, T]$. This allows a calculation of the expenses per design aspect, as well as the related energy capacities in PetaJoules (PJ). Both the costs and the energy capacity are a way to normalize between the different design aspects. I.e. one conversion asset might have an entirely different capacity than one storage asset, or even other conversion assets. In short, the main result values for each experiment outcome include the total system cost in MEur, and for each design aspect the total number of investments, and the energy capacity in PJ.

Classification

First, the sensitivity of these results to each uncertain parameter individually is analyzed using an Extra Trees classifier [133]. Similar to a Random Forest, it uses an ensemble of weak classifiers to obtain a high performing one; though at even less computational expense. This technique is employed because, compared to Sobol indices and linear regression, it requires relatively limited computational resources, does not assume linearity and lacks a restrictive assumption for unimodal symmetry [108]. This is fitting to our application, given the complexity of the optimization framework and the fact that the case includes heterogenous uncertainties: some of them are discrete, non-linear and not continuous. Moreover, the goal is not an exact classification, but merely to determine the relative influence of each uncertain parameter on the outcomes. The Extra Trees classifier is used to provide feedback to both the decision maker and the exploratory modeling process.

Correlation & partitioning

For an urban decision maker, it can be valuable to know whether there are trade-offs, or conversely positive correlations, between different investments. This can help steer their policy decisions. A correlation analysis compares the influence of each result value to each other. This leads to a large set of pair plots, where different patterns can be analyzed. To aid this analysis and quickly determine relevant positive and negative correlations, the pair plots are aggregated into one correlation matrix, which is visualized as a heat map.

In addition, it can be useful to know the exact tipping point(s) of uncertain parameter values, or their ranges that drive these investment trade-offs. To find these tipping points, or uncertainty ranges, a PRIM (Patient Rule Induction Method) technique is applied [109]. PRIM is a lenient hill climbing

optimization algorithm which recursively *peels* away small slices of an input space based on simple rules to find subregions where the target variable is relatively high (or low). Figure 3.4 gives an example for a combination of continuous and categorical values. The range of the experiments of interest (red dots) needs to be found by finding the best fitting box (green line), removing those areas (grey box) which contain mostly other experiments (blue dots). The input space, initial box B , can be reduced either by removing an entire category, candidate boxes b_1 , b_2 , and b_3 , or removing a slice of continuous data, candidate boxes b_4 and b_5 , which works similarly for integer variables. Based on a certain objective function, the best candidate box is calculated and then the process repeats itself.

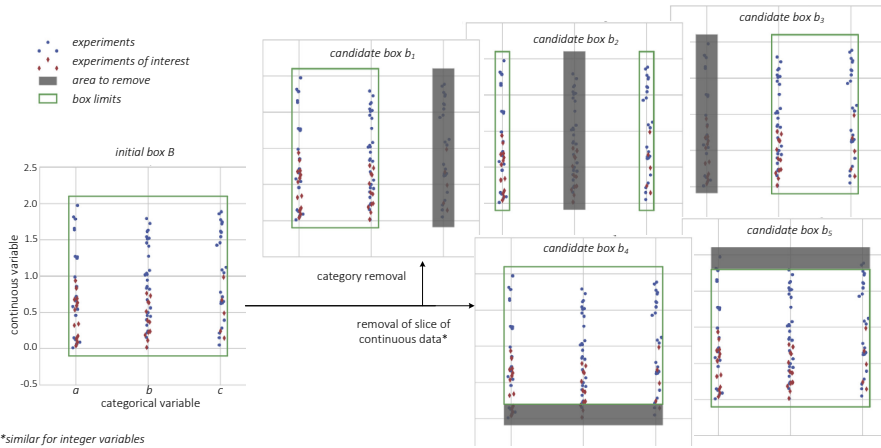


Figure 3.4: Patient Rule Induction Method (PRIM) algorithm visualization, adapted from [108]

This creates a *peeling trajectory*, which finishes at a pre-determined density or coverage threshold [134]. Density is defined as the fraction of experiments in the box that are of interest. Coverage is the fraction of all experiments of interest in the box. Both are relevant to aid decision making, yet they are in tension with each other. To find exact uncertainty ranges that drive certain investment levels, a high density is more important. Hence, a density threshold of 0.8 is used.

Similarity & clustering

To further analyze the practical relevance of the results, a clustering approach is used. This can determine significant system design clusters, or investment patterns, and see which parameter combinations caused them. By knowing which decisions the optimization framework tends to take under which circumstances, robust decision support can be provided to urban decision makers.

Distance measuring - To compare and cluster results, a certain value needs to be assigned to each individual experiment outcome. Commonplace is to use a so-called distance measure to calculate the difference, or conversely the similarity, between each experiment outcome. In this work, the *cosine distance* is preferred. As explained in Section 2.6, it is well suited for high-dimensional and sparse vectors, as opposed to vectors with high magnitude. Result vector $[RV]$ is exactly such a vector, given how its defined and that the number of investments is limited by N . The cosine distance is calculated as the inverse of cosine similarity:

$$1 - \cos\theta = 1 - (\mathbf{A} \cdot \mathbf{B}) / (\|\mathbf{A}\| \|\mathbf{B}\|) \quad (3.30)$$

where \mathbf{A} and \mathbf{B} represent two result vectors. A distance of zero represents the highest similarity and inversely, a distance of 1 means a 90 degree angle between vectors and the lowest similarity.

Clustering - A clustering algorithm can be applied to the cosine distance matrix. An *hierarchical* [112], *agglomerative* [113] clustering algorithm with a *complete linkage* criterion [114] is applied, as explained in Section 2.6. These clusters are analyzed first on which uncertainty (ranges) shaped them using a Classification and Regression Tree (CART) [115], to determine broad investment trends. Then, patterns of their investment design aspects are evaluated: asset type, location, and time period. The exploratory methodology is explained in a more general sense in [106].

3.4 Computational approach

The proposed framework for multi-energy design investment planning translates to a mixed-integer linear program (MILP), combining a capacitated facility location problem with a multi-dimensional, capacitated network design problem. Both problems separately are NP-hard (if not NP-complete) and the combination is highly combinatorial. It contains a three-dimensional network

expansion, as a conversion unit creates a virtual network between energy carriers, besides the individual network expansion options (see Figure 3.5). The use of storage assets significantly increases the solution space, as more trade-offs have to be made across certain time periods, most notably between supply or storage. This creates a strongly NP-hard problem; even with just two energy carriers and one time period [38]. This complexity has consequences for how to tractably solve the optimization problem.

3.4.1 Solving the MILP

Practical mixed integer (linear) programs are typically solved by state-of-the-art MIP solvers like Gurobi or CPLEX (Klotz and Newman, 2013). Ever continuing advances in implementation of algorithms and hardware improvements in these solvers allow formulation of increasingly large and complex models. A MIP solver reads a MIP problem, executes an optimization procedure, containing both exact and heuristic methods, and returns the best solution found. For obtaining solutions to the multi-energy framework, the Gurobi MIP solver is used. Besides state-of-the-art, it is also open source, which makes the findings

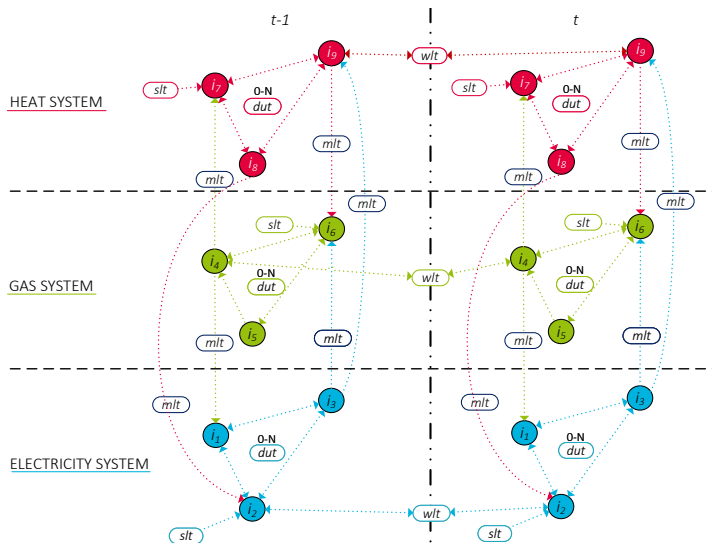


Figure 3.5: Optimization framework modeling decisions within and in between energy systems, and between time periods

in this thesis easier to reproduce, also enabling future research. The methods that Gurobi applies for solving MIPs are a branch and bound (B&B) procedure combined with problem reductions, cutting planes and various heuristic methods (Figure 3.6) [135]. After a general description of B&B methods, we shortly introduce how these components are implemented in the solver.

For many optimization problems, direct solution methods might not exist, or they might be highly inefficient. Branch and bound methods can solve these *difficult* problems by applying existing methods to *easy* sub-problems. Through solving a collection of those, a solution for the original problem might be found. For MILPs, the *easy* sub-problems are linear programs (LPs) that can be solved with the simplex method [136]. In B&B methods, such LPs are in fact linear relaxations of the original integer program, where the integrality constraints are relaxed. From the root node of the B&B solution tree, which contains the linear relaxation of the original problem, tree branches to new nodes are made to continuously solve new relaxations. The algorithm keeps track of the best current feasible solution; the *incumbent* and if all original integer variables have an integer value in the optimal relaxed solution, an optimal integer solution to the original problem is found. If this is not the case, then an integer variable with a non-integer value is chosen and restricted to be lower than the rounded down non-integer value or higher than the rounded up non-integer value.

The Gurobi algorithm uses several building blocks in its MIP algorithm as depicted in Figure 3.6 [137]:

- Presolve - The presolve is a collection of problem reductions to reduce the problem size and tighten its formulation.
- Branch and bound - In the root node of the branch and bound tree (the first node selection and presolve), the LP relaxation is solved. After that, a branch and bound tree search is generated by iteratively selecting nodes as the next sub-problem to process. The solver keeps track of the incumbent, the global lower bound and the gap between the incumbent and the lower bound throughout the whole procedure (optimality gap). When this gap is equal to 0, optimality is reached and the solver terminates.
- Cutting planes - The implementation of cutting planes is the most important contributor to computational advances in integer programming over the last years. During the B&B procedure, different relaxed solutions are cut off from the solution space.

- Heuristics -The branching part of the branch and bound algorithm is not the only method that the solver uses to find new feasible solutions. Gurobi includes multiple heuristics, such as feasibility heuristics, local search heuristics and some heuristics in the root node. Good heuristic methods find solutions earlier than branching. By exploiting the problem structure, Gurobi adapts its strategy deciding when to apply which heuristics.
- Additional techniques - Besides the above mentioned components, many additional techniques are included in the solver's optimization procedure, such as sophisticated branch variable techniques, symmetry detection, disjoint subtree detection, etc. In most cases, their goal is to limit the size of the branch and bound tree that must be explored.

Although the standard algorithm is powerful, our highly combinatorial

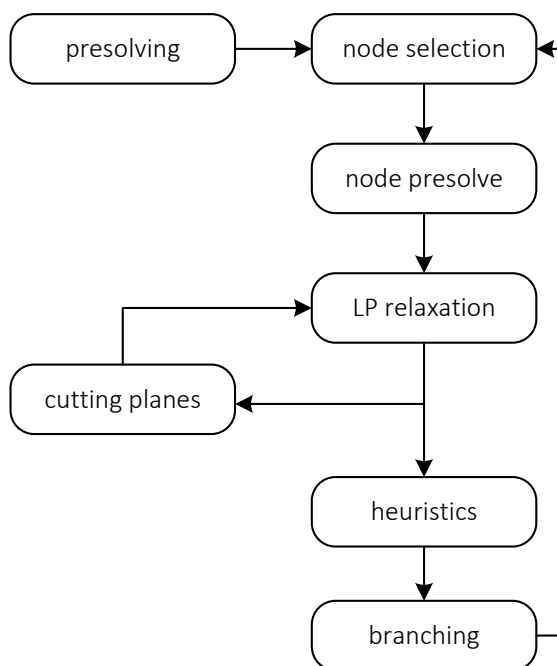


Figure 3.6: Gurobi MIP algorithm building blocks, adapted from [137]

problem is still challenging to solve for large cases. Different improvements can be applied from both mathematical and computational points of view. For example, it can be interesting to vary the aggressiveness of cutting planes in some cases, especially with model-specific knowledge. Also, the parameters of the algorithm can be tuned, e.g. instead of solving the LP relaxations with a primal simplex method, a dual simplex, or a barrier method can be selected. The latter showed promise, yet was still unable to feasibly solve large urban cases [38]. Similar challenges remained with the use of valid inequalities, different decomposition methods and heuristics [37], [38]. Hence, the proposed modeling framework is demonstrated with a long-term, but spatially small-scale case to showcase all its functionalities without losing tractability. For this case, the B&B algorithm setting using the primal simplex method is preferred, as it is less numerically sensitive than the barrier method [138].

3.4.2 Programming details

The model is programmed in Pyomo, which is an open-source collection of Python software packages (version 3.7) specific for optimization modeling. It is solved with the Gurobi Parallel Mixed Integer Programming (MIP) solver version 8.1.1. All runs were executed using laptop with Windows 10, a 2.3GHz processor and 16 GB of RAM. The optimality (MIP-)gap is set as low as possible, balancing run time and memory usage, to an absolute value of 0.1%.

For the implementation of the uncertainty, exploratory methodology, the optimization framework is connected to the EMA Workbench [110]. This package supports LHS sampling of the input parameters using the ranges as described, and it provides the validation techniques as described in section 2.4.1.

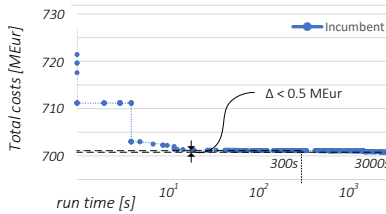


Figure 3.7: Solution progress of a typical experiment run

For the individual policy and weather variations, the MIP-gap is combined with a run time limit of 3000s. For the exploratory analysis, the run time for

each experiment is reduced to 300s. This balanced the computational burden well with sufficient result accuracy. Figure 3.7 shows this in the solution progress of a typical experiment run: with a 20x longer run time, and significant additional memory use, the solution improves less than 1%. This is mainly due to the similarity between the relative costs of different solutions, especially conversion versus storage. There are many different solution options which are often only marginally better, so the solver finds little additional improvement, which highlights the relevance of investment patterns as opposed to investment magnitude.

3.5 Conclusion

This concludes the description of the multi-energy framework, including the formulation of the optimization model, the uncertainty analysis, and the computational approach. More information on the code itself and the programming details can be found in the Github repository [139]. The next chapter will describe the extensive urban case study on which the framework and uncertainty approach were tested.

Chapter 4

Urban case study based on a large Dutch city

4.1 Introduction

To demonstrate the benefits of the multi-energy optimization framework developed in Chapter 3, an extensive, multi-energy case study is assembled based on the city of Eindhoven, the Netherlands. It includes all energy carriers present in the city: electricity, gas, and heat. This case study forms the basis of the next two chapters, in which the framework is applied to tackle the three main challenges of the energy transition: the carrier and temporal mismatches (Chapter 5), and the deep uncertainty (Chapter 6). Each of these chapters contains more details on the specific application of the case study described in this chapter.

First, the heterogeneous data sets forming the basis of the case, are described and depicted in Section 4.2. First, the demand-side, then the supply-side, and finally the pathway effects are discussed. Section 4.3 translates this data to a case fitting the multi-energy framework, including a description of relevant assumptions, specific details of each asset category, and how this shapes part of the mathematical formulas and sets. The remaining complexity of the case study is briefly highlighted at the end of that section. Finally, the chapter is summarized and preliminary conclusions are drawn in Section 4.4.

4.2 Data

The city of Eindhoven is the fifth largest city in the Netherlands with 235.691 inhabitants [140]. Its municipality has considerable climate ambitions to achieve a 95% reduction of carbon emissions by 2050, compared to 1990 [141]. In 2016, the municipality made its first high-level projections on how to achieve these ambitions, in which they incorporated the need for a multi-energy systems perspective [122]. Consequently, they consider three energy carriers, which correspond to the current energy networks present in the city: electricity, gas, and heat. Figure 4.1 shows a depiction of the municipality and its seven city parts, including hypothetical energy networks.

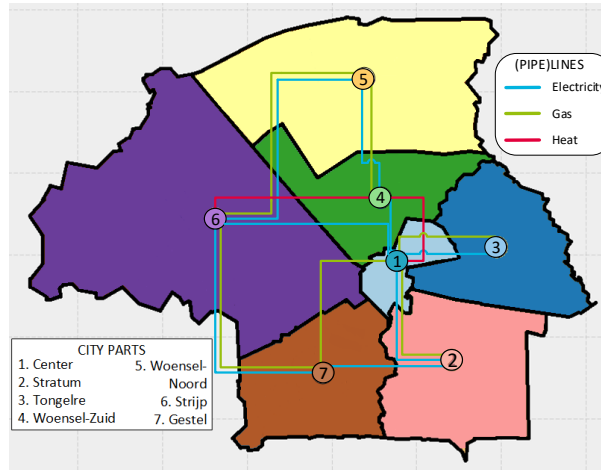


Figure 4.1: City parts of Eindhoven with multi-energy network projections

4.2.1 Demand-side

The current energy demand levels are based on the situation of Eindhoven in 2011, depicted in Figure 4.2, which formed the basis of their high-level projections [122]. The figure shows the demand for different energy carriers per sector, including residential, commercial, industrial, and local transportation demand (*mobility*). Note that this includes a demand for fuel, coal and oil. The latter two arise from national estimates for industrial energy demand,

which complements the actually available data from a handful of local industries. These carriers were allocated to the most similar energy carrier: gas. In addition, the demand figures were updated using 2018 data from the local District System Operator (DSO) [142]. This led to a total of 15.6 PJ, of which 28% is electric, 45% is gas, and 27% is heat. These values are allocated to Eindhoven's seven city parts using bottom up input from detailed residential demand figures from the DSO combined with local, expert knowledge on commercial, industrial and transportation data [143]. This led to a demand distribution per sector and energy carrier for each city part, or location L , as shown in Table 4.1. Each location contains a node for each energy carrier, translating to a total of 21 nodes.

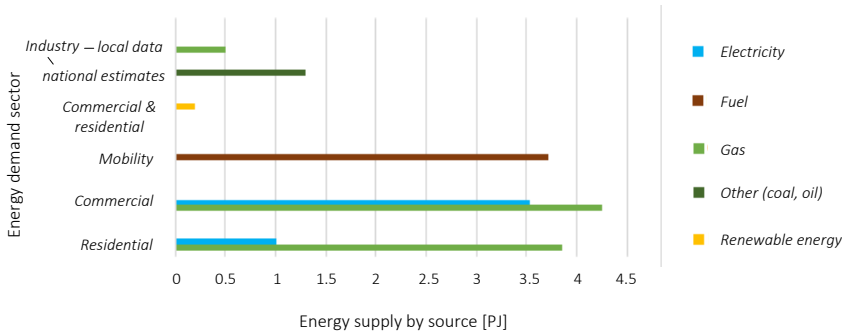


Figure 4.2: Eindhoven energy demand by sector and energy supply by source in PJ in 2011, from [122]

In the municipality's high-level projections, demand developments up to 2040 were provided based on a number of relevant factors, e.g. population changes, energy efficiency increases, and % adoption of electric vehicles (EVs). Figure 4.3 shows the details of the energy savings caused by an increase in energy efficiency. The isolation of homes and buildings shows a particularly high potential (reducing residential gas usage, and commercial energy usage). Using Dutch national energy data [144], projections [145], and statistics [123], these developments were extended to 2050 to match the final year of Eindhoven's climate goals. The most notable change compared to Eindhoven's projections is a much higher EV adoption, as their potential was not yet recognized as it is now. This especially led to an even lower gas demand, and higher electricity demand by 2050. The total energy demand in 2050 equals 10 PJ, of which 43% is electric, 13% is gas, and 44% is heat.

Table 4.1: Demand distribution per carrier e and per sector for each Eindhoven city part L [in %]

L	D_{e_1}	D_{e_2}	$D_{e_3}^a$	Rs.	Cm.	In.	Mb. ^b
l_1	8.6	9.7	8.9	1.2	4.7	0.0	3.1
l_2	17.1	18.1	14.3	2.3	7.1	3.6	3.1
l_3	8.6	9.7	8.9	1.2	4.7	0.0	3.1
l_4	9.2	9.7	11.0	4.7	2.4	0.0	3.1
l_5	9.2	9.7	11.0	4.7	2.4	0.0	3.1
l_6	30.1	25.0	31.7	2.3	18.8	2.4	6.2
l_7	17.1	18.1	14.3	2.3	7.1	3.6	3.1
Totals	100	100	100	18.7	47.1	9.5	24.6

^a e_1 = electricity, e_2 = gas, e_3 = heat

^bResidential, Commercial, Industrial, and Mobility [122]

4.2.2 Supply-side

To further shape the case study from the supply-side of the energy system in Eindhoven, data on relevant conversion, network, supply, and storage assets is required. To this end, data from the local DSO is combined with international data sets, including techno-economic data from the International Energy Agency's (IEA) Energy Technology Systems Analysis Program [120], from manufacturers, research papers, and other relevant databases. Table 4.2 lists the assets used in this case study and includes relevant sources for each of them. Why these assets were used is discussed next. More details about each asset, including relevant assumptions, is included in the next section.

Given that incorporating all three energy carriers increases the model complexity significantly (see Section 3.4), three asset options per category were allowed. Each asset is modeled using one average energy capacity, to limit further computational cost. Most of the selected assets were already present in the city, including all three network types (electricity lines, gas, and heat pipelines); both Combined Heat & Power (CHP) and Heat Pump (HP) conversion; gas, photovoltaic (PV) and wind supply; heat and gas storage. Some assets were selected given their future and/or multi-energy potential: power-to-gas (P2G) conversion, and electricity storage. Note that there is no heat supply currently present in the city and neither is it part of the investment op-

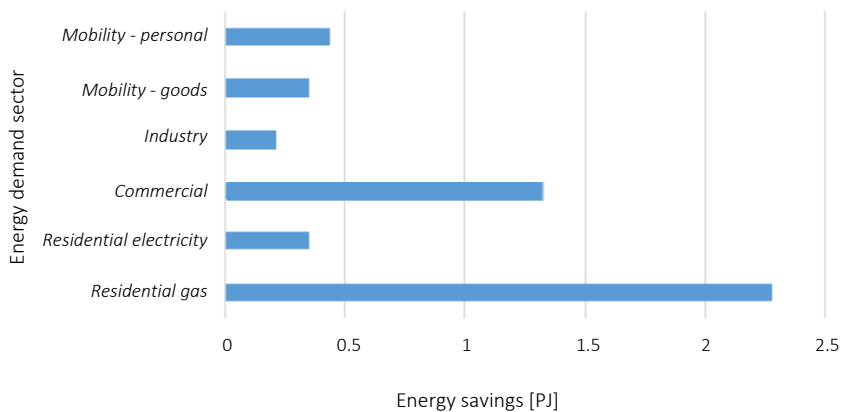


Figure 4.3: Energy savings in Eindhoven in PJ by sector in 2040, from [122]

tions, as there are no significant, economic, non-carbon emitting heat sources. This means that any heating network cannot be supplied directly, only indirectly via conversion assets.

4.2.3 Pathway effects

In addition to the demand developments in the city, there are also other developing factors that can influence the energy system design. These factors include social, economic, environmental and technical developments and are used to incorporate *pathway effects* during the time frame of the energy transition as introduced in Chapter 1. In the multi-energy framework, this is captured in the social discount factor δ , the external supply factor σ_{st} which includes the policy factor Π_{st} and the relative capacity factor (CF) $\eta_{st}^{CF}/\eta_s^{CF_{avg}}$, and the technological development rate ϕ_x for each asset x .

The main data for most of these parameters are included in Table 4.3. The policy factor is derived from Eindhoven's climate goal of a 95% reduction of CO_2 emissions by 2050. In order to reach this goal, the fossil gas supply has to decline by 2.97% annually. With regard to the CFs of PV and on- and offshore wind, the table only contains the Dutch averages. The entire range of historical capacity factors can be found in the Appendix in Table 8.2.

Table 4.2: Asset investment input data including capital cost C , energy (and power) capacity Γ , efficiency η and relative annual operating time ρ

I	Asset name	C [M€/ z] ¹	Γ [PJ] (MW)	η [%]	ρ [%]	Ref.
B_{d_1}	Electricity netw.	$0.65e^{-4}$	0.179 (5.7)	97.5	100	[69]
B_{d_2}	Gas network	$1.00e^{-4}$	0.123 (3.9)	99.9	100	[146]
B_{d_3}	Heat network	$5.50e^{-4}$	0.284 (9.0)	95.0	100	[120]
B_{m_1}	CHP conversion ²	2.73	0.142 (5.0)	90 ³	90	[120]
B_{m_2}	HP conversion ⁴	0.75	0.027 (1.0)	400 ⁵	84.5	[120]
B_{m_3}	P2G conversion ⁶	18	0.397 (18)	55	70	[119]
B_{s_2}	PV supply ⁷	2.56	0.012 (3.0)	-	12.2 ⁸	[147]
B_{s_3}	Wind supply	6.63	0.054 (6.0)	-	28.7 ⁸	[147]
B_{w_1}	Electricity storage	1.12	$2.9e^{-5}$	4.0	100	[148]
B_{w_2}	Gas storage	1.99	0.36	99.8	100	[120]
B_{w_3}	Heat storage	0.8	$1.08e^{-2}$	90	100	[120]

¹ $\forall d : z = \text{meter}$, $\forall m, s, w : z = \text{asset}$ ² Combined Heat and Power; ³ 36% to electricity, 54% to heat; ⁴ Heat Pump; ⁵ Coefficient-of-Performance (COP); ⁶ Power-to-Gas; ⁷ Photovoltaic; ⁸ Capacity factor.

4.3 Case application and assumptions

In the case demonstrated in this thesis, the current situation in Eindhoven and its 2050 climate goal is followed as closely as possible. This requires several general assumptions about all the assets and limitations due to the climate goal (4.2.1), as well as assumptions for each asset specifically, which is elaborated on per asset category (4.2.2-4.2.5). Finally, the resulting case complexity is briefly highlighted in Section 4.2.6.

4.3.1 General

First, the municipality is interested in a future multi-energy systems perspective and wants to include all the energy carriers currently present in the energy infrastructure of the city: electricity (e_1), gas (e_2), and heat (e_3). As mentioned in the previous section, three options per asset category were selected; either based on their current presence in the city, or based on future potential.

Table 4.3: Pathway effect parameter input data

Description	Parameter	Value	Source
Social discount rate	δ	4%	[124]
Policy factor	$\Pi_{s_1 t}$	-2.97%	[141]
Avg. PV CF	$\eta_{s_2}^{CF_{avg}}$	0.122	[149], [150]
Avg. Wind ^{ON} CF	$\eta_{s_3}^{\bar{C}F_{avg}}$	0.243	"
Avg. Wind ^{OFF} CF	$\eta_{s_3}^{CF_{avg}}$	0.330	"
P2G conversion	ϕ_{m_3}	7.9%	[119]
PV supply	ϕ_{s_2}	5%	[151]
Wind supply	ϕ_{s_3}	2.2%	[151]
Electricity storage	ϕ_{w_1}	5%	[152]

To ensure the city meets its climate goal, the existing fossil gas supply is forced to decrease to zero in 2050. Investments can be made in the other, renewable supply options, PV and wind, to decarbonize the energy supply. Note that there are many other renewable energy sources, e.g. geothermal, wave, hydropower, yet these are not (significantly) part of the Dutch energy mix, or not applicable specifically in Eindhoven.

The resulting mathematical sets are defined in Table 4.4. The topology of the city is depicted in Figure 4.4, where the energy systems are projected next to each other. It shows the gas supply locations, and all candidate investments within and across the three networks using dotted lines. To aid interpretation of the figure, only the heat system displays all potential network connections and each other potential asset is depicted only twice. All assets are also displayed with their respective indices. Note that this is merely a static depiction, while the model can invest in assets at each time period.

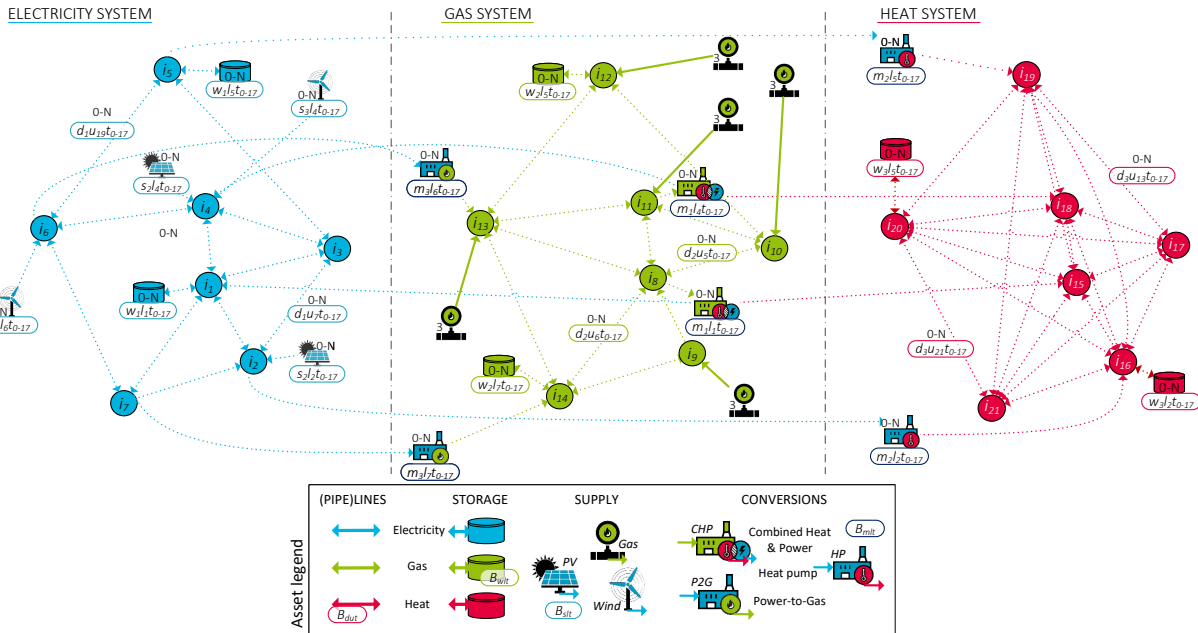


Figure 4.4: Eindhoven topology of its three carrier energy system shaping the 21-node case study - including potential asset investments

Table 4.4: Demonstration cases - set definitions

Set	Math elements	Actual elements
DA	$\{d_1, d_2, d_3\}$	{electricity, gas, and heat (pipe)line}
E	$\{e_1, e_2, e_3\}$	{electricity, gas, and heat (pipe)line}
L	$\{l_1, l_2, \dots, l_7\}$	{City Part 1, ..., City Part 7}
MA	$\{m_1, m_2, m_3\}$	{CHP, HP, P2G}
SA	$\{s_1, s_2, s_3\}$	{gas supply, PV supply, wind supply}
T	$\{t_1, t_2, \dots, t_{17}\}$	{2018, ..., 2050}
U	$\{u_1, u_2, \dots, u_{210}\}$	$ U = V (V - 1)/2$
V	$\{v_1, v_2, \dots, v_{21}\}$	$ V = E L $
WA	$\{w_1, w_2, w_3\}$	{electricity, gas, and heat storage}

Given limited spatial data about existing infrastructure, the case study is modeled as a largely *greenfield* situation. Except for existing gas supply assets, no previous investments have occurred, and only the node locations and the demand development per carrier is known. That means $F_{e,u,0}^{d,max} = M_{e,l,0}^{m,max} = S_{e,l,0}^{s,max} = W_{e,l,0}^{start} = W_{e,l,0}^{w,max} = 0$: no energy transport is yet possible. In other words, the current situation is constructed in the first time period t_0 , which corresponds to 2018. The time periods are modeled annually, with a 2-year time step. From 2018 to 2050, this gives 17 time periods.

Generally, the model assumes all assets can be constructed at each location or on each relevant edge. This can be adjusted using different investment constraints, which can be spatial, economical, or even social/regulatory: some assets might not geographically fit at certain locations, construction is limited by a budget per time period, or certain areas could be exempt from construction due to zoning restrictions (e.g. near schools or playgrounds).

Finally, in this case study, the combined fixed and variable operational costs amounted to less than 5%, and in most cases less than 2.5%, of the capital costs per asset [153] [120]. Including these did not significantly change the model decisions, though it did incur much additional computation time. Hence, only the operational energy and time losses (η and ρ in Table 4.2) were included in the case.

4.3.2 Network assets

The electricity and gas networks are modeled after the MV-network and its medium-pressure gas equivalent. These are the main energy distribution networks at city scale. The technical and economic characteristics were collected from the local distribution system operator [146], [79] and relevant technology providers [154]. No cost or capacity data is known on the geographically limited district heating network currently present in Eindhoven. Hence, the heat network characteristics are retrieved from [120], aligning with an average urban district heating network. From these references, linearized energy network losses are determined which can be found in Table 4.2.

4.3.3 Conversion assets

Three conversion assets are modeled (m_1, m_2, m_3): combined heat and power systems (CHPs), heat pumps (HPs), and power-to-gas systems (P2Gs). This aligns with what is currently present in the city (CHP), and includes the most likely (HP), or highest future potential (P2G) investment options.

In a CHP, gas is used to power a turbine, which generates electricity and simultaneously, the residual heat generated in this process is also extracted [120]. The use of residual heat is what makes their total efficiency much higher than regular gas power plants where only electricity is produced and the generated heat is merely disposed of. A combined efficiency of up to 95% is reached in some instances [64]. In this case, an efficiency of 90% is assumed, with a 36% electrical and a 54% thermal efficiency; modeled after the most common CHPs used in the Netherlands, which are either based on a gas engine or a gas turbine [155].

HPs use a process fluid and electricity to extract thermal energy from a low-temperature source (e.g. air, water, ground or waste heat) and provide heat to a higher temperature sink (and simultaneously refrigerate the heat source). They are widely used to supply heating and cooling for residential, commercial, and industrial applications. The 'efficiency' of this process, which is based on thermodynamic refrigeration cycles, is referred to as a coefficient-of-performance (COP), which is greater than one. In this case the COP is assumed to be 4 [156].

P2Gs are the most novel conversion asset. Many different systems have been tested in labs and pilot settings, which show significant future promise [157]. For this base case, data from an existing system is implemented [119]. This pilot plant first generates hydrogen using a platinum-electrode electrolyser with 70% efficiency. Subsequently, the hydrogen is converted to methane

gas via a methanation process in a bioreactor with 78% efficiency. This leads to a combined efficiency of 55% from power to gas.

Using these conversion efficiencies, the *coupling matrix* can be constructed, which shows the conversion from each energy carrier to the other, and three *carrier specific matrices*, which show the conversion for each carrier via the three conversion assets.

$$\text{Coupling matrix } M = e_2 \begin{pmatrix} e_1 & e_2 & e_3 \\ 1 & 0.4 & 4 \\ 0.36 & 1 & 0.54 \\ e_3 & 0 & 0 & 1 \end{pmatrix}$$

$$\text{Electricity conversion matrix } \sum M_{e_1} = e_2 \begin{pmatrix} m_1 & m_2 & m_3 \\ e_1 & -0 & -1 & -1 \\ +0.36 & +0 & +0 \\ e_3 & +0 & +0 & +0 \end{pmatrix}$$

$$\text{Gas conversion matrix } \sum M_{e_2} = e_2 \begin{pmatrix} m_1 & m_2 & m_3 \\ e_1 & +0 & +0 & +0.4 \\ -1 & -0 & -0 \\ e_3 & +0 & +0 & +0 \end{pmatrix}$$

$$\text{Heat conversion matrix } \sum M_{e_3} = e_2 \begin{pmatrix} m_1 & m_2 & m_3 \\ e_1 & +0 & +4 & +0 \\ +0 & +0 & +0.54 \\ e_3 & -0 & -0 & -0 \end{pmatrix}$$

With these matrices, $\Delta M_{e,l,t}$ from Equations 3.4 and 3.5 can be specified, which is defined as the sum of the following equations:

$$\Delta M_{e_1,l,t} = -M_{e_1,l,t}^{m_2} - M_{e_1,l,t}^{m_3} + 0.36M_{e_2,l,t}^{m_1}, \quad \forall l, t \quad (4.6a)$$

$$\Delta M_{e_2,l,t} = -M_{e_2,l,t}^{m_1} + 0.4M_{e_1,l,t}^{m_3}, \quad \forall l, t \quad (4.6b)$$

$$\Delta M_{e_3,l,t} = 4M_{e_1,l,t}^{m_2} + 0.54M_{e_2,l,t}^{m_1}, \quad \forall l, t \quad (4.6c)$$

4.3.4 Supply assets

One investment constraint applied to this urban case refers to the supply locations and potential imports. Five nodes, 9-13, have access to gas supply (s_1), as these are connected to the national gas grid. PV supply (s_2) can be generated locally and inserted at each electricity node. Similar to gas, wind

supply (s_3) is imported at a limited number of locations (nodes 3, 4, 6, and 7), as this is also where HV-MV transformer stations are located. Given the city's climate ambitions, more constraints are added to the energy supply. Gas supply is forced to decrease as mentioned before, this is implemented using the policy factor $\Pi_{S_1,t}$, which means the variable gas supply $S_{e_2,l,t}$ is limited by a decreasing maximum value $S_{e_2,l,t}^{max}$. No investments can be made in any additional gas supply ($B_{s_1,l,t}^{SA} = 0$), only in the renewable energy sources (RES) producing electricity ($B_{s_2,l,t}^{SA}$ and $B_{s_3,l,t}^{SA}$). The economic data for both the PV and wind assets is from [151]. The capacity of both RES is very modular and were selected to fit an urban scale, with one wind asset being slightly larger than a PV asset in view of its geographical restrictions.

4.3.5 Storage assets

Finally, three storage assets can be constructed, one for each energy carrier. The electricity storage (w_1) or Battery Electric Storage (BES) assets are modeled using data from [158], [151], and [148]. For gas storage (w_2), there are many different options, from salt caverns to depleted oil fields, but their (underground) application potential is very dependent on local geography. However, the gas storage systems in the Netherlands are generally constructed to service much more than just one city [159]. Hence, Dutch data [160] is complemented with international data to determine an asset that could be assumed to operate at an urban setting [161], [162]. Heat storage (w_3) is similar to gas, in the sense that it comes in many different shapes and sizes [120] and is very dependent on geography. To determine average techno-economic characteristics for one asset, Dutch data on heat storage in urban settings is used [160], [163]. Generally, these are underground or aquifer thermal energy storage systems (U/ATES).

Note that despite their differences, all storage assets display both storage and withdrawal (or charging/discharging) losses, as well as standing losses (included in Table 4.2). In long-term investment scenarios with annual time periods, standing losses vary widely per storage asset, which is expected to significantly influence their application potential.

4.3.6 Complexity

The only set that has not yet been defined is I , the set of investments, which is defined as a union of several other sets and elements: $I = DA \cup MA \cup \{s_2, s_3\} \cup WA$. This leads to a total number of 1972 candidate investments. Of these,

there are 1071 potential network assets $B_{d,u,t}$, 357 potential conversion assets $B_{m,l,t}$, 187 potential supply assets $B_{s,l,t}$, and 357 potential storage assets $B_{w,l,t}$. Using a step function for B , larger assets are constructed. In the current case study, $N = 5$ (see Equation 1) for most assets¹, so up to 5 times the standard capacity can be built per location and time period. That means the number of potential solutions is at least $(N + 1)^{1972} = 3.268e + 1534$, underlining the remaining computational challenge even with a spatially limited case.

4.4 Conclusion

This chapter described the extensive, multi-energy urban case study that was constructed for the purpose of this thesis. First, the different data sources for the demand-side, as well as the supply-side were presented. Next followed a description of how this data was applied to the multi-energy framework, including assumptions for each asset category. The chapter ended with a brief highlight of the remaining case complexity and the resulting computational challenge.

With this input the multi-energy exploratory framework 3 can be applied to tackle the three energy transition challenges. The next two chapters discuss these results. Chapter 5 includes two sets of what-if scenarios, varying the climate policy and long-term weather, and tackles the carrier and temporal mismatch. Chapter 6 provides the results for the uncertainty analysis, exploring simultaneous variations in demand development, the social discount rate, and technological development rates and thus handling the underlying deep uncertainty in the energy transition.

¹the RES are more modular; wind assets go up to $N = 15$ and PV up to 30

Chapter 5

Application of the framework to climate policy & weather variation scenarios

5.1 Introduction

The energy transition translates to an energy supply that needs to shift from fossil fuels to mainly renewable energy sources (RES). That also implies a shift to a mainly electric energy supply, because this is the one area where renewable supply is currently cost effective with today's technologies. Yet currently only 25% of the world's energy demand is electric and in the Netherlands it is even lower: just 17% in 2018 [164]. As only 2% of infrastructure is renewed annually [165], this demand might not shift as fast as supply, causing a *carrier mismatch*. Moreover, a dependency on mainly variable and uncertain renewables is a momentous technological challenge. Besides daily and seasonal fluctuations, some renewable energy sources (RES) display significant inter-annual fluctuations [30], up to 30% in high wind areas [166]. If these fluctuations do not occur at the same time as demand fluctuations, a *temporal mismatch* occurs. These first two challenges of the energy transition are addressed in this chapter.

Chapter 3 established the multi-energy optimization framework to help urban decision makers design the energy transition of their city. Chapter 4 framed the urban case study. For the first demonstration of the multi-energy

framework, two distinct sets of *what-if* scenarios were designed as depicted in Figure 5.1: one to generate solutions for the *carrier mismatch* by varying climate policy options (Section 5.2, and another for the *temporal mismatch* by varying weather conditions (Section 5.3). Given the long-term planning perspective of the current investment model, the sets of scenarios are focused on long-term climate policy, and inter-annual weather variations. This chapter ends with a preliminary conclusion on the results of these scenarios (5.4).

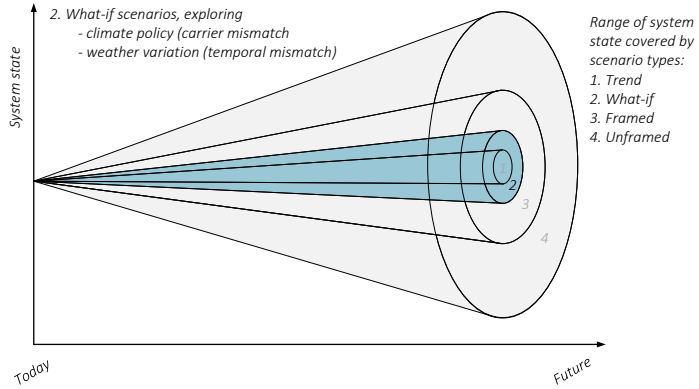


Figure 5.1: What-if scenarios - demonstrating uncertainty in long-term climate policy and inter-annual weather variations, adapted from [96]

5.2 Climate policy scenarios

In the modeled city climate change driven policy targets are in line with the EU goal of a 95% reduction of CO_2 emissions by 2050 [141]. In the case study this translates to a linear reduction of fossil gas supply, which is also in line with Dutch ambitions to phase out fossil gas usage [167]. Yet the corresponding forecast for the demand development of this city shows significant non-electric demand remaining in 2050 (see Section 4.2.1). Indeed, at the end of the time horizon of the urban case study a gas demand still remains, causing a carrier mismatch. In the first set of what-if scenarios, the climate policy is varied around this original climate goal, with some even stricter and some more lenient scenarios. These scenarios are compared to business-as-usual (BAU) Scenario 0, which implements no policy.

In this section, the setup of these eight scenarios is described first (5.2.1), including how this is implemented into the multi-energy framework. Then the main results are discussed in 5.2.2, which includes an in-depth analysis of the scenarios with a linear CO_2 emission reduction to 2050 and then the alternative scenarios. This section ends with a summary of the main findings (5.2.3) for the effects of climate policy variations on the energy transition designs for the city of Eindhoven.

5.2.1 Scenario setup

First, a *business-as-usual* (BAU) scenario (#0) is defined where the gas supply, and thus the CO_2 emissions, do not change at all. The reduction is then gradually increased, all the way to the final scenario (#8), where a 100% emission reduction is required by 2030. Figure 5.2 shows the different scenarios, where Scenario 4 represents the original climate ambition of Eindhoven of a 95% reduction by 2050. Note that the timeline is not linearly represented, even though all scenarios but Scenario 6 adopt a linear reduction. Scenario 6 also ends with a 100% reduction by 2050, like Scenario 5, yet the decline is now shaped parabolically, which allows for a slow start to ease the climate policy adoption; followed by an acceleration in later years. Appendix Section 8.1 provides additional background data for these scenarios.

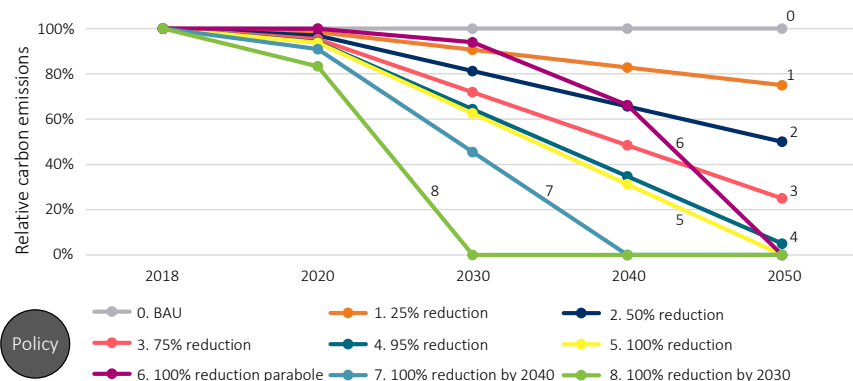


Figure 5.2: Climate policy scenarios 0-8 with relative carbon emissions from 2018 to 2050

The scenario variations are implemented using the external factor σ_t^s , which is used to influence the maximum energy supply of a supply asset (see Con-

straint 3.18). This external factor is defined by a policy factor Π_t^s and the ratio of RES capacity factors $\eta_t^{s,CF}/\eta^{s,CF_{avg}}$ (Constraint 3.19). The climate policy variation is applied via the policy factor Π_t^s , which is translated from a percentage of CO_2 -emissions reduction and causes an increasingly lowered maximum gas supply. As described in Chapter 3 (3.4.2), the optimality gap is set as low as possible, while balancing run time and memory usage. This is achieved by setting the optimality gap to an absolute value of 0.1%, and the run time to 3000 seconds.

5.2.2 Results

The main results for all the climate policy scenarios are found in Table 5.1. This includes the number of investments I , the total installed capacity Γ in petajoules, the total costs in million Euros, and the cost difference of each *carrier mismatch* scenario compared to BAU Scenario 0. A clear upward trend is visible: the more strict the required CO_2 reductions, the higher the total investment costs. In the extreme scenario of a 100% reduction in 2030, the costs more than double.

Figure 5.3 shows this same trend, depicting the additional investment costs (*green*) and additional number of investments per conversion (*purple*), network (*grey*), storage (*yellow*), and supply (*blue*) asset required for each scenario beyond the base level of Scenario 0. The figure shows how a variety of different assets are required in most scenarios, which are discussed below in more detail.

Linear scenarios to 2050

Business-as-usual The results of the BAU scenario nearly equate to the *brown-field* energy infrastructure, which is equal to all the assets required to manage the 'current' energy balance of the modeled city in 2018. This is depicted in Figure 5.4, showing the electricity (*blue*), gas (*green*), and heat (*red*) systems in parallel. All unlabelled assets are constructed in t_0 , or 2018. Only two assets are labelled: two Heat Pump (HP) investments in 2040 (t_{12}) and 2048 (t_{16}), one new asset in node i_{17} (or location 3), and one additional asset in node i_{20} . These are used to meet the slightly increasing heat demand. In terms of network infrastructure, gas networks are highest in number and capacity (~70%), followed by electricity (~20%), and then heat networks (~10%); typical for Dutch cities (if heat networks are present). With regard to conversion assets, mostly Combined Heat and Power assets (CHPs) are required (about 5 PJ), followed by a significant number of Heat Pumps (HPs), which in capacity

Table 5.1: Climate policy results - Main quantitative results per scenario in number of investments I , total installed capacity Γ in PJ, total costs in MEur and cost difference Δ with BAU Scenario 0

#	Climate policy	# of I	Total Γ [PJ]	Total costs [M€]	Cost Δ [%]
0	BAU	210	24.15	582.32	-
1	25% reduction	210	24.15	582.32	-
2	50% "	211	24.28	582.37	0.01
3	75% "	271	26.33	620.30	6.5
4 ^a	95% "	334	28.80	682.76	17.2
5	100% "	328	30.29	700.75	20.3
6	100% " parabole	304	34.89	627.21	7.7
7	100% " by 2040	341	45.72	893.26	53.4
8	100% " by 2030	424	50.12	1286.52	120.9

^aEindhoven climate policy

amount to about 1 PJ. In the figure, these assets are depicted in the system to which they deliver energy, which means CHPs are shown both in the electricity and heat system, and HPs only in the heat system. Given that the BAU scenario has a steady supply of gas, with a diminishing gas demand and remaining electricity and heat demand over the entire time period, constructing a CHP that converts said gas to both electricity and heat is favorable. Several RES are built, both photovoltaics (PV) and wind, to satisfy the remaining electricity demand and to supply the HPs for the remaining heat demand. The geographical spacing of the RES assets closely follows the demand weight of the different locations, with the most assets supplying node i_6 , followed by i_2 and i_7 . No Power-to-Gas (P2G), nor storage assets are required.

25-75% reduction The next two scenarios, with 25 and 50% reduction, do not deviate much from the BAU results. This can be explained from the demand development in the case study. Due to expected energy efficiency implementations and increased electrification, especially the gas demand decreases over time. That gives room for the maximum gas supply to decrease before additional investments are required. Even a 75% CO_2 -emissions reduction only increases the total costs by 6.5%. It is the first scenario to require storage assets, and mostly requires additional conversion and supply assets to manage the energy balance in later time periods.

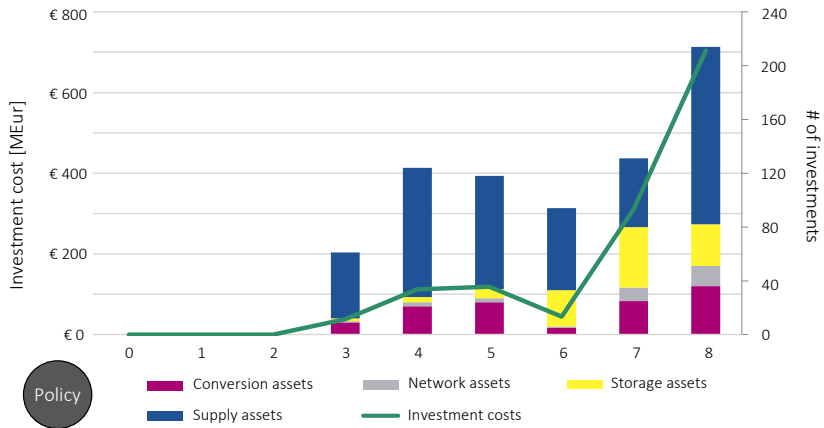


Figure 5.3: Climate policy results - Total investment costs in MEur (green line) and number of investments per asset (stacked bars) for Scenario 1-8 in comparison to Scenario 0

95-100% reduction As the carbon limit moves towards stricter values (Scenarios 4-8), the investment mix changes in a number of ways. There is no longer enough gas supply to generate enough heat through CHPs, so it is generated using electricity through HPs instead. In addition, in the final time periods there is still a gas demand, yet no longer sufficient gas supply. This is where the *carrier mismatch* starts to manifest. To manage the energy balance per carrier and time period, investments in additional wind supply combined with additional gas storage assets are made. To arrive at a 100% linear reduction, a handful of additional conversion assets are required and a lot of additional RES supply assets are constructed. No Power-to-Gas (P2G) assets are required yet, however, that might change beyond 2050.

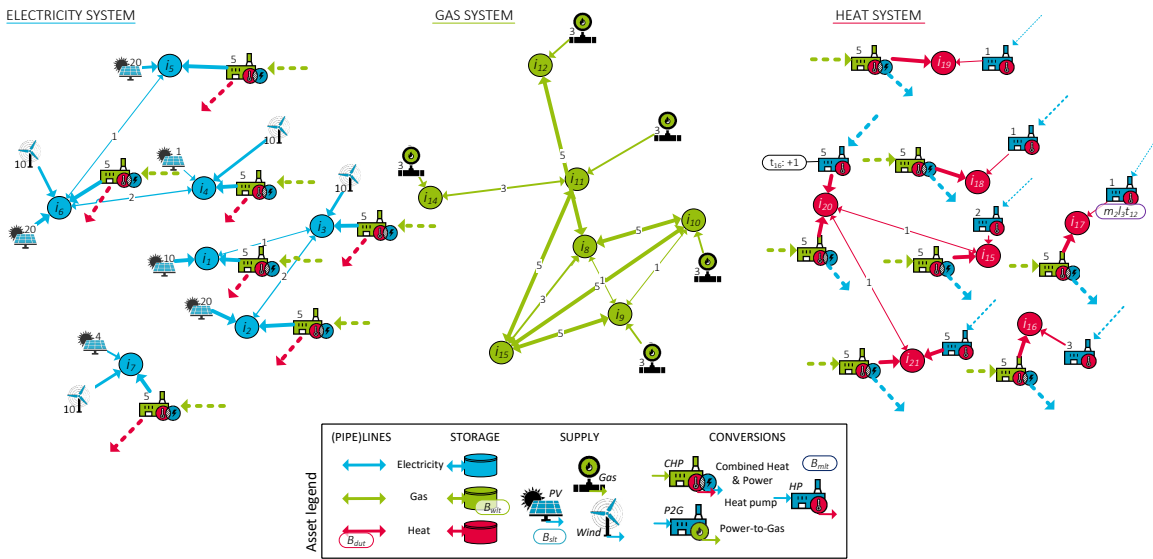


Figure 5.4: Climate policy BAU Scenario 0 - Geographical results showing the assets^a constructed in the electricity, heat, and gas systems in parallel^b

^aConversion assets are depicted only in the receiving system ^bOnly assets constructed after t_0 are labelled

This is shown in more detail in Figure 5.5 for Scenario 4, the main scenario for the modeled city where a 95% CO_2 -reduction is required by 2050. The large stacked bars show the developing energy demand for electricity (blue), gas (green), and heat (red), where especially gas demand is reduced substantially. The overall downward trend results from energy savings as discussed in Chapter 4, Section 4.2.1. The orange line shows the decreasing maximum gas supply, and the yellow line shows the increasing, renewable electricity supply. Four lines with markers show how much electricity (dark blue) and gas (dark green) is used for conversion, and how much heat (purple) and electricity (light blue) that results in. This confirms the switch from CHP conversion to HP conversion. Finally, two columns show how gas is stored (brown) and then extracted (coral) in alternating waves. All the remaining gas in storage is extracted in 2050, which is due to the artificial end of the optimization by 2050 and causes what is called a *boundary effect* [168]¹.

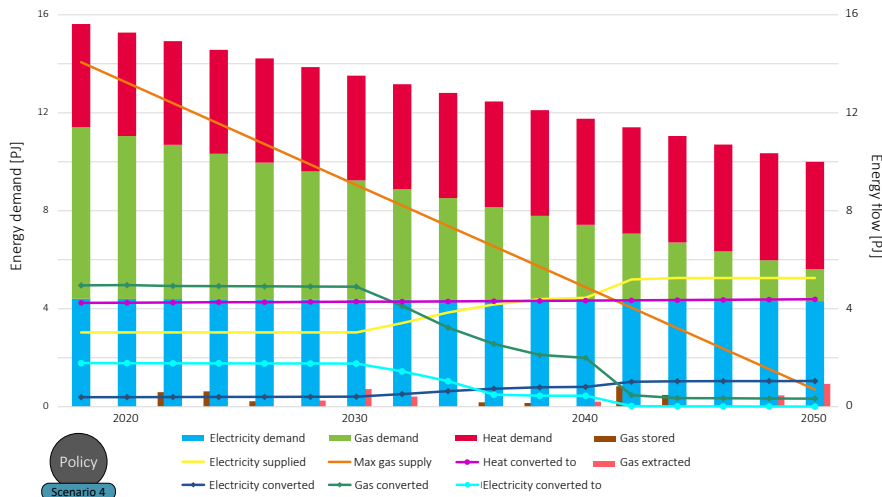


Figure 5.5: Climate policy Scenario 4 - Energy demand (stacked bars), supply, conversion from and to (lines), and storage (columns) in PJ from 2018 to 2050

¹If the optimization model is allowed to run up to 2060, while reducing gas demand in the same linear fashion (which means it reaches zero by 2058), a handful of additional gas storage assets and one P2G asset are constructed to ensure any remaining gas demand is met. Besides using more gas via storage, it is also extracted at a slightly slower pace than in Scenario 4.

Alternative scenarios

Parabolic policy An interesting result to highlight is shown in Scenario 6, or the parabolic pathway to 100% CO_2 -reduction, which is depicted in Figure 5.6. The orange line of the maximum gas supply is shaped parabolically, instead of linearly to zero. This means its maximum level of gas supply in 2040 is at the same level as the 50% reduction scenario, before dropping to zero in 2050. That means most investments to manage the carrier mismatch can be concentrated in the last decade, when they are at their lowest cost. As a result, Scenario 6 is almost as cheap as the 75% reduction Scenario 3.

The ability to postpone certain expensive investments is highly beneficial from an economic point of view. This is driven by the *techno-economic effects* the model accounts for. First of all, future investments are discounted using the social discount factor δ , which is 4%. Hence, the further into the future, the higher the discounted investment values. This effect is especially beneficial to make relatively expensive technologies more cost-competitive; like long-term gas storage. Second, different assets are assigned different technological development rates (ϕ_x), which compounds upon the interest rate. This effect is notably beneficial for Power-to-gas (P2G) conversion investments, as this technology is very expensive initially, yet is expected to make significant development steps ($\phi_{m_3} = 7.9\%$ [119]). Specifically for the RES investments, PV supply has a much higher ϕ_x than wind (5% vs 2.2% [151]), making it more favorable in the final time periods. While most other scenarios favor wind supply investments, Scenario 6 favors PV supply.

However, the economic advantage does come at a different sort of 'cost', namely an increase in total CO_2 emissions. Given that the gas supply remains higher throughout the time frame, the cumulative carbon emissions are much higher than in Scenarios 4 and 5. In fact, they are at the same level as for Scenario 2, which only reaches a 50% reduction of CO_2 emissions by 2050. Since the consequences for the global temperature rise largely depend on the total greenhouse gases emitted [169], this Scenario might not be as favorable after all. In fact, when it comes to the overall goal of the city of Eindhoven, this scenario technically does not meet a 100% reduction of CO_2 -emissions (or even 95%). Although the fossil gas supply is reduced to zero by 2050 (orange line in Figure 5.6), from 2032-2040 its excess is injected into gas storage (brown bars), and extracted from 2046-2050 (coral bars). That extraction is simply postponed use of fossil gas and actually amounts to almost half of the remaining energy demand in 2050.

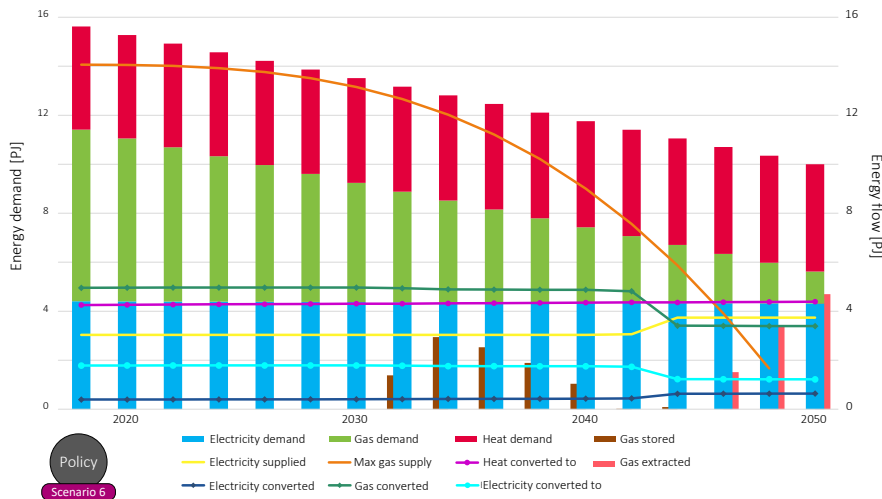


Figure 5.6: Climate policy Scenario 6 - Energy demand (stacked bars), supply, conversion from and to (lines), and storage (columns) in PJ from 2018 to 2050

Accelerated policy The final two scenarios 7 and 8 show the consequences of considerable policy acceleration, and provide a glimpse of what could happen in the other scenarios after 2050. The total investment costs increase immensely, by 53% and 120%, as much of the gas demand needs to be met through alternative routes: either via additional gas storage, or by additional RES supply and P2G conversion, or both. All of these assets are still very expensive so early in the planning period. Scenario 7 requires one P2G asset, Scenario 8 requires 12 of them. Even in these extreme scenarios, heat storage is never required as there are many cheaper conversion options to generate heat within a time period. Electricity storage is also not considered, as annual standing losses for electricity storage assets are very high. This makes it much less cost-efficient to use than other balancing options from the inter-annual perspective. Although these scenarios require much higher investments, their cumulative CO_2 emissions are 46% and 68% lower than Scenario 0, and actually 30% and 59% lower than Scenario 4, which is a significant acceleration of the energy transition.

5.2.3 Main findings

Overall, although the BAU scenario is the least costly, it is interesting to note that significant carbon emission reductions can be achieved with little cost increase. A 75% reduction is just 6.5% more expensive. The city's target of 95% CO_2 -emissions reduction induces 17.2% additional costs. And if the municipality decides to implement a parabolic reduction target, they can achieve a 100% reduction in 2050 for just a 7.7% increase in investments. However, this causes significantly more cumulative CO_2 -emissions and is not entirely carbon neutral. If they adopt a linear approach to a 100% reduction, it would cost 20.3% extra by 2050, but this would guarantee a carbon neutral solution. Yet if the climate goals are required to become even more stringent, investment costs increase exponentially: with 53.4% and even 120.9% if the 100% target needs to be achieved by 2040 or 2030 respectively.

The main question that these results raise is whether these demand projections will actually come to pass. If the demand for gas does not decrease as significantly as it does in these scenarios, the carrier mismatch is even higher and the investment costs are bound to increase. This is illustrated by the final two scenarios and in the substantial difference between the parabolic scenario and the linear scenarios. Since demand development is one of the main uncertainties in nearly all energy models, it warrants further analysis. Additionally, the development of both economic and technological characteristics, especially on such long time scales, are also very uncertain. And both can significantly impact the results. If certain technologies develop or are discounted differently, the trade-offs between different investments can shift. Finally, instead of a top-down climate policy a (range of time-dependent) policy-driven carbon tax(es) could be employed, altering the costs of using fossil fuels and thus changing optimal energy transition designs.

5.3 Weather variation scenarios

Large amounts of implemented RES lead to a supply-driven energy system, with a varying energy supply dependent on weather conditions. If the variable supply is high due to favorable weather conditions, while demand is low, or vice versa due to unfavorable weather, temporal mismatches can occur. The second, different set of 8 what-if scenarios portrays these effects, all comparing to a 'steady weather' Scenario 0. Half of the scenarios use inter-annual variations of historical weather amplitude, and the other half use variations of the average capacity factors of photovoltaic (PV) and wind supply.

This section also starts with a description of the different scenarios (5.3.1), including the implementation into the multi-energy framework. The results (5.3.2) are organized in two categories: historical amplitude and capacity factor variations. Following that, the main findings for the inter-annual weather variations are given 5.3.3.

5.3.1 Scenario setup

To find solutions for the long-term temporal mismatch, the investment model is tested on eight different weather scenarios, where all scenarios follow the same 95% reduction of CO_2 emissions. The increased implementation of variable RES causes a more supply-driven system and makes the energy system more sensitive to temporal mismatches. The resulting designs are compared to the base scenario (#0), which displays no inter-annual variation in weather, making it equal to Climate policy Scenario 4 (Section 5.2.1).

The weather scenarios are based on historical weather data from the Netherlands, from 1980-2018, derived from [149], [150] (see also Table 8.2 in the Appendix). These data show average capacity factors for PV and wind energy, the latter for both on- and offshore. Currently, capacity for offshore wind amounts to 30% of total wind capacity [170]; yet the Dutch government aims for offshore wind to provide far more than 50% of all renewable electricity supply by 2030 [171]. Given these structural uncertainties, the main weather scenarios use a 50/50 combination of on- and offshore so as not to make a specific distinction, and to allow for comparison of scenarios using solely on- or offshore wind (Scenarios 7-8).

Figure 5.7 shows the different scenarios and the effects on the relative capacity factors for the PV supply (top half) and wind supply (bottom half) from 2018 to 2050. The Appendix contains the two tables forming the basis of this figure, showing the relative capacity factors for PV (Table 8.3) and wind (Table 8.4) for all eight scenarios. Scenario 1 (*coral*) depicts the historical weather and forms the basis of all the other weather variations. In Scenarios 2-4, the amplitude of the average capacity factors for both PV and wind is varied by multiplying them with 0.5, 1.5, and 3 (*cyan, yellow, and light blue*). This is used to display a wide range of potential inter-annual weather variability impacting both solar [172] and wind energy [173]. The lowest and highest amplitudes are not as likely, but are a way of testing the multi-energy framework and showing the effect of best and worst cases on the energy system design.

Scenarios 5-8 vary by the absolute capacity factors in different combinations. First, both PV and wind are varied by - and + 50% (*green, and dark*

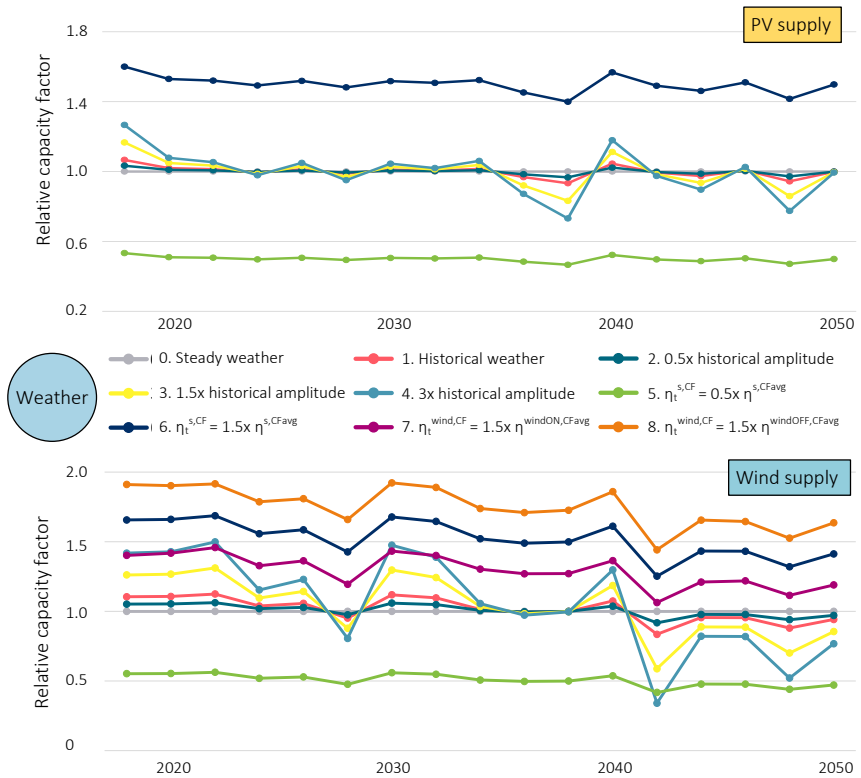


Figure 5.7: Weather variation scenarios 0-8 with relative capacity factors for PV^a and Wind supply from 2018 to 2050

^a N.B. In Scenarios 7 and 8 the PV capacity factor is equal to Scenario 1

blue). Although a 50% lower output for both RES is highly unlikely, it is another way to test the energy transition design on a worst case scenario. A 50% higher output could be more likely, because of technological advances, or better site selection with a higher energy potential, and again is a good test of the design. For the final two scenarios, only the output of wind supply is varied. First, it is assumed that all supply is onshore and again 50% higher (purple), then again for only offshore wind supply (orange). Combined, these scenarios represent weather variation in different areas, from (extremely) cloudy/calm to (extremely) sunny/windy areas.

These scenario variations are also implemented using the external factor

σ_t^s , yet this time using the average and the varying capacity factors, $\eta^{s,CF_{avg}}$ and $\eta_t^{s,CF}$ respectively. The average capacity factors are given in Table 8.2 (Appendix 8.1), using the varying capacity factor as described above, relative capacity factors are calculated and used in the model (Tables 8.3 and 8.4). While the climate policy scenarios only limited the supply of gas, the varying capacity factor can both increase and decrease the average RES supply depending on the weather conditions. As before, the optimality gap is set to 0.1% with a 3000s run time for each scenario. Other relevant settings, values, and code can be found in the Appendix ??.

5.3.2 Results

The main results are shown in Table ??, for each scenario including the total number of investments I , the total installed capacity Γ in petajoules, the total costs in million Euros, and the cost difference compared to the base Scenario 0. This base scenario is modeled with a 95% CO_2 -reduction and no inter-annual weather variations, which is equal to Climate policy Scenario 4. These results are quite different from the climate policy variations, showing much more fluctuations especially in the number of investments and the costs. In addition, nearly all scenarios are less costly than the base scenario, Scenario 8 by more than 40%. Yet Scenario 5 is almost 70% more expensive. Both highlight the significant impact of inter-annual weather fluctuations.

Figure 5.8 visualizes these results by showing the difference in the total investment costs and in the cumulative number of investments per asset for each weather variation scenario compared to Scenario 0. This figure emphasizes the intricacies of modeling a multi-energy system with a range of assets, while including pathway effects like long-term weather variations. For the last four scenarios, the results are straightforward: scenarios requiring more assets are more expensive than the base scenario, and those requiring less assets are less expensive. Yet all of the first four scenarios require extra assets, while incurring *less* costs than the base scenario. More details about these results per scenario are provided next.

Amplitude variations

Historical weather In Scenario 1, historical weather variation is included and this leads to 42 additional asset investments, including 0.51 PJ more HPs, 0.37 PJ more RES, and 0.36 PJ more network assets. Counter-intuitively, the total investment costs are lowered, as this scenario requires less investments in earlier time periods and adds all its additional investments in later time

Table 5.2: Weather variation results - Main quantitative results per climate policy scenario in number of investments I , total installed capacity Γ in PJ, total costs in MEur and cost difference Δ with Scenario 0

#	Weather scenario	# of I	Total Γ [PJ]	Total costs [M€]	Cost Δ [%]
0 ^a	Steady	334	28.80	682.76	-
1	Historical	376	30.03	652.41	-4.4
2	0.5x hist. ampl. ^b	353	28.97	665.88	-2.5
3	1.5x hist. ampl.	410	31.79	608.18	-10.9
4	3x hist. ampl.	439	35.70	604.88	-11.4
5	0.5x $\eta_t^{s,CF_{avg}}$	542	37.38	1,159.07	69.8
6	1.5x $\eta_t^{s,CF_{avg}}$	260	27.20	440.94	-35.4
7 ^c	1.5x $\eta_t^{s_{3a},CF_{avg}}$	216	30.23	501.84	-26.5
8 ^d	1.5x $\eta_t^{s_{3b},CF_{avg}}$	178	24.98	402.19	-41.1

^aEindhoven climate policy

^bhistorical amplitude

^c s_{3a} = onshore

^d s_{3b} = offshore

periods, once capital costs have declined. This is possible because especially the wind resource benefits from a higher capacity factor in the earlier time periods, leading the earlier RES investments to provide higher outputs. The first time period with a relatively lower capacity factor, or a 'bad weather' year, is in 2028. At that point, the combined techno-economic effects of the social discount factor and the technological development rates for PV and wind supply cause the investment costs to be lower. In other words, Scenario 1 is able to benefit more from good weather years than that it is hindered by bad weather years.

0.5-3x amplitude In Scenarios 2-4, where the amplitude of historical weather variations (Scenario 1) is varied, there is a slight upward trend compared to Scenario 0 in the number of investments. Yet again, none of the scenarios incur higher total investment cost. Scenario 4 is especially striking, even though it invests in almost 25% more asset capacity spread across conversion, storage, and supply, it is 11.4% cheaper than Scenario 0. Although the supply output after 2040 is relatively low for both PV and wind, investments are much less expensive. Figure 5.9 shows specific results for Scenario 4, where the extreme amplitude variation of the PV and wind capacity factors is clearly visible in the

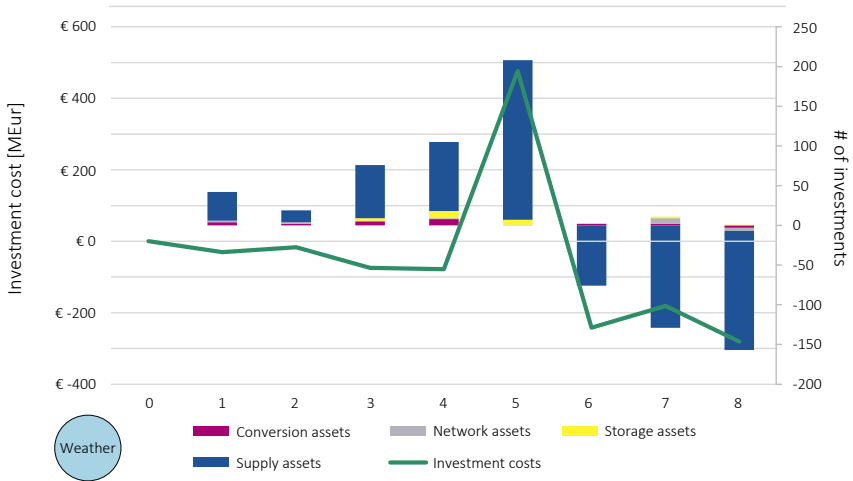


Figure 5.8: Weather variation results - Total investment costs in MEur (green line) and number of investments per asset (stacked bars) for Scenario 1-8 in comparison to Scenario 0

variation of the electricity supplied. Compared to the Climate policy scenarios (Figures 5.5 and 5.6), much more response is shown to solve the mismatch between supply and demand.

Capacity factor variations

In the second set of scenarios (5-8), the results are even more pronounced. If the overall output of the RES supply is lower (Scenario 5), the required investments in renewable supply are much higher, and vice versa (Scenarios 6-8).

Lower capacity factor Scenario 5 is almost 70% more expensive than the steady weather Scenario 0. Most additional investments are required in the RES supply, followed by the number of storage assets. In terms of energy capacity, both more than double. The storage assets particularly influence the total investment cost, as these are required in the beginning of the time frame, limiting any future year discounting or cost decreases. The reason these storage assets are required so early, is due to the first 'bad weather' year in 2028 as mentioned before. At that point, the gas stored in the first time periods is

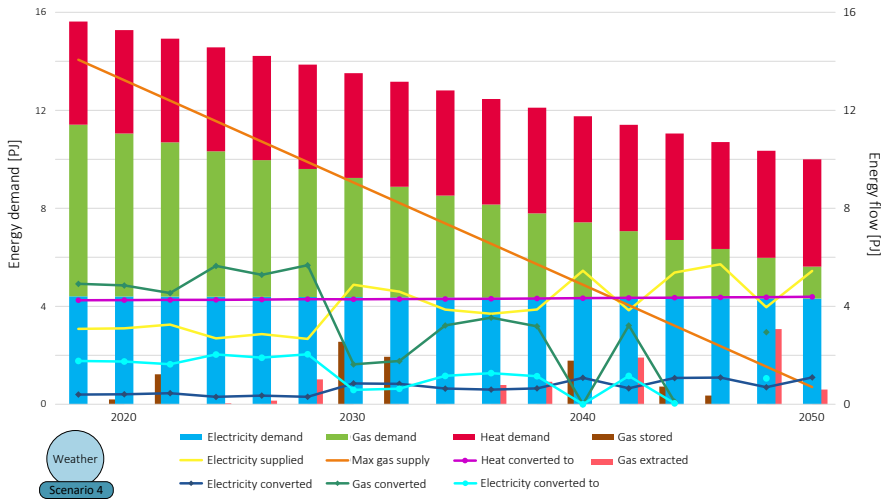


Figure 5.9: Weather variation Scenario 4 - Energy demand (stacked bars), supply, conversion from and to (lines), and storage (columns) in PJ from 2018 to 2050

extracted steadily, to help run the CHPs at a higher rate to generate enough heat and electricity. As the RES supply picks up through later time periods and the gas supply is steadily decreased, the CHPs are replaced by the use of HPs. Yet even in the final time periods, stored gas is extracted again to use in the CHPs and balance against lower RES outputs. The use of these conversion units to balance the ongoing temporal mismatches is depicted in Figure 5.10. This compares the use of CHP and HP conversion for Weather Scenario 0 and Scenario 5, the latter showing much more volatility, accentuating the importance of incorporating inter-annual weather variations.

Higher capacity factor The last three scenarios highlight three different results: the consequence of better site location of renewables, the inclusion of more (or less) sunny weather, and the difference between on- and offshore wind patterns.

First, the total costs in all three scenarios are significantly lower than the steady weather scenario, as well as the amplitude varying scenarios (see both Figure 5.8 and Table ??). This confirms the value of locating renewable assets at areas with high energy potential, causing the RES provide a higher total energy supply. Given that only the capacity factors are increased, and the

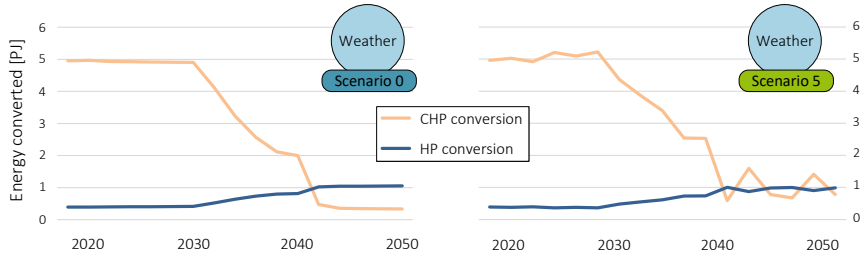


Figure 5.10: Weather variation Scenario 0 compared to Scenario 5 - use of Combined Heat and Power (CHP) and Heat Pump (HP) conversion in PJ from 2018 to 2050

amplitude remains the same, the inter-annual weather variations are not as significant as in Scenarios 3 and 4. This means much less response is required to solve any mismatches between supply and demand. Figure 5.11 shows the results for Scenario 8, which depicts steadier behavior than compared to Scenario 4 in Figure 5.9. Although Scenarios 6-8 also require significantly less investments, in terms of invested asset capacity, the scenarios are within 10% of Scenario 0.

In Scenario 6, the capacity factor of both wind and PV supply are increased, whereas the last two scenarios only increase the capacity factor of the wind supply. Since PV supply has no spatial restrictions, it can be supplied more directly where demand arises and thus Scenario 6 prefers PV investments. Hence, less network assets are required in this scenario. At an inter-annual level, PV also displays less overall variation than wind, reducing the need for long-term storage assets. Contrarily, in the last two scenarios the higher output for wind tips the investment balance in its favor, leading to zero PV supply investments.

Finally, the difference between the last two scenarios is also quite interesting. If the wind supply is strictly offshore, especially in windy conditions (i.e. with an increased capacity factor), the actual supply is much higher, requiring less RES assets than if the wind supply is strictly onshore; causing a 20% cost difference. Though it should be noted that the current scenarios do not incorporate transportation losses in national grids, which would increase with an offshore wind supply. Yet the difference is such that the attractiveness of an offshore wind supply in general can be confirmed, as it generally has a much higher annual capacity factor than onshore wind [150].

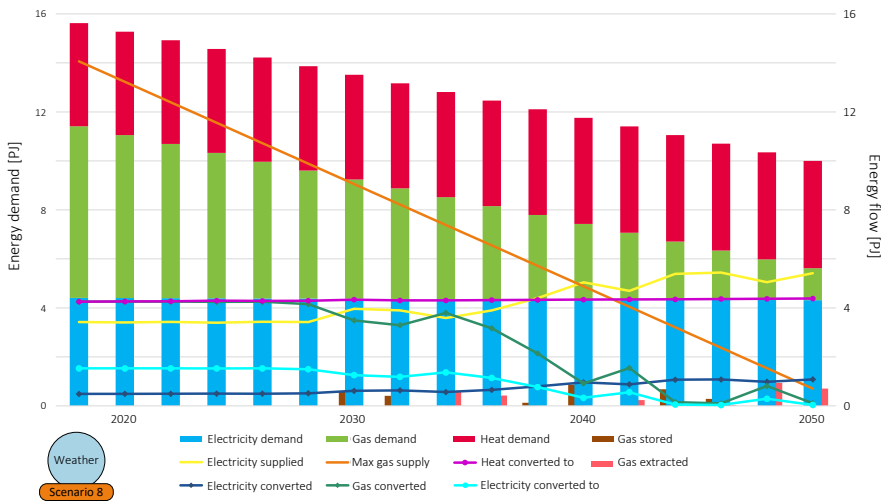


Figure 5.11: Weather variation Scenario 8 - Energy demand (stacked bars), supply, conversion from and to (lines), and storage (columns) in PJ from 2018 to 2050

5.3.3 Main findings

In these scenarios, the main fluctuations are created in the RES supply, causing some similar and some differing effects. Nearly all scenarios show a significant response in the number of supply assets constructed. A portion of the scenarios require an increase in supply assets to balance amplitude variations, while other scenarios are able to decrease investments when the supply per asset is higher. Yet additional investments do not necessarily mean a higher total investment cost: a threefold increase of the amplitude of historical weather requires 31% more assets compared to steady weather, yet a 11% lower investment cost. This is due to the techno-economic effects, which cause a lower cost level for investments in later time periods. The most striking scenario is #5, which is nearly 70% more expensive than Scenario 0. This scenario underlines the importance of locating renewable energy sources (RES) in areas with a high supply potential. The last three scenarios confirm this finding, showing how the total design costs can be up to 41% lower if the RES supply is relatively higher. This also confirms the value of investing in further technological innovations beyond mere cost reductions, to make the RES assets more efficient and as such increase their capacity factors endogenously. These fluctua-

tions also highlight the value of incorporating inter-annual weather variations in long-term planning models.

Compared to the policy variation scenarios, the weather variations generate substantially different results. Most of the fluctuations in asset investments are found in the RES supply, while the policy variations create much more variation in all types of assets. For example, none of the weather scenarios invest in P2G assets. Although the temporal mismatch results in significant investment fluctuations, there is no carrier mismatch and thus no requirement for an alternative source for gas. In addition, the response in the use of the different assets is much more volatile for the weather scenarios. To ensure system reliability heat- and gas-related conversion and storage assets respond to the variable electric supply, confirming the potential of a multi-energy system to absorb these fluctuations. This is most visible in the lines of Figure 5.9, and the comparison of Figure 5.10 (recall that Weather Scenario 0 is equal to Climate Policy Scenario 4). These fluctuations are in fact a clear response to the timing of the inter-annual weather variations (the long-term *temporal mismatch*). Consequently, many scenarios profited from relatively higher capacity factors in early time periods, while the actual capacity factors could turn out quite differently.

5.4 Conclusion

The results presented in this chapter show how the multi-energy framework could provide solutions for the first two challenges of the energy transition: the carrier mismatch and the temporal mismatch. The carrier mismatch relates to the difference in the type of energy carrier supplied and demanded, while the temporal mismatch is defined as the difference in timing between energy supply and demand. The effects of policy and weather variations and the resulting mismatches on the multi-energy transition design for the city of Eindhoven were analyzed. For both challenges, 8 different sets of widely ranging what-if scenarios were used to test the multi-energy framework.

First, both sets of scenarios show very divergent, sometimes drastically different results, yet every time the multi-energy optimization framework is able to provide energy transition designs capable of handling the demand and supply mismatches. Even for the most extreme the scenarios, the framework can ensure demand is met and climate goals are reached.

In short, the multi-energy optimization framework is able to design a logical transition pathway for a wide range of scenarios. An increasingly strict climate policy results in increasing investment cost, while reducing cumulative

CO_2 -emissions. With a notable exception being the parabolic climate policy, which is able to benefit more from techno-economic effects, yet induces much more carbon emissions. Inter-annual weather variations created more varied results, showing both more costly, and cheaper scenarios, depending on the supply potential of the renewable assets. Especially closer to 2050, several years of lower RES output required more response from the conversion assets to manage the temporal mismatch. These results underline the value of including inter-annual weather variations in long-term planning models with renewable energy supply [29], [28].

The results of these what-if scenarios provide valuable insights for urban decision makers and for future research. Yet the same time, given the widely different results, it becomes evident that a combination of different parameter variations can create a more fundamental understanding of potential energy transition futures. Chapter 6 shows the results for simultaneous parameter variations, addressing the final challenge of deep uncertainty present in long-term planning of energy transition designs.

Chapter 6

Application of the framework to deep uncertainty

6.1 Introduction

In the previous chapter (5) the first results are presented, demonstrating solutions to the first two challenges of the energy transition (carrier and temporal mismatch). Yet future projections of the energy system are deeply uncertain, which is represented in Figure 6.1 by the *unframed* system state. This uncertainty should be incorporated into energy planning models, and forms the final energy transition challenge of this thesis. In Section 3.3, the approach to an appropriate uncertainty analysis is defined, incorporating multiple uncertainties simultaneously. Given the complex nature of the multi-energy framework, an exploratory modeling methodology is selected. To fully demonstrate the multi-energy framework, this approach is tested on the same case study of the city of Eindhoven presented in Chapter 4.

The exploratory modeling methodology was visualized previously, and it is repeated here as it forms the core structure of the current chapter (see Figure 6.2). First, the uncertain parameters are selected, including demand development D , the social discount rate δ , and relevant technological development rates ϕ_x , and their range and distribution are characterized. To systematically explore the multi-dimensional range of parameters with the least amount of bias, 800 samples are generated from each of these parameters using Latin Hypercube Sampling (LHS) (6.2). Together these combine into 800 experiments. A brief description of the experimental setup is given in Section 6.3,

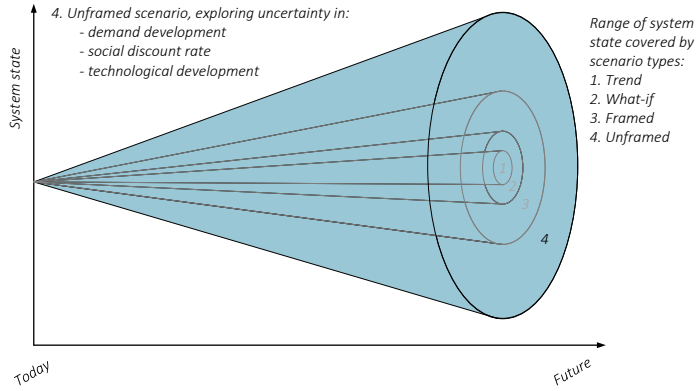


Figure 6.1: Unframed scenario - exploring uncertainty in demand development, social discount rate and technological development simultaneously, adapted from [96]

which describes how the optimization model is applied.

Section 6.4 presents the results of the influence of the combined uncertainty of demand projections and techno-economic parameters on the optimal energy transition design for the city of Eindhoven. To distinguish investment patterns and relate these to the underlying uncertainties, a combination of data processing techniques is used. The results are analyzed and compared to the result of the municipality's base case from different angles to find valuable insights for the municipality's decision makers, providing an additional demonstration of the multi-energy framework, and tackling the final energy transition challenge of deep uncertainty. This section ends with a reflection on the implications of the exploratory results, on the influence of uncertainty on the results, and on how this information can be used by decision makers. Finally, Section 6.5 provides the conclusions of this chapter.

6.2 Uncertainty characterization and sampling

Several parameters are specific to the city case study and hence not subject to parametric uncertainty, including the climate policy Π , the asset capital and operational costs C and O , and asset capacities Γ and efficiencies η . However, variations on climate policy were still tested before (Section 5.2), as were

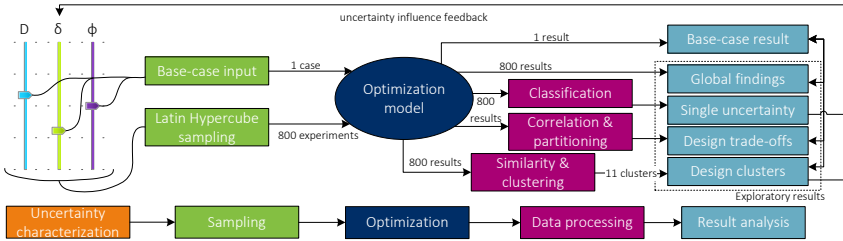


Figure 6.2: Exploratory modeling methodology visualisation, including demand development D , social discount rate δ , and technological development rates ϕ_x

inter-annual weather variations (Section 5.3). From the remaining parameters three major long-term uncertainties are selected: energy demand development $D_{e,l,t}$, the social discount rate δ and the technological development rates ϕ_x . These parameters are discussed in the next subsections, including their general or specific case relevance, the ranges that are used and how everything is translated into the 800 samples used for the experiments as specified in Chapter 3, Section 3.3.

6.2.1 Energy demand

Energy demand development is heavily influenced by energy efficiency developments, GDP per capita, policy instruments such as taxes, and population development [126]. Given the highly uncertain energy transition, simply describing energy demand development by extrapolating and manipulating present-day demand data is inadequate [174]. Instead, different demand development time-series were defined using on three factors:

- **Total demand in 2050** - depends on the combined effect of population growth and the implementation of energy efficiency solutions;
- **Energy demand mix in 2050** - relates to the phase-out speed of (fossil) gas reliance towards increased renewable electricity and/or heat reliance;
- **Demand development curve** - connects to the implementation pace of climate and energy policy targets due to societal and/or political pressure.

This resulted in 12 demand development time-series, which are displayed in Table 6.1 with their total demand value in PJ, the demand mix in 2050, and the

shape of their demand curve from 2018 to 2050. The first row (#0) shows the values for the current situation in 2018. The second row (#1) is the timeseries for the base case of the municipality. The first few series (#2-5) explore a different total demand in 2050, both + 50% and + 25% compared to the 10 PJ base value. Series #6-9 implement different demand ratios, modeling a higher demand of each energy carrier and one extreme case (#9). The final three series #10-12 follow different demand curves besides the linear curve in the base case: an 'Exponential' curve with delayed efficiency implementations, an 'S-shaped' curve with accelerated change, and a 'Constant' curve, which means no change occurred.

Given the high level of uncertainty on future demand development, each scenario is treated as equally likely in the Latin Hypercube Sampling (LHS) setup (Section 3.3.2). So each demand scenario is applied 800/12 times, or approximately 67 times. A graphical overview of the sample distribution of the demand scenarios across the 800 experiments is given in Figure 6.3. Appendix Section 8.2 provides additional background data for these scenarios.

Table 6.1: Uncertainty ranges for 12 demand development time-series compared to the current situation, including final demand value D , demand mix, and curve

#	Description	D [PJ]	Demand mix [e_1 e_2 e_3] ^a	Demand curve
0	Current situation	15.63 ^b	28% 45% 27%	N\A
1	Base case	10 ^c	43% 13% 44%	Linear
2	VH ^d demand	15	43% 13% 44%	Linear
3	VL ^e demand	5	43% 13% 44%	Linear
4	High demand	12.5	43% 13% 44%	Linear
5	Low demand	7.5	43% 13% 44%	Linear
6	H e_1 L e_2 L e_3	10	54% 11% 35%	Linear
7	L e_1 L e_2 H e_3	10	35% 11% 55%	Linear
8	L e_1 H e_2 L e_3	10	33% 34% 33%	Linear
9	VL e_1 VH e_2 VL e_3	10	27% 45% 28%	Linear
10	Fast change	10	43% 13% 44%	Exponential
11	Very fast change	10	43% 13% 44%	S-shaped
12	No change	15.63	28% 45% 27%	Constant

^a electricity, gas, heat

^b $t_0 = 2018$

^c $t_{16} = 2050$

^d Very High

^e Very Low

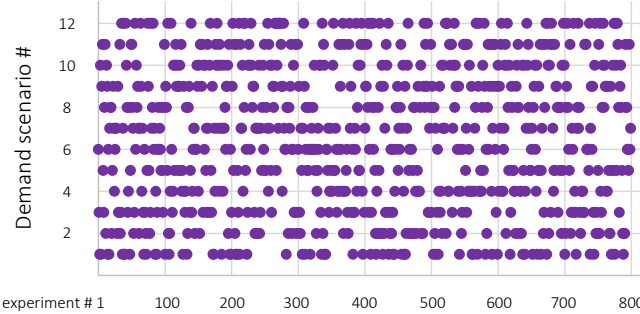


Figure 6.3: Samples for all 800 experiments for each demand scenario

6.2.2 Social discount rate

The social discount rate, δ in Equations 3.9-3.12, is used to put a present value on costs and benefits that occur in the future, specifically for social projects or societal investments. The choice of discount rates has a significant impact on the evaluation of climate (policy) options [175]. Generally, discount rates used by EU Member States' government agencies as well as in energy scenarios range between 1% and 7%, as there is a consensus of using declining risk-free discount rates over a long time horizon to describe the social perspective [124]. Yet, many different values have been used in energy system modeling, as some use an individual (investor or consumer) perspective to evaluate. That generally leads to much higher values, up to 15%, as this is based on what rates of discount individuals actually apply in their day-to-day decisions [102]. Although this thesis applies a social perspective, aiming to minimize the required societal investments to manage the energy transition, to analyze a broad enough range of uncertainties the total range for the social discount rate is set from 1 to 15% (see also Table 6.2).

Given that this entire range is possible in energy system modeling, the social discount rate parameter is inserted into the LHS setup with a uniform probability distribution (see Figure 6.4). Across the 800 experiments, differing values of δ are selected to explore the entire parameter range.

6.2.3 Technological development rate

The technological development rate ϕ is captured as a specific development parameter per asset. This allows the development curve of novel technologies,

Table 6.2: Uncertainty ranges for social discount and technological development rates

Description	Parameter	Base case	Range	Source
Social discount rate	δ	4%	1-15%	[124]
P2G conversion	ϕ_{m_3}	7.9%	$\pm 50\%$	[119]
PV supply	ϕ_{s_2}	5%	$\pm 50\%$	[151]
Wind supply	ϕ_{s_3}	2.2%	$\pm 50\%$	[151]
Electricity storage	ϕ_{w_1}	5%	$\pm 50\%$	[152]

so-called *learning curves* [176], to be incorporated. Assets that are expensive today, can become competitive in the future, as experience with the technology increases. E.g. photovoltaic and wind energy systems saw cost decreases of more than 80% and 50% respectively over the last 10 years [151]. Given such significant developments, these effects are very important to capture in long-term models [177]. However, the actual rates of development are also very uncertain, depending on many factors, from straightforward R&D investments due to economic potential, to unpredictable political drive and social acceptance [125]. Following the example of [178], a range of minus-plus 50% of the estimated base value is assumed as the uncertainty range for the development rates.

To focus on the technologies with the most potential for impactful changes in development rate, only the development rates of assets with a base value larger than 2% are included in the analysis. This threshold is selected because it is assumed that technology units with a faster predicted future development have a higher probability of deviations from this presumed development rate, and thus more uncertainty. Consequently, the development rates for the following technology units are endogenously considered (Table 6.2): P2G conversion ϕ_{m_3} [119], PV supply ϕ_{s_2} [179], wind supply ϕ_{s_3} [151], and electricity storage ϕ_{w_1} [152].

No data is available on the probability density of any of these parameters, as such, the whole range of each uncertain technology development rate is treated as equally likely in the LHS setup. The resulting sample values of the uniform distributions across the 800 experiments are depicted in Figure 6.4. The brackets indicate the range of each distribution. Since PV supply and electricity storage have the same techno-economic development rate, their brackets overlap. Essentially, this is a visual representation of Table 6.2.

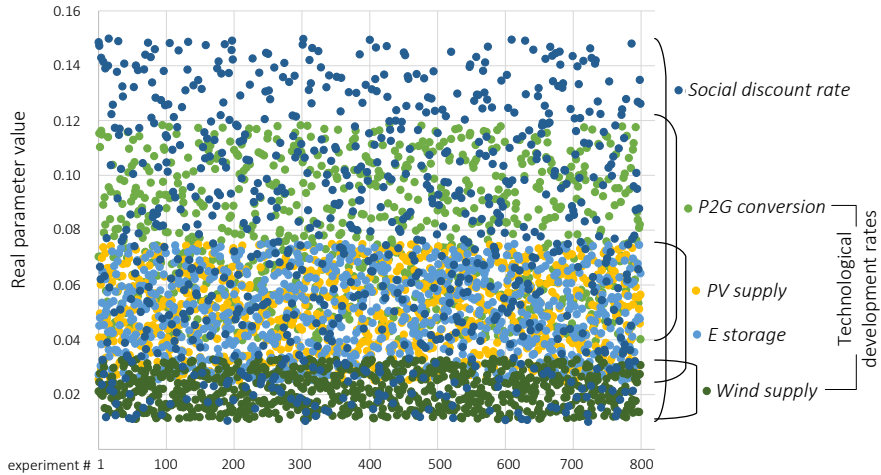


Figure 6.4: Sample distribution for all 800 experiments for each uncertain real parameter: the social discount rate δ (dark blue), the technological development rates for P2G conversion ϕ_{m_3} (light green), PV supply ϕ_{s_2} (yellow), electricity storage ϕ_{w_1} (light blue), and wind supply ϕ_{s_3} (dark green).

6.3 Experiment setup

Although three different types of uncertainty are described, in the optimization framework this leads to 6 uncertain parameters ($k = 6$): energy demand D , social discount rate δ , and the four selected technological development rates ϕ . To ensure $N > 100k$ (see also Section 3.3.2, 800 experiments were defined to examine simultaneous variations of all uncertain parameters. The total number of investment possibilities is 1972, of which 901 are non-network investments and 1071 are network investments. The result matrix $[N, X^E ET + X^L LT]$ becomes [800, 1972].

For the experiments, the optimality gap is set to an absolute value of 0.1%. To manage total computation time and memory without compromising the distinction between the different experiments, the maximum run time per experiment is set to 300 seconds. This is explained in more detail in Section 3.4, and Figure 3.7. Other relevant settings, values, and code can be found in Appendix 8.2 and 8.3.

6.4 Results

The large number of results is split into five distinct sections. First, the results of the base case, in which no uncertainty is incorporated, are presented (6.4.1). This provides a baseline to which we can compare the exploratory results. Section 6.4.2 introduces the exploratory results from a global perspective on all the experiments. This is followed by an analysis on the influence of each uncertain parameter individually (6.4.3). The next two sections focus on the influence of the combination of uncertainties, as this is the key to the exploratory approach. Section 6.4.4 explores relevant design correlations or trade-offs with specific tipping points for the uncertain parameters. Section 6.4.5 uncovers broad investment trends using clustered results. Each cluster is analyzed on three design aspects: investment asset type, location, and timing. All these results provide input for both the municipality and the local Distribution System Operator (DSO) on specific policy directions and the city's infrastructure plans. Finally, the sixth subsection reflects on the main findings of this exploratory modeling demonstration (6.4.6).

6.4.1 Base case results

To help interpret the results of the uncertainty exploration, the results of the base case are presented. For these, demand scenario #1 is used, which is the current demand projection of the municipality, and the base case values for the social discount, and technological development rates (see Tables 6.1 and 6.2). A slight modification from the original CO_2 emission reduction goal is made, using a 100% reduction by 2050 instead of 95% (corresponding to Climate Policy Scenario 5 in the previous chapter). This creates a more challenging case, leading to more distinct and interesting results. The base case is deterministic, assuming no uncertainty, and corresponds to the *trend* in Figure 6.1.

The total costs for the base case are 701 MEur and it requires 328 investments, of which 63% are made in the first time period t_0 (2018). This is due to the largely greenfield nature of the case. Figure 6.5 shows the resulting energy transition design from 2018 to 2050 for the electricity (blue), gas (green), and heat (red) systems in parallel. All assets are numbered according to their installed capacity. The unlabeled assets depict those constructed in t_0 . This includes most network assets and all Combined Heat and Power (CHP) conversion assets. Black-lined labels show additional assets that were constructed in later time periods.

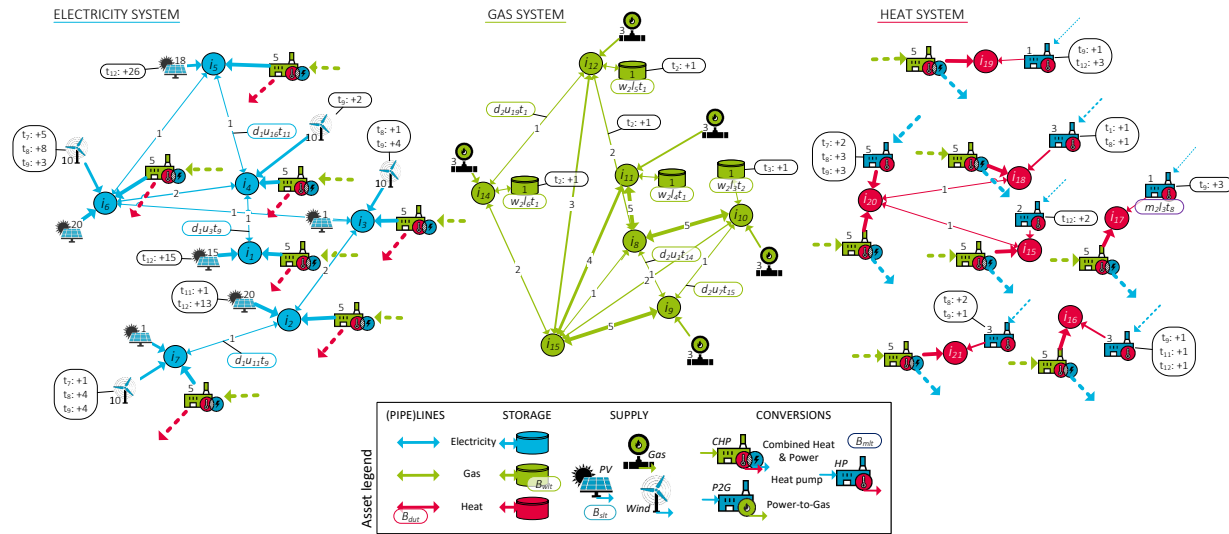


Figure 6.5: Deterministic results showing the electricity (blue), gas (green), and heat (red) systems in parallel. All assets are numbered according to their installed capacity. Conversion assets are shown in the system that they deliver to, so CHP conversion assets are shown in both the electricity and the heat system. All assets without a label were built at t_0 . Black-lined labels show additions per time period.

Many additional Heat Pump (HP) conversion, wind supply, and several photovoltaic (PV) supply assets are constructed as time progresses. All gas storage assets are constructed later, a few time periods before gas supply is no longer high enough to meet gas demand, building up a reserve. In this base case, no Power-to-Gas (P2G) conversion assets are constructed, because gas storage is more economical within this time frame¹. Neither electricity nor heat storage assets assets are constructed, because their annual standing losses makes neither economically favorable.

Table 6.3 shows the quantitative results of the base case in the first column; this includes both the energy and the power capacity when relevant. The next columns contain the exploratory results with only the energy capacities.

6.4.2 Global findings

For the exploratory approach, 800 samples within the ranges of each of the six uncertain parameters were combined into an equal amount of experiments. These were inserted into the optimization framework and generated 800 different results. The distribution of most experiment results is not Gaussian, but discrete. Consequently, the standard deviation is not suitable to represent the data spread. Instead, the median (50%) is used to indicate the most common result. The Inter Quantile Range (IQR), the range between the 25% (Q1) and 75% (Q3) quantiles, is used to indicate the most common variability across experiments. The minimum and maximum values show the entire result variability. Table 6.3 gives a quantitative summary of these values.

One of the most important things to notice in these results is the difference between the base case and the median. If the municipality had not assumed any uncertainty, they would have used the base case and overestimated the investment costs in more than half of the 'potential futures', or underestimated them in 25% of the future scenarios. More specifically, they would have assumed there is no use for P2G conversion, even though it plays a role in many samples, sometimes a major one. Using the exploratory approach, it is clear that the variance in the results is quite different and the median could be a better starting point for their projections. This is an important affirmation of the utility of endogenous consideration of uncertainty.

The next four figures include more detailed result graphics for all 800 experiments, giving one example for each asset type: electricity network in Figure 6.6, P2G conversion in Figure 6.7, wind supply in Figure 6.8, and gas

¹Note that P2G will get built after 2050, when all stored gas runs out, as demonstrated in Section 5.2.2 when discussing *boundary effects* of Climate Policy Scenarios 4 and 5.

Table 6.3: Quantitative results of the base case compared to all 800 experiments

Result value	Base case	Median	Q1	Q3	IQR	Min	Max
Total costs [M€]	701	655	617	702	85	581	966
No. of investments	328	330	294	422	128	220	914
Total capacity	[PJ] (MW)			[PJ]			
Electricity network	1.79 (57)	1.97	1.61	2.33	0.72	1.07	4.48
Gas network	3.94 (125)	4.55	4.31	4.67	0.37	3.81	6.15
Heat network	0.57 (18)	0.57	0.57	0.57	-	0.57	0.85
CHP conversion	4.97 (175)	4.97	4.97	4.97	-	4.97	5.53
HP conversion	1.15 (43)	1.07	0.91	1.36	0.45	0.59	1.70
P2G conversion	- (0)	0.40	-	0.79	0.79	-	7.54
PV supply	1.50 (389)	0.95	0.87	2.54	1.68	0.87	8.41
Wind supply	3.96 (438)	3.69	2.71	4.56	1.84	2.17	9.55
Electricity storage	-	-	-	-	-	-	-
Gas storage	2.52	2.16	1.44	3.24	1.80	0.72	16.20
Heat storage	-	-	-	-	-	-	0.01
Totals [PJ]	20.40	20.31	17.38	25.03	7.65	14.76	60.43

storage assets in Figure 6.9. These line plots include on the left-hand side the cumulative capacity in PetaJoule (PJ) for each individual experiment. On the right-hand side, the result density of the experiments is displayed, including the median, and a highlighted band containing 50% of the experiment results. The far right shows a probability density. To facilitate comparison between the assets, the y-axes all range from 0-10 PJ. The lineplots for the cumulative costs of these assets, as well as those for all the other assets can be found in the Appendix Section 8.2.

Most interesting to note in these figures is the timeline of the investments, which is not visible in the static Table 6.3. This shows the progressing energy transition, which in most experiments requires increasing investments in wind supply, electricity network and gas storage assets. Investments in P2G conver-

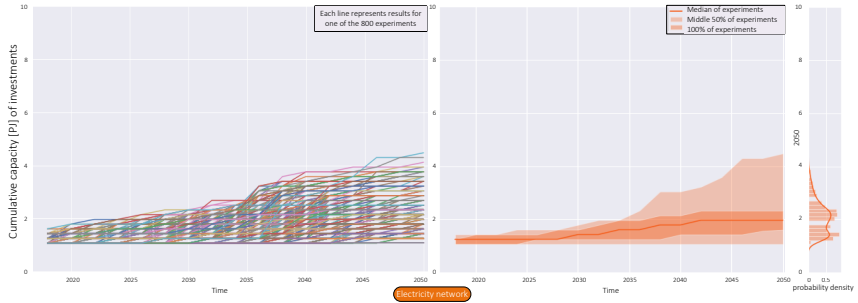


Figure 6.6: Lineplot of the cumulative capacity for all electricity network investments per experiment, the result and probability density for all 800 experiments

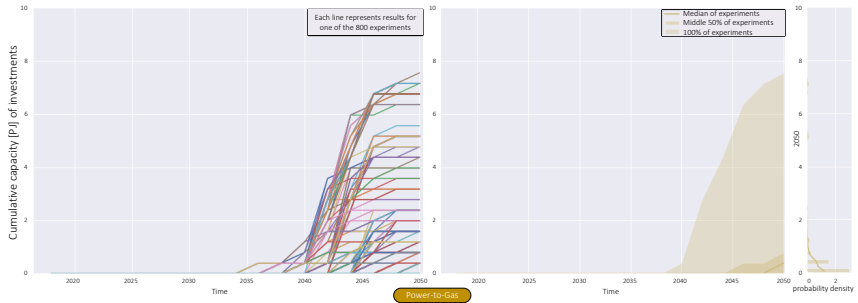


Figure 6.7: Lineplot of the cumulative capacity for all Power-to-Gas conversion investments per experiment, the result and probability density for all 800 experiments

sion assets only start from around 2035, when they becomes more economic and the energy transition becomes more challenging. Additionally, the result density emphasizes the large distribution of the experiments. Especially the highest 25% of the experiments (shown in a lighter color above the highlighted band) show the impact of the more challenging samples. In the worst-case experiments, the capacity requirements for each of these assets could increase significantly: more than double for electricity network assets, triple for wind supply assets, an 8-fold increase for gas storage assets, and even a 20-fold increase for P2G assets. Of course, the occurrence of these maxima are not as likely, but it is worth taking it into account as decision maker. Ensuring some of these situations do not materialize, or at least planning for contingencies,

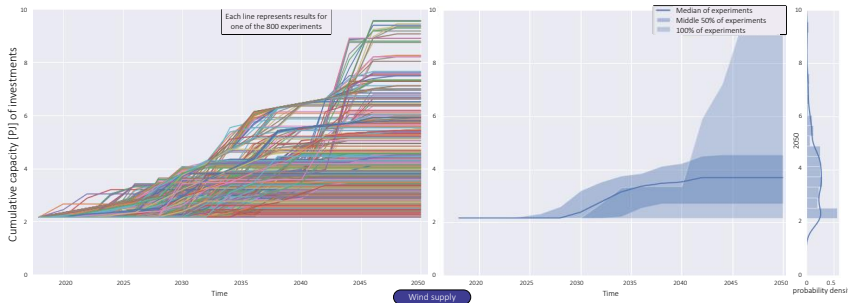


Figure 6.8: Lineplot of the cumulative capacity for all wind supply investments per experiment, the result and probability density for all 800 experiments

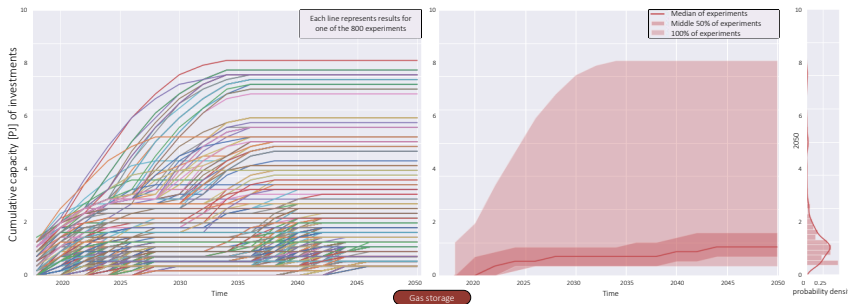


Figure 6.9: Lineplot of the cumulative capacity for all gas storage investments per experiment, the result and probability density for all 800 experiments

can save a significant amount of costs.

6.4.3 Individual uncertainty

Figure 6.10 shows the relative sensitivity of the result values to the six different uncertain parameters; scored using the Extra Trees classifier as described in Subsection 3.3.3. A higher percentage means a result is more influenced by a particular uncertainty. All percentages sum to 100% for each of the columns (note that these results are rounded to two digits).

Across all result parameters, the development of energy demand is the most influential uncertainty. All infrastructure investments are driven by the need to ensure demand is met at every node and in every time period. This

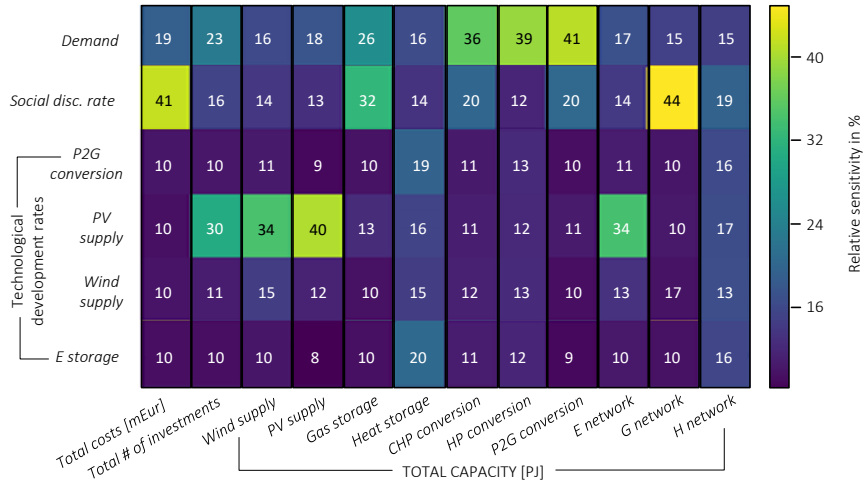


Figure 6.10: Sensitivity of the result values to all 6 uncertain parameters using the feature score in % (yellow = high sensitivity, dark blue = low sensitivity)

is captured in the main energy balance constraint (Equation 3.2). The investments in conversion assets are especially driven by demand uncertainty, which has slightly differing causes. For CHP conversion, the level of investments in the first time period is quite high, leaving little room for variation. However, as it is a very efficient conversion technique, it is beneficial to use in the highest demand experiments. Supporting this analysis is Figure 6.11; a boxplot with the distribution and shape of the cumulative investment capacities in PJ for each asset type. HP conversion is a relatively small asset and easily accommodates all heat demand fluctuations. Finally, P2G conversion assets are very large and expensive and the median number of investments are quite low. Yet in the highest demand cases, the number of investments can grow by an order of magnitude.

The uncertainty in the social discount rate δ is most influential on the total costs of the energy system designs, the gas storage and gas network assets. It has an exponential effect directly on all costs and ranges from 1-15%, so its influence on the total cost is expected. When it comes to gas storage, although the assets are relatively expensive, they are one of the few that can *transfer* energy between time periods. Additionally, and unlike several other assets, it is not influenced by uncertainty in its own technological development rate.

Given that the social discount rate is classically used to influence investment timing, this result makes sense. A high δ makes it more beneficial to wait to make investments, and by waiting, other assets become increasingly more economic than gas storage. Yet a low δ makes the difference in costs between earlier investments and future investments lower, which leads to more gas storage. The same effect applies to gas network assets. Although these are not as expensive as gas storage, they are more expensive than electricity network assets, which is its main distribution competitor. δ also influences most other (relatively) expensive assets to a certain degree: CHP and P2G conversion, as well as heat network assets. A high δ can make these investments more rapidly economical than a low δ .

When it comes to the technological development rates, the highest relative sensitivity is of the total photovoltaic (PV) supply capacity to the technological development rate of PV supply ϕ_{s_2} . Clearly, if PV costs decrease more rapidly, it is more economical to install them, and vice versa. Yet, ϕ_{s_2} also substantially influences the total number of investments, the wind supply, and the electricity network investments. These are *cascading effects*. First, PV supply assets are relatively small and many are required to meet all demand by the end of the time frame considered. Hence, they cause the highest variation in investment numbers. The influence on wind supply is a competing effect and already points to a trade-off. Although wind supply is generally more cost-efficient than PV, if the technological development rate further helps or hinders the attractiveness of PV investments, that can be influential in its competition with wind. Examining the data from the opposite perspective, the total PV capacity is influenced a little by the development rate of wind, but not nearly to the same degree. This can be explained by the fact that the technological development rate of PV supply is much higher than that of wind supply ($\phi_{s_2} \gg \phi_{s_3}$ [151]), giving it a larger range and more influence on the results (see Table 6.2). Finally, more (or less) PV assets would also require more (or less) electricity network assets to distribute the electricity generated. However, this result could also point to a second cascading effect: a varying ϕ_{s_2} causes a varying wind supply, which can also cause a varying number of electricity network assets. Given that wind supply is geographically constrained, it would require more electricity network to distribute. The correlation analyses in the next paragraph show more details on these findings.

6.4.4 Design trade-offs

Next, the simultaneous influence of the uncertainties is analyzed. This resembles the unframed system state (Figure 6.1) and is the main goal of the

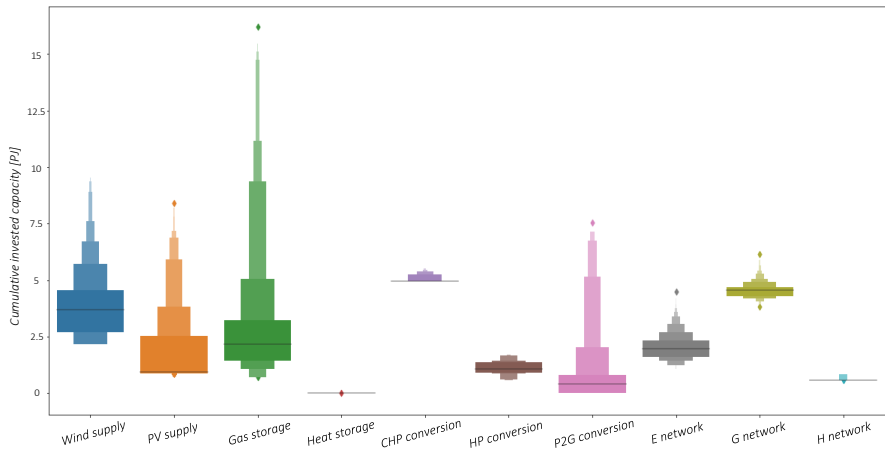


Figure 6.11: Boxplot portraying the distribution and shape of the cumulative investment capacities for each asset type for all 800 experiments from 2018-2050

exploratory approach. First, a correlation analysis is applied to find investment trade-offs as well as which uncertainty ranges or tipping points drive them. This can be relevant for decision makers especially when they want to determine which technology (areas) to stimulate.

Figure 6.12 shows a heat map of the correlation matrix for all result values. Mostly positive (red) and a few slightly negative (blue) correlations were found. First, correlations across all the assets are evaluated to find which assets most influence the total costs and number of investments. This is followed by an analysis of several specific positive and negative correlations or design trade-offs, with a main focus on the largest trade-off between PV and wind supply investments. A combination of all pair plots showing the results of each individual experiment, forming the basis of the correlation matrix, can be found in Appendix 8.2, Figure 8.13.

Total costs and investments

The largest positive correlation is between the total number of investments and the total PV supply capacity built. This confirms what is mentioned in the previous paragraph, that the number of PV assets vary most (see Figures 6.10 and 6.11). Yet when it comes to energy capacity, gas storage shows the

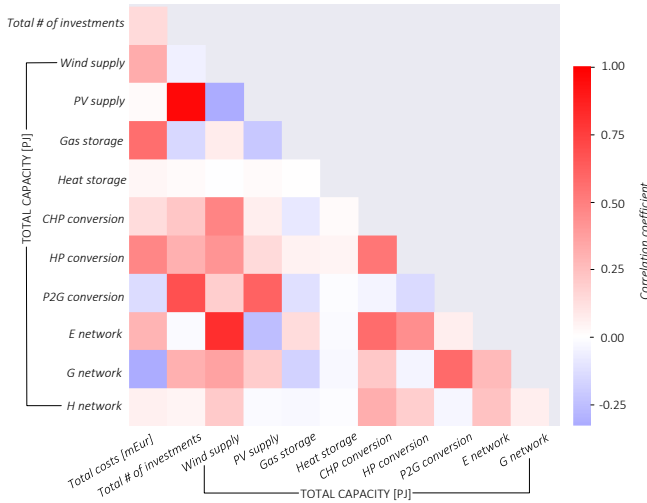


Figure 6.12: Correlation Matrix Heatmap of result values

most variation and indeed it has a significant correlation with the total costs (see Figure 8.12 in Appendix 8.2). Interesting to note is that gas storage has a slightly negative correlation with the number of assets. This can be explained by the fact that in most of the experiments, the number of investments in gas storage lie below its median. So its costs are more significant than its numbers. Similar reasoning explains why P2G conversion and gas network assets are negatively correlated with the total costs. Their numbers are more significant than their costs.

Specific trade-offs

The largest trade-off is between wind and PV supply, again confirming that these are competing technologies. Interesting to note is that there is a specific tipping point that leads to the highest wind investments: when the technological development factor ϕ_{s_2} of PV is smaller than or equal to 4.7%. On the contrary, the highest PV investments are minimally affected by the technological development factor of wind (ϕ_{s_3}). Despite this competition, both investments are required for each energy system design, so the trade-off is not that strong (25%).

The second largest correlation is between the electricity network and the

wind supply capacity, confirming the second cascading effect mentioned the Subsection 6.4.3. More wind supply requires more electricity networks, due to its distance from certain demand locations. On the contrary, more PV supply requires (slightly) less electricity networks as it can be generated locally. For both other networks, as well as for gas storage, wind supply has a (stronger) positive correlation which again relates back to its geographical limitations. It is more likely to be generated somewhere it is not (entirely) needed, so it either needs to be distributed or stored for later use. At a first glance, wind supply is the cheaper option, yet a deeper analysis shows more aspects of the energy system need to be considered. This is valuable input for a decision maker.

The investment effects of PV and wind supply also show similarities, since they both generate electricity. For example, both positively correlate with the number of P2G conversion and gas network assets. This effect arises from the energy transition. When gas supply diminishes, the remaining gas demand needs to be met either via storage, or by generating electricity and converting it to gas. So a higher electricity supply leads to more P2G conversion and indirectly to a larger gas network.

6.4.5 Design clusters

After analyzing the global findings, the individual influence of each uncertain parameter, and specific trade-offs between technologies, many useful insights have been gained. The final step to add even more value for an urban decision maker is to gain insight into investment trends across the entire energy system design. To determine which designs perform well across what range of uncertainties; to know which investments are prudent, no matter what future comes to pass; and to find a robust investment strategy and see if certain policies can manage or even reduce uncertainties. These trends are captured by arranging the results into design clusters. Each cluster contains experiments with similar output, often driven by similar input ranges of the uncertain parameters.

First, the highlights of all the cluster results are given, including their total investment numbers, capacity, and which uncertainty input ranges differentiate them. Then these are further analyzed on the three investment design characteristics: investment asset type, location, and time period. For a municipality and a local DSO, knowing which asset types are robust investments helps shape technology-specific policies. Second, knowing the optimal physical locations of investments is very helpful input for spatial planning purposes. Finally, knowing the optimal investment timing can help drive policy timing and even provide a sense of urgency if delays lead to more expensive designs.

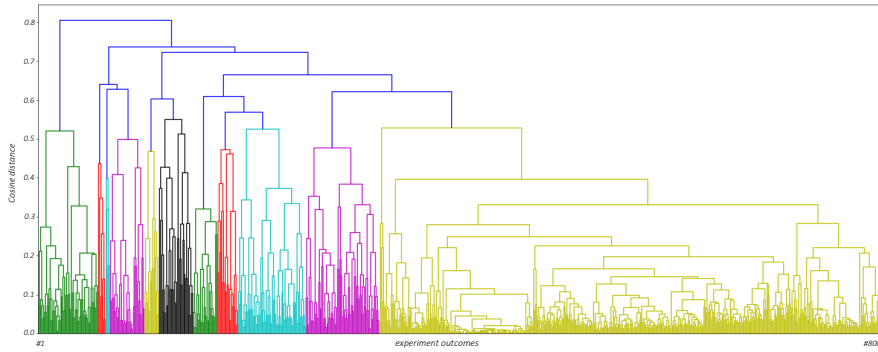


Figure 6.13: Dendrogram showing the hierarchical clustering of the cosine distance matrix, with 800 experiment outcomes arranged in 11 clusters with cosine distance value threshold at 0.6

Cluster highlights

Using hierarchical agglomerative clustering (Section 3.3.3) and a cosine distance value threshold of 0.6, 11 clusters are identified. Figure 6.13 depicts the underlying dendrogram. Table 6.4 shows how many experiments each cluster contains, their total median investment numbers (I) and capacity (Γ), and their distinguishing uncertainty drivers. These drivers were found using a classification and regression tree (CART) analysis on the clusters (see paragraph 3.3). Note that although many clusters do not have demand as a main driver in the CART analysis, this does not mean demand scenarios were unimportant; only that the CART analysis is not able to distinguish between them.

Cluster 2 is by far the largest cluster, containing more than half of the experiments, which means it resembles the most likely energy system design. It is mainly driven by experiments where the technological development factor of PV ϕ_{s_2} is in a lower part of its range [0.025-0.045]. This leads to a preference for wind supply, and a lower total number of investments due to the fact that wind assets are four times larger than PV supply assets. The experiments in the cluster are on the lower end of capacity requirements, which corresponds to the average and lower demand scenarios, including the municipality's base case (10 PJ by 2050).

Table 6.4: Design cluster characteristics - ordered by number of experiments and showing the average number of investments I , installed energy capacity Γ in PJ, and the main uncertainty drivers

Cluster	# exp.	# I	Γ [PJ]	Main drivers ¹
All	800	282	20.3	-
2	476	284	20.7	$\phi_{s_2} \leq 0.045; \phi_{s_3} > 0.015$
8	70	396	19.8	D#11; $0.059 \leq \phi_{s_2} \leq 0.07$
5	64	355	19.5	$\delta \leq 0.075; 0.056 \leq \phi_{s_2} \leq 0.066$
4	57	776	29.2	$\delta > 0.075; 0.059 \leq \phi_{s_2} \leq 0.07$
3	33	495	22.6	$\delta \leq 0.075; \phi_{s_2} > 0.066$
1	32	574	24.9	$\delta > 0.075; \phi_{s_2} > 0.059$
9	23	461	23.3	$\delta \leq 0.075; 0.048 \leq \phi_{s_2} \leq 0.066$
11	20	460	21.0	$\delta > 0.075; \phi_{s_2} > 0.059$
10	14	475	28.5	$\delta > 0.075; 0.048 < \phi_{s_2} \leq 0.059; \phi_{s_3} > 0.022$
6	7	379	23.7	$\delta > 0.075; \phi_{s_2} > 0.066$
7	4	746	26.6	$\phi_{s_2} > 0.066$

¹ D# = demand scenario, δ = social discount rate, ϕ = technological development factor, of which s_2 = PV, and s_3 = wind supply

The next two largest clusters are 8 and 5. Half of the experiments in Cluster 8 relate to demand scenario #11 (*very fast change*), which is characterized by an early, accelerated reduction of gas demand, and they are all driven by a high ϕ_{s_2} . Cluster 5 is shaped as well by a high ϕ_{s_2} , combined with a discount rate δ lower than 7.5%. Both clusters have a much higher average number of investments than Cluster 2, without requiring a higher total asset capacity, indicating a preference for PV supply assets.

Clusters 4 and 10 require the highest installed energy capacity, indicating a need to meet higher demand levels. While Cluster 4 uses mainly PV assets to do so, driven by the high ϕ_{s_2} , Cluster 10 requires significantly less assets, indicating a high number of wind supply assets. Both clusters are also driven by a high δ , which incurs on average lower costs for all installed capacity.

Asset type

Figure 6.14 depicts the median number of investments per asset type for all experiments and each of the eleven clusters. Note that the numbers do not necessarily correspond to energy capacity, see also Figure 6.11 and Table 4.2.

	11	10	13	9	11	9	8	10	8	10	18	8
E network – B_{d_1}	11	10	13	9	11	9	8	10	8	10	18	8
G network – B_{d_2}	37	39	37	35	40	36	37	36	36	36	37	37
H network – B_{d_3}	2	2	2	2	2	2	2	2	2	2	2	2
CHP conversion – B_{m_1}	35	38	35	35	35	35	35	37	35	35	38	35
HP conversion – B_{m_2}	40	54	36	51	34	35	35	63	42	54	63	43
P2G conversion – B_{m_3}	1	4	0	0	13	0	2	3	0	1	2	0
PV supply – B_{s_2}	82	353	76	304	585	177	194	532	220	247	184	281
Wind supply – B_{s_3}	68	70	79	49	53	58	51	56	47	67	121	47
G storage – B_{w_2}	6	4	6	10	3	5	15	7	6	9	10	7
Clusters –	All	1	2	3	4	5	6	7	8	9	10	11

Figure 6.14: The median number of investments aggregate to asset type for all non-clustered experiments and each cluster

A few trends are found across the clusters when analyzing the asset types. First, the current energy infrastructure in Eindhoven (and most of the Netherlands) is heavily gas-oriented. The electricity network has around half the energy transport capacity of the gas network, while the heat network is almost non-existent. This can be explained by the differing costs between the three networks and the fact that heat is an energy carrier to which other sources can easily be converted. Second, the number of investments in heat network and CHP conversions assets are quite similar across the clusters. Most of these assets are part of the infrastructure foundation required to balance the current energy system (in time period t_0). Finally, no electricity storage assets were constructed. And although heat storage assets are expected to have higher relevance seasonally, they were constructed in 2 of the most expensive scenarios

(see Table 6.3). As this is not reflected in the median, both asset options were not included in Figure 6.14.

Most of the variance is found in the P2G conversion, PV supply, wind supply, and gas storage assets. As discussed before, these differences are mainly driven by the different demand scenarios. A higher demand requires more RES investments, which in turn can make P2G conversion assets more economical than gas storage to cover the remaining gas demand. The variance between PV and wind supply is due to the different technological development values, and again the geographical constraints, as previously discussed. Note that a wind asset has about four times the capacity of a PV supply asset, so there are more clusters with a wind preference than the number of assets portray. Most notable is Cluster 2, where the capacity of wind supply is 5 times higher than that of PV. In most clusters, especially those driven by low demand scenarios (Clusters 2, 5, and 8), P2G conversion has little to no presence. Any remaining gas demand at the end of the time frame is fulfilled using gas stored in previous periods. However, in the clusters driven by the highest demand scenarios (Clusters 1, 4, and 7), the number of P2G assets can become substantial; complementing the gas storage investments. Note that the capacity of a P2G asset is also higher than the other conversion assets.

Location

Figure 6.15 depicts the median number of investments per location and edge for all experiments in the first column, and for each cluster in the following columns. Note that edges with less than two network investments were omitted to focus on significant results.

Overall, the geographical placement of the investments is quite similar in all the clusters. Most non-network assets are placed on location 6 (nodes 6, 13, and 20), followed by locations 2 and 7. This corresponds to the demand weight of these locations. Consequently, most network connections are built around these locations, though the central position of location 1 also attracts many edge investments. Several edges receive no investments, which is generally related to their relative distance to each other (see also Figure 4.1).

In these results, the effect of the geographical constraints on gas (locations 2-6) and wind supply (locations 3, 4, 6, and 7), and lack thereof for PV supply are evident. In those experiments with a preference for wind supply (Clusters 2 and 10), more investments are found in locations 3 and 4. Contrarily, Clusters 1, 4, and 7 all show a significant preference for PV supply and investments that correspond far more to the demand weight of each location.

	29	64	24	63	85	50	46	76	52	63	66	53
Location 1 – B_{l_1}	29	64	24	63	85	50	46	76	52	63	66	53
Location 2 – B_{l_2}	37	134	32	102	128	67	70	151	82	98	62	85
Location 3 – B_{l_3}	29	38	30	26	82	21	24	48	21	25	44	21
Location 4 – B_{l_4}	28	36	28	34	83	24	27	54	23	30	42	24
Location 5 – B_{l_5}	34	72	29	70	95	55	54	86	57	71	62	59
Location 6 – B_{l_6}	71	126	67	112	150	69	85	195	95	79	90	114
Location 7 – B_{l_7}	32	50	30	49	89	31	30	73	41	40	41	45
Edge 2 (1,3) – B_{u_2}	5	5	5	4	5	5	3	5	5	4	5	5
Edge 4 (1,5) – B_{u_4}	5	6	5	5	5	5	5	5	5	5	5	5
Edge 5 (1,6) – B_{u_5}	4	4	5	4	4	4	3	3	4	4	6	3
Edge 6 (1,7) – B_{u_6}	3	3	3	2	3	3	2	2	3	2	2	3
Edge 7 (2,3) – B_{u_7}	4	3	5	4	5	3	5	4	3	4	7	3
Edge 11 (2,7) – $B_{u_{11}}$	5	5	5	5	5	5	5	6	5	5	5	5
Edge 12 (3,4) – $B_{u_{12}}$	1	3	1	1	2	2	1	2	1	2	2	2
Edge 15 (3,7) – $B_{u_{15}}$	5	5	5	5	5	5	5	5	5	5	5	5
Edge 16 (4,5) – $B_{u_{16}}$	1	1	2	1	1	1	0	0	1	1	3	0
Edge 17 (4,6) – $B_{u_{17}}$	4	4	4	4	5	4	4	4	4	5	5	4
Edge 18 (4,7) – $B_{u_{18}}$	5	5	5	5	5	5	5	5	5	5	5	5
Edge 20 (5,7) – $B_{u_{20}}$	2	2	2	3	2	2	2	3	1	2	3	2
Clusters –	All	1	2	3	4	5	6	7	8	9	10	11

Figure 6.15: The median number of investments aggregated to location or significant edge (≥ 2 investments) for all non-clustered experiments and each cluster

Time period

The largely greenfield investment character of the case study creates a *foundation* of investments in the first time period. Given the large size of this foundation, the presence and differences between smaller investments in later time periods are poorly registered by the cosine distance algorithm. Moreover, the investment differences in the first time period are minimal. Therefore, the analysis focuses on the investments after the first time period, as shown in Figure 6.16.

	1	2	3	4	5	6	7	8	9	10	11
Clusters – All	1	2	3	4	5	6	7	8	9	10	11
2020 – B_{t_2}	1	2	2	7	0	1	4	10	0	5	8
2022 – B_{t_3}	3	7	3	7	0	3	3	8	1	7	8
2024 – B_{t_4}	3	4	2	4	3	3	2	6	0	4	6
2026 – B_{t_5}	2	4	2	3	2	2	3	6	2	3	5
2028 – B_{t_6}	2	8	2	2	1	2	4	10	2	2	10
2030 – B_{t_7}	3	13	3	2	3	2	0	13	1	9	16
2032 – B_{t_8}	9	12	9	2	16	9	1	100	1	10	12
2034 – B_{t_9}	8	16	6	25	22	6	95	42	6	15	25
2036 – $B_{t_{10}}$	9	28	7	86	12	7	4	44	27	26	36
2038 – $B_{t_{11}}$	10	32	6	71	3	26	0	92	26	104	26
2040 – $B_{t_{12}}$	8	61	4	9	3	50	1	20	30	20	8
2042 – $B_{t_{13}}$	6	22	3	7	57	19	29	18	74	8	10
2044 – $B_{t_{14}}$	3	10	3	7	194	2	14	54	11	7	18
2046 – $B_{t_{15}}$	2	100	2	6	185	2	1	78	1	9	62
2048 – $B_{t_{16}}$	1	36	1	1	3	1	0	12	1	2	4
2050 – $B_{t_{17}}$	1	1	0	0	1	1	0	1	1	1	0

Figure 6.16: The median number of investments aggregated to time period for all non-clustered experiments and each cluster

Overall, the investment timing shows that most investments are planned later in the time frame. This has two major causes. First is the timing of

the energy transition. In this case study of the city of Eindhoven, the city's climate goals were translated to their fossil gas supply linearly reducing to zero by 2050. Yet at that last time period, a demand for gas still remains. This either needs to be fulfilled via P2G conversion, or from gas storage, or a combination of both. For many demand scenarios, 2034 is the first time period when the remaining gas supply is lower than gas demand; creating a surge of investments. Second, some asset types are still in their early stages of development and have significant techno-economic cost reduction potential. That means these assets, especially P2G conversion and PV supply, can become increasingly more cost-effective in later time periods.

6.4.6 Main findings

Reflecting on the implications of the exploratory results, the influence of uncertainty on the long-term planning of energy systems is unmistakable. Compared to the results of the base case of 701 million Euros, the total system design costs range from 581 to 966 million Euros under the uncertainty assumptions utilized in this study. In addition, assets that not built in the base case, such as P2G conversion and heat storage, ended up being built in multiple experiments, in some cases playing a significant role: the maximum capacity of P2G is higher than the combined maximum capacities for the other two conversion assets.

Regarding the uncertain parameters individually, the first notable result is that the development of demand is the most influential. Differences in high and low total demand drove the main differences between the minimum and maximum number of investments. Especially the speed of electrification, or conversely the decrease in gas reliance, given the municipality policy to reduce fossil gas supply, is quite dominant in driving the costs down. Second, the variations in the social discount rate clearly affected the total costs of the solutions. It also showed effects on those assets which were more relevant in later time periods especially, without high technological development rates. Third, the different technological development rates showed how preferences for different assets could shift. Higher base rates inherently caused more variation, which is clearly shown in the results: from the enormous variation in P2G conversion assets, to the clear trade-off between PV and wind supply with a tipping point in favor of wind at $\phi_{s_2} \leq 0.047$, consistent with its lower cost per energy generated. Yet in certain scenarios the geographical constraints on wind supply incurred more network and storage requirements, tipping the balance in favor of PV.

It is also relevant to see the interactive effects of the different uncertainties, underlining the value of analyzing them simultaneously. Although all 800 experiments differed, they also showed many broad similarities in investments across asset type, location, and timing. Long-term gas storage assets are invaluable for balancing the entire energy system; there is a slight preference for wind supply assets, though always complemented by PV supply; and P2G conversion only plays a role in the most difficult demand scenarios, while the other two conversion assets are always applicable. The latter finding underlines the benefits of a multi-energy systems perspective. If this case is approached by analyzing each network individually, additional network and storage assets would have been required and higher costs incurred. The geographical spread of the investments generally aligns with the differences in demand per location, with the highest demand location l_6 always containing the most investments. In some experiments, the effects of the geographical constraints on wind and gas supply were notable, causing up to 50% higher investment numbers in low-demand locations. The investment timing is influenced most by the specific timing in the case study, most investments were made in the second half of the time frame, when the energy transition becomes most challenging for the municipality and highly developing assets most economic. All of these results which provide useful knowledge for an urban decision maker and confirm the value of the exploratory approach.

6.5 Conclusion

In this chapter, the multi-energy framework was applied to explore deep uncertainty in the long-term, multi-period investment planning case of the energy system in Eindhoven. An unframed system state was explored by analyzing multiple uncertain parameters simultaneously: demand, social discount rate, and four technological development rates. Using Latin-Hypercube sampling to generate 800 experiments, the framework produced different optimal designs for the energy transition of the city from today to 2050. Applying multiple different data science techniques, the experiments were compared to the municipality's base case and to each other, to determine the influence of the uncertainties on the results.

The results were consistent and responsive to the uncertain parameter changes, again confirming the value the multi-energy case study, as well as the proposed methodology to expand the optimization framework to explore multiple uncertainties simultaneously. Specifically, there were three important findings. First, ignoring uncertainty can lead to significant under- (-17%)

or overestimation (+38%) of investment costs. Second, demand uncertainty is the largest driver of the results, especially showing high costs when gas demand remains high around 2050. This provides an opportunity for the municipality, showing that it can be very beneficial to focus on policy aimed at accelerating electrification or a reduced dependency on gas. Such an acceleration of the energy transition leads to a lower level of investments required. On the flip-side, if an accelerated reduction of gas demand is challenging, investing in the development of P2G can be worth while. Finally, broad investment trends were visible for all three design aspects. Conversion assets were important in almost every design, underlining the benefits of a multi-energy systems perspective. Variations in investment location and timing were also consistent with our expectations: most investments were made at locations with the highest energy demand and during the second half of the time frame, when the energy transition becomes most challenging for the municipality and highly developing assets most economic.

These results confirm the value of the multi-energy framework for urban decision makers and policy advisors. A clear spread of different designs was found, as befits an unframed, deeply uncertain future scenario; emphasizing the impact of uncertainty on the planning of future energy systems. More specifically, the results show a distinct difference between the base-case and the spread of all the experiments, uncovering multiple different policy opportunities. These results also tackle the final challenge of the energy transition, which is to incorporate deep uncertainty.

Chapter 7

Conclusions

7.1 Introduction

In order to remain below 1.5°C global warming, nearly all carbon dioxide emissions need to be reduced to zero by 2050. The majority of these emissions originate in the energy system, which contains a myriad of existing infrastructure, with a diverse mix of multiple energy carriers and a largely fossil energy supply. An energy transition towards solely zero carbon, or renewable energy sources (RES) is required, which is complex and uncertain, as the transition is influenced by all sorts of social, technological, political, and environmental pathway effects. For the implementation of stringent climate actions, cities play a large role given their increasing population density and resource intensity. Furthermore, many cities are already dealing with the effects of climate change, leading to a strong motivation to act, and at the same time this scale of energy systems has been surprisingly understudied in the literature and is thus ripe for developing actionable policies that can have a clear impact.

In the final chapter of this thesis, overall conclusions are drawn on the value of the multi-energy framework, the integrated urban case study, and the combined results tackling the challenges of the energy transition (7.2). The next section summarizes the contributions of this thesis (7.3). Section 7.4 concludes on the entirety of this thesis by formulating recommendations for future work.

7.2 Conclusions

In this thesis three specific challenges were examined at an urban scale: the carrier mismatch, the temporal mismatch, and the deep uncertainty present in long-term energy models. To tackle these challenges, this thesis proposed a multi-energy optimization framework for long-term, multi-period investment planning of integrated urban energy systems, including an exploratory modeling methodology to incorporate uncertainty. It aims to help urban decision makers design a pathway for their energy transition such that climate goals are reached, and large-scale implementation of zero carbon or RES is achieved in the most cost-efficient manner, all while assuring a safe and reliable energy system. The framework allows for a fully coupled network planning, including investments in conversion, supply, and storage assets for each energy carrier considered. It incorporates both relevant physical constraints as well as techno-economic effects for each of these assets. It is formulated as a mixed integer linear program, and translates to a novel application of the combined facility location network design problem.

In order to test and demonstrate the added value of the framework, an extensive, multi-energy case study was assembled based on Eindhoven, a large city in the Netherlands. The first demonstration used two distinct sets of what-if scenarios to tackle the carrier- and the temporal mismatch, varying climate policy and inter-annual weather. The climate policy scenarios showed two central results:

1. As expected, the more stringent the climate policy, the more investments were required, yet with increasingly lower cumulative CO_2 -emissions. The *carrier mismatch* becomes evident as both the fossil gas supply, as well as any fossil gas in storage, eventually run out. Then the only remaining option to meet remaining gas demand is to invest in Power-to-Gas (P2G) conversion assets;
2. Additionally, delaying stringent climate actions to later time periods significantly reduces the required investments. However, this also causes much higher cumulative CO_2 -emissions, which can have considerable consequences for the global temperature increase. This is an important finding and demonstrates the real-world value for decision makers, as well as the deliberations they need to make.

For the inter-annual weather variation scenarios, three conclusions were drawn:

1. First, especially in the second half of the planning scope as RES become more prevalent, more temporal mismatches occurred during so-called *bad weather years*. To ensure a continued reliable energy supply, the model invests in long-term storage and conversion assets, as well as more RES supply, which is similar to the climate policy scenarios;
2. Different from the climate policy scenarios, PV supply investments are favored over wind, as the inter-annual variation in wind supply is much more significant. This confirms relevance of incorporating long-term weather variations and shows that the model responds appropriately to differing inputs;
3. Finally, the worst case weather scenario is 70% more expensive than the steady weather scenario, while the best scenario is 41% cheaper. This shows the potential both of optimal siting of RES projects, as well as of further technological innovations beyond mere cost reductions to increase RES asset efficiency and endogenously raise their capacity factors.

The second demonstration included the exploratory modeling approach, simultaneously varying demand developments, the social discount rate, and several technological development factors, tackling the deep uncertainty present in long-term planning of energy transition designs. The results were consistent and responsive to the uncertain parameter changes. Besides clear differences between the experiments, there were also many similarities in the investment patterns. Both of which provide useful knowledge for an urban decision maker and confirm the value of the exploratory approach. There were three main conclusions:

1. The exploratory modeling approach gives a much wider view of model sensitivity and allows decision-makers to determine robust and effective investments, trade-offs between different investments, and tipping points in the energy system design. For example, there was a clear trade-off between PV and wind supply: both renewable resources are required, yet differing circumstances can change their preferred share in electricity generation;
2. Uncertainty had a significant impact on the spread of the expected investment costs: the cheapest energy system design was 17% below the base case, and the most expensive one was 38% higher. Specifically, demand development was the most influential uncertain parameter, impacting nearly all result values and showing the benefits of a policy aimed at accelerating electrification;

3. For the three investment design specifics on asset type, location, and timing, broad investment trends showed the importance of a combination of conversion assets in almost every design, underlining the benefit of a multi-energy perspective. Variations in investment location and timing were also consistent with expectations. Most investments were made at locations with the highest energy demand and during the second half of the time frame. The years approaching 2050 are when the energy transition becomes most challenging for the municipality and highly developing assets most economic.

7.3 Contributions

There are five major contributions in this thesis. The first and main contribution is the development of the multi-energy framework for long-term, multi-period investment planning of integrated urban energy systems and contains three parts:

- First, it is a novel framework for multi-energy systems, combining a generic way to include different types of conversion, supply, and storage assets, with a network layout and corresponding constraints for each carrier; effectively leading to a 3D-network design.
- Second, it is novel for long-term, multi-energy investment planning models to include multiple time periods, and different types of pathway effects, not just technology-related, but also social, economic, environmental, and political.
- In mathematical terms, the resulting optimization problem was formulated as a multi-period, mixed-integer linear program (MILP), combining a capacitated facility location problem with a multi-dimensional, capacitated network design problem, which is a novel application of the facility location network design problem.

The second contribution is the expansion of the framework to include an uncertainty and sensitivity analysis befitting the complex mathematical problem that the framework tackles, using an exploratory modeling approach. This includes the application of a Latin Hypercube Sampling (LHS) method, a PRIM partitioning technique, an hierarchical, agglomerative, completely linked clustering algorithm based on a cosine distance measure, and the CART analysis of these clusters, which is a novel combination and first application to such an energy system optimization model.

The third contribution is the assembly of a comprehensive, multi-energy urban case study based on the city of Eindhoven. It combines a multitude of heterogeneous data sets from the municipality, the local distribution system operators (DSOs), national forecasts and statistics, European and international asset data, research labs, energy consultancies, and historical environmental data. The assembly of this multi-energy case study sharply contrasts with standard, single-network cases like the IEEE 33-bus distribution system of the power sector [121], which is readily available for research in power systems. Such standard test systems do not yet exist for multi-energy research.

The final two contributions relate to the demonstration of the framework using the case study. The fourth contribution is to show the impacts of both climate policy adjustments and inter-annual weather effects on the transition of urban energy systems, demonstrating how the framework can handle the carrier and temporal mismatches and help an urban decision maker plan for the challenges of an increasingly renewable energy supply, with a transitioning energy demand.

The fifth and final contribution is the demonstration of the entirety of the framework including the exploratory approach, to handle the deep uncertainty present in long-term planning of energy systems. Specifically, the effects of top-down climate constraints were analyzed, while simultaneously varying demand developments, technology improvements, and investment factors. This constitutes an extensive application and further validation of the framework and its added value for energy transition design in urban areas.

7.4 Recommendations

The research field of multi-energy systems is novel, given that the term was first coined just 15 years ago [39]. As such, there are still many interesting research directions to be explored. Additionally, the work in this thesis is highly multi-disciplinary: it is based on the practical challenge of the energy transition, which requires a multi-energy systems engineering approach, combined with a consideration of economic, social, and environmental factors. Simultaneously, the framework combines a mathematical optimization model of considerable computational complexity with a data science-oriented exploratory modeling approach. In each of those disciplines, recommendations for future work can be made. To provide some structure to the recommendations, they are organized along two angles: where further scientific research can be applied, and which practical implementations are interesting.

7.4.1 Scientific research

The following recommendations relate to future scientific research:

- First, including additional *brownfield* data would allow further testing of the multi-energy framework and makes it more applicable for cities. Existing infrastructure has significant impact on the cost-effectiveness of certain solution directions. Furthermore, incorporating such information as a starting solution can reduce the number of potential solutions, which reduces complexity and could increase computation speed.
- Though broad ranges of different uncertain parameters were tested, the geographical constraints, the asset types and their respective capacities, and the original supply and demand values were strong determining factors for the results. Hence it would be very interesting to test completely different cases, e.g. cities where heat networks are much more prevalent, or exponentially growing cities with entirely different demand development projections.
- To further increase applicability, future work can aim to expand towards larger cases, ultimately aligning with the actual energy assets of a city. In an average city, that could mean anything from zero up to tens of heat stations, hundreds of gas stations, and even three to four times as many electricity stations at MV-equivalent level.
- To fully capture the impact of existing infrastructure, it helps to include asset age and expected lifetimes. Both can be incorporated into the framework by adjusting the investment costs to reflect maintenance and replacement options, to make the modeling more realistic. Such additions do add considerable complexity and have large data acquisition challenges.
- The computational complexity also affects the level of detail possible in modeling of the decision-making process of urban planning. For some of the more modular assets, integer investment variables form an acceptable approximation, while for most assets it is more realistic to model them differently: using binary variables to determine the minimum capacity, combined with a continuous variable including cost digression to determine the actual asset size.
- To manage the computational complexity, it can be helpful to either find or develop another solution method that can solve the problem more

efficiently. Either using different mathematical formulations or decomposition methods, using or developing different solution algorithms, or both. For example, column generation and interior-point methods are both algorithm classes that can be used to find optimal solutions to large linear problems, or bespoke algorithms could be created specifically to the structure of the formulated CFLND problem;

- To facilitate testing and proper comparison of new mathematical formulations, solution methods, and algorithms, developing standardized multi-energy test cases (like the IEEE test systems [121]) can be helpful.
- Another research direction is to include the operational challenges of these integrated energy systems in transition. From daily and seasonal weather effects on the supply side, to the use of demand-side flexibility, which generally occur at shorter timescales. Given the model complexity, incorporating such operational challenges can be more effective in an iterative manner; similar to how generation expansion planning and dispatch models can be coupled in power systems [168].
- Similarly, the full dimensioning of storage systems in multi-energy systems is its own research topic and needs analyses at different timescales. It requires short-term analysis to capture daily balancing requirements, medium-term analysis to capture seasonal balancing requirements, and finally, as this work demonstrated, long-term analysis to capture inter-annual balancing requirements. The latter is an aspect that is widely overlooked in the existing literature. While this thesis provides a glimpse into some of these requirements in decarbonized energy systems, this is an area that would benefit from extensive further research. For example, by integrating operational models of multi-energy storage systems with related planning models.
- Finally, the framework can also be applied to different geographical scales, e.g. to a country or a set of countries, or to a set of buildings, or even just one building, if conversion assets have application potential. The general relationships, such as the energy balance and the flow calculations, still hold, though system parameters would need adjustment.

7.4.2 Practical implementations

In order to apply the framework in practice, several recommendations arise:

- Standardize the current open source data set, record current sources, and create a manual on how to insert relevant input data. This stimulates replicability, reduces time spent, and enhances result confidence for users.
- To enable easy implementation of different data sets, an application can be developed to automatically read and incorporate data sources (e.g. GIS, demand statistics, asset data bases).
- Develop a cloud-based framework, to reduce the hurdle of computing power requirements;
- Implement the framework into a user friendly tool, or add a graphical user interface (GUI), to make it easier to use;
- Develop an application to plot the results onto a map, to immediately display spatial consequences of an energy system design;
- Develop an application to allow expert users to manually adjust the optimized results, automatically recalculating the consequences of the manual adjustments.

7.4.3 Recommendation note

While developing any of the above-mentioned recommendations, it is imperative to remain aware of the goal of the multi-energy framework: to help (urban) decision makers design a robust, integrated energy infrastructure to manage the energy transition and reach their climate goals. As George Box said in 1979 [180]: "All models are wrong, some are useful." Since replicating a future energy system in an actual experiment is impossible, it is up to researchers, policy advisors, and decision makers to determine what is useful within the means of what is possible. For complex problems such as this one, sometimes that means finding more computing power, sometimes it means not including everything that seems relevant, and focusing on what actually is.

Chapter 8

Appendix

The appendix contains additional data on the climate policy and weather scenarios (8.1), supporting data, settings, and additional results for the exploratory demonstration (8.2), and some of the code used for the multi-energy framework (8.3). All of this and more can also be found in the Github [139]. Note that the github environment has three branches:

- *main*, which contains the code and a short read-me file,
- *data*, which contains the original and processed data files, and
- *figs*, which contains all the figures used in this thesis and several more.

8.1 Scenario data

This section contains additional data sets that were used to construct the scenarios for the climate policy and inter-annual weather variations presented in Chapter 5.

8.1.1 Climate policy scenarios

This subsection provides additional data on the climate policy scenarios, as described in Chapter 5, Section 5.2.1. Table 8.1 provides the gas supply trajectories for each of the eight scenarios, which were defined as follows:

0. Business-as-usual (BAU)
1. 25% reduction by 2050
2. 50% reduction by 2050
3. 75% reduction by 2050
4. 95% reduction by 2050
5. 100% reduction by 2050
6. 100% reduction by 2050 in parabole
7. 100% reduction by 2040
8. 100% reduction by 2030

Table 8.1: Climate policy Scenarios 0-8 - gas supply from 2018 to 2050

Year	0	1	2	3	4	5	6	7	8
2018	14.1	14.1	14.1	14.1	14.1	14.1	14.1	14.1	14.1
2020	14.1	13.8	13.6	13.4	13.2	13.2	14.1	12.8	11.7
2022	14.1	13.6	13.2	12.7	12.4	12.3	14.0	11.5	9.38
2024	14.1	13.4	12.7	12.1	11.6	11.4	13.9	10.2	7.03
2026	14.1	13.2	12.3	11.4	10.7	10.5	13.8	8.95	4.69
2028	14.1	13.0	11.9	10.8	9.89	9.67	13.5	7.67	2.34
2030	14.1	12.7	11.4	10.1	9.05	8.79	13.2	6.39	0
2032	14.1	12.5	11.0	9.45	8.22	7.91	12.7	5.11	0
2034	14.1	12.3	10.5	8.79	7.38	7.03	12.0	3.84	0
2036	14.1	12.1	10.1	8.13	6.55	6.15	11.2	2.56	0
2038	14.1	11.9	9.67	7.47	5.71	5.27	10.2	1.28	0
2040	14.1	11.6	9.23	6.81	4.88	4.40	9.00	0	0
2042	14.1	11.4	8.79	6.15	4.04	3.52	7.56	0	0
2044	14.1	11.2	8.35	5.49	3.21	2.64	5.87	0	0
2046	14.1	11.0	7.91	4.83	2.37	1.76	3.91	0	0
2048	14.1	10.8	7.47	4.18	1.54	0.88	1.67	0	0
2050	14.1	10.5	7.03	3.52	0.70	0	0	0	0

8.1.2 Weather scenarios

This subsection provides additional data on the weather variation scenarios, as described in Chapter 5, Section 5.3.1. First, the historical weather data is given in Table 8.2, collected from [149], [150]. The next two tables include the relative capacity factors used for Scenarios 0-1, for photovoltaic (PV) supply in Table 8.3 and for wind supply in Table 8.4. Recall, the scenarios are defined as follows:

0. Steady weather (no variations)
1. Historical weather
2. 0.5x historical weather amplitude
3. 1.5x historical weather amplitude
4. 3.0x historical weather amplitude
5. 0.5x $\eta_t^{s,CF_{avg}}$
6. 1.5x $\eta_t^{s,CF_{avg}}$
7. 1.5x $\eta_t^{windON,CF_{avg}}$
8. 1.5x $\eta_t^{windOFF,CF_{avg}}$

Table 8.2: Average Dutch national capacity factors for photovoltaic (PV) and on- and offshore wind energy from [149], [150]

Year	PV	$Wind^{ON}$	$Wind^{OFF}$
1980	0.118	0.253	0.348
1981	0.108	0.243	0.334
1982	0.121	0.237	0.321
1983	0.116	0.270	0.364
1984	0.116	0.232	0.311
1985	0.117	0.233	0.319
1986	0.121	0.268	0.365
1987	0.116	0.220	0.299
1988	0.115	0.271	0.363
1989	0.122	0.234	0.317
1990	0.122	0.278	0.366
1991	0.124	0.234	0.314
1992	0.118	0.253	0.341
1993	0.120	0.247	0.329
1994	0.121	0.260	0.345
1995	0.127	0.256	0.346
1996	0.127	0.228	0.317
1997	0.126	0.228	0.308
1998	0.113	0.273	0.367
1999	0.124	0.258	0.349
2000	0.118	0.267	0.361
2001	0.120	0.238	0.329
2002	0.123	0.249	0.332
2003	0.132	0.212	0.291
2004	0.122	0.242	0.326
2005	0.124	0.233	0.320
2006	0.123	0.242	0.329
2007	0.122	0.261	0.347
2008	0.120	0.260	0.355
2009	0.126	0.231	0.315
2010	0.123	0.203	0.275
2011	0.125	0.243	0.330
2012	0.121	0.231	0.316
2013	0.122	0.232	0.321
2014	0.123	0.233	0.314
2015	0.125	0.260	0.348
2016	0.124	0.213	0.291
2017	0.119	0.230	0.314
2018	0.130	0.227	0.312
2019	0.126	0.241	0.324

Table 8.3: Weather variation Scenarios 0-8 - relative capacity factors for PV from 2018 to 2050

Year	0	1	2	3	4	5	6	7	8
2018	1	1.066	1.033	1.166	1.266	0.533	1.599	1.066	1.066
2020	1	1.019	1.009	1.048	1.078	0.509	1.529	1.019	1.019
2022	1	1.013	1.006	1.033	1.053	0.506	1.520	1.013	1.013
2024	1	0.994	0.997	0.986	0.978	0.497	1.491	0.994	0.994
2026	1	1.012	1.006	1.030	1.049	0.506	1.518	1.012	1.012
2028	1	0.987	0.993	0.968	0.950	0.493	1.481	0.987	0.987
2030	1	1.011	1.005	1.028	1.044	0.505	1.516	1.011	1.011
2032	1	1.004	1.002	1.012	1.019	0.502	1.507	1.004	1.004
2034	1	1.015	1.007	1.037	1.060	0.507	1.522	1.015	1.015
2036	1	0.967	0.983	0.919	0.871	0.483	1.451	0.967	0.967
2038	1	0.932	0.966	0.832	0.731	0.466	1.399	0.932	0.932
2040	1	1.044	1.022	1.112	1.179	0.522	1.567	1.044	1.044
2042	1	0.993	0.996	0.984	0.974	0.496	1.490	0.993	0.993
2044	1	0.974	0.987	0.935	0.896	0.487	1.461	0.974	0.974
2046	1	1.006	1.003	1.016	1.025	0.503	1.509	1.006	1.006
2048	1	0.943	0.971	0.859	0.774	0.471	1.415	0.943	0.943
2050	1	0.998	0.999	0.996	0.993	0.499	1.497	0.998	0.998

Table 8.4: Weather variation Scenarios 0-8 - relative capacity factors for wind from 2018 to 2050

Year	0	1	2	3	4	5	6	7	8
2018	1	0.941	0.970	0.854	0.767	0.470	1.412	1.189	1.635
2020	1	0.880	0.940	0.700	0.520	0.440	1.320	1.115	1.525
2022	1	0.954	0.977	0.887	0.819	0.477	1.432	1.219	1.645
2024	1	0.955	0.977	0.888	0.821	0.477	1.432	1.210	1.655
2026	1	0.835	0.917	0.587	0.340	0.417	1.252	1.063	1.442
2028	1	1.074	1.037	1.186	1.297	0.537	1.611	1.363	1.859
2030	1	0.999	0.999	0.997	0.996	0.499	1.498	1.271	1.726
2032	1	0.993	0.996	0.983	0.972	0.496	1.489	1.269	1.709
2034	1	1.014	1.007	1.035	1.056	0.507	1.521	1.303	1.739
2036	1	1.097	1.048	1.243	1.389	0.548	1.645	1.401	1.890
2038	1	1.118	1.059	1.296	1.475	0.559	1.678	1.432	1.923
2040	1	0.951	0.975	0.878	0.805	0.475	1.427	1.195	1.659
2042	1	1.057	1.028	1.143	1.228	0.528	1.585	1.362	1.808
2044	1	1.038	1.019	1.096	1.153	0.519	1.557	1.328	1.787
2046	1	1.124	1.062	1.311	1.498	0.562	1.687	1.458	1.915
2048	1	1.106	1.053	1.267	1.427	0.553	1.660	1.418	1.902
2050	1	1.104	1.052	1.261	1.418	0.552	1.657	1.402	1.911

8.2 Exploratory data & results

This section contains several parts to support the results presented in Chapter 6. First additional background data for the demand scenarios is provided. Next, the settings applied to generate and analyse the experiments are listed. Finally, some additional results are given.

8.2.1 Uncertainty characterization

The uncertainties are characterized in different manners, the technological development factors and the social discount rate are both real parameters, varying with a certain numerical range as defined in Table 6.2. The demand scenarios are categorical, and the extensive underlying data for each demand scenario is not depicted in Table 6.1. Instead, this section of the appendix contains several tables and figures to define the most distinct demand scenarios. Recall, the following twelve scenarios were used:

1. Base case
2. Very high demand
3. Very low demand
4. High demand
5. Low demand
6. High electricity, low gas, and low heat demand
7. Low electricity, low gas, and high heat demand
8. Low electricity, high gas, and low heat demand
9. Very low electricity, very high gas, very low heat demand
10. Fast change (exponential)
11. Very fast change (S-curve)
12. No change (constant)

Demand Scenarios 1-5 only vary in the total demand, not in the ratios between the different energy carriers demanded, nor in the timing. As such, one table for the base case is given in Table 8.5, with a corresponding Figure 8.1. Scenarios 6-9 do not vary in the total demand, just in the ratios between the energy carriers. Scenario 6 is given in Table 8.6 and Figure 8.2 as an example. Finally, Scenarios 10-12 vary in the timing of the demand change, although the final scenario simply does not change from 2018 onward. Scenario 11 is depicted in Table 8.7 and Figure 8.3.

Table 8.5: Demand Scenario 1

Time Period	Electricity	Gas	Heat	Total
2018	4.408	7.007	4.211	15.62
2020	4.402	6.651	4.221	15.27
2022	4.396	6.294	4.232	14.92
2024	4.390	5.938	4.243	14.57
2026	4.384	5.582	4.253	14.22
2028	4.378	5.225	4.264	13.86
2030	4.372	4.869	4.274	13.51
2032	4.366	4.513	4.285	13.16
2034	4.360	4.156	4.296	12.81
2036	4.354	3.800	4.306	12.46
2038	4.348	3.444	4.317	12.11
2040	4.342	3.087	4.328	11.75
2042	4.336	2.731	4.338	11.40
2044	4.330	2.375	4.349	11.05
2046	4.324	2.018	4.359	10.70
2048	4.318	1.662	4.370	10.35
2050	4.312	1.306	4.381	10

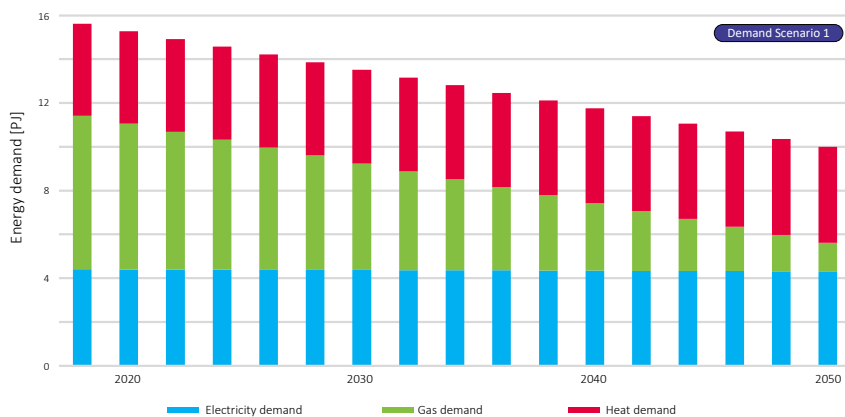


Figure 8.1: Demand Scenario 1

Table 8.6: Demand Scenario 6

Time Period	Electricity	Gas	Heat	Total
2018	4.408	7.007	4.211	15.62
2020	4.469	6.635	4.170	15.27
2022	4.530	6.263	4.128	14.92
2024	4.592	5.891	4.087	14.57
2026	4.653	5.519	4.046	14.22
2028	4.715	5.148	4.005	13.86
2030	4.776	4.776	3.963	13.51
2032	4.837	4.404	3.922	13.16
2034	4.899	4.032	3.881	12.81
2036	4.960	3.660	3.840	12.46
2038	5.022	3.289	3.798	12.11
2040	5.083	2.917	3.757	11.75
2042	5.145	2.545	3.716	11.40
2044	5.206	2.173	3.675	11.05
2046	5.268	1.801	3.634	10.70
2048	5.329	1.430	3.592	10.35
2050	5.390	1.058	3.551	10.00

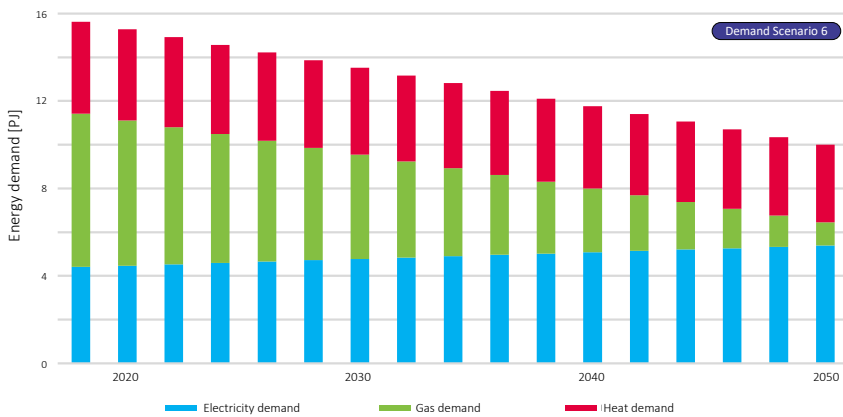


Figure 8.2: Demand Scenario 6

Table 8.7: Demand Scenario 11

Time Period	Electricity	Gas	Heat	Total
2018	4.408	7.007	4.211	15.62
2020	4.408	7.006	4.211	15.62
2022	4.408	7.004	4.211	15.62
2024	4.408	7.001	4.211	15.62
2026	4.408	6.991	4.211	15.61
2028	4.408	6.967	4.212	15.58
2030	4.407	6.902	4.214	15.52
2032	4.404	6.734	4.219	15.35
2034	4.397	6.325	4.231	14.95
2036	4.383	5.471	4.257	14.11
2038	4.360	4.155	4.296	12.81
2040	4.338	2.839	4.335	11.51
2042	4.323	1.986	4.360	10.67
2044	4.316	1.578	4.372	10.26
2046	4.314	1.410	4.378	10.10
2048	4.313	1.345	4.380	10.03
2050	4.312	1.306	4.381	10

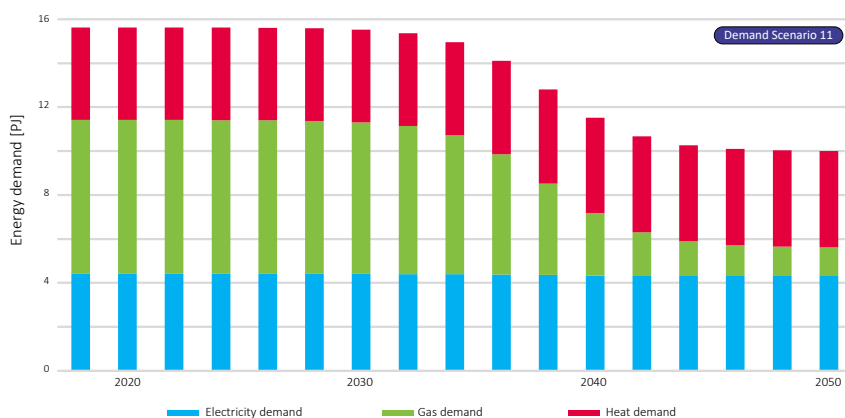


Figure 8.3: Demand Scenario 11

8.2.2 Experiment settings

For the exploratory approach, many different settings were required. First to generate the samples, then to run the optimization model, and finally to process the results. Some of these settings were mentioned in either Chapter 3 or Chapter 6. To enable result replication and further understanding of the approach, all relevant, non-standard settings are collected in Table 8.8.

Table 8.8: Exploratory approach - experiment settings

Definition	Settings
Uncertainty sampling Experiments	Demand = #1-12, $\phi_{m3}=0.0395, 0.1185, \phi_{s2}=0.025-0.075, \phi_{s3}=0.011-0.033, \phi_{w1}=0.025-0.075, \delta=0.01-0.15$ k=6, n=800
Gurobi solver	MIP-gap=0.1%, run time = 300s
PRIM algorithm	threshold=0.8, peel alpha=0.05, mass min=0.05
Clustering	agglomerative, affinity='precomputed', linkage='complete'

8.2.3 Additional results

In this part of the appendix, additional figures were added to help interpret the 800 experiment results. First, we display the complete line plots for all the assets, the electricity network assets in Figure 8.4, the gas network assets in Figure 8.5, the heat network assets in Figure 8.6, the CHP conversion assets in Figure 8.7, the HP conversion assets in Figure 8.8, the P2G conversion assets in Figure 8.9, the PV supply assets in Figure 8.10, the wind supply assets in Figure 8.11, and the gas storage assets in Figure 8.12. This is an expansion from what was displayed in Section 6.4.2, including on the left-hand side the cumulative costs in million Euros, as well as the cumulative capacity in PetaJoules for each individual experiment over time (from 2018-2050). On the right-hand side, the figures show the result density of the experiments for both result values (cumulative cost and capacity), including the median, and a highlighted band containing 50% of the experiment results, also over time. The far right shows a probability density. Please note the difference in y-axes for the different types of assets.

Next is a pair plot for all the result values as defined in Table 6.3, Section 6.4. It shows the results for all 800 experiments in pairwise relationships. For example, it shows the clear positive correlation between PV supply and the

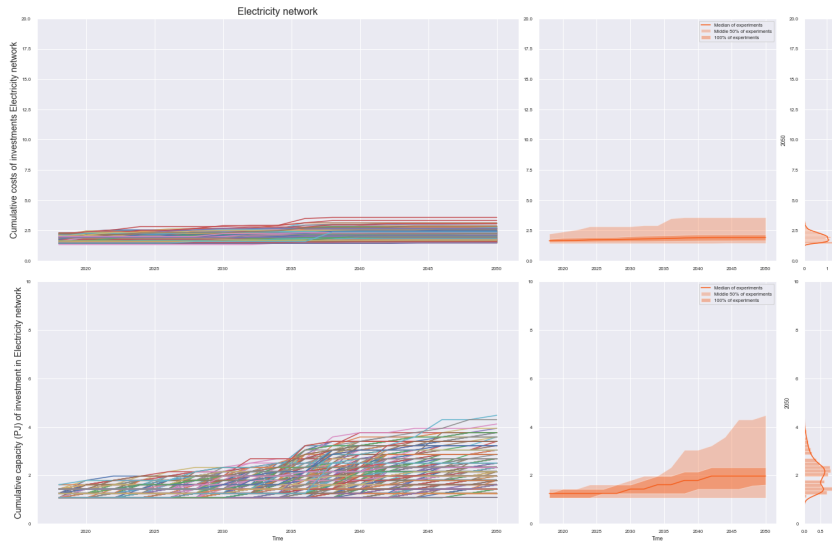


Figure 8.4: Lineplot & result density of the cumulative cost & capacity of all electricity network investments made from 2018-2050 per experiment

total number of investments. And along the main diagonal, the distribution of a result value across the experiments is depicted (e.g. most experiments have a low total costs, but a handful are more than 900 million Euros). It is a more detailed visualization of the correlation plot in Figure 6.12, Section 6.4.4.

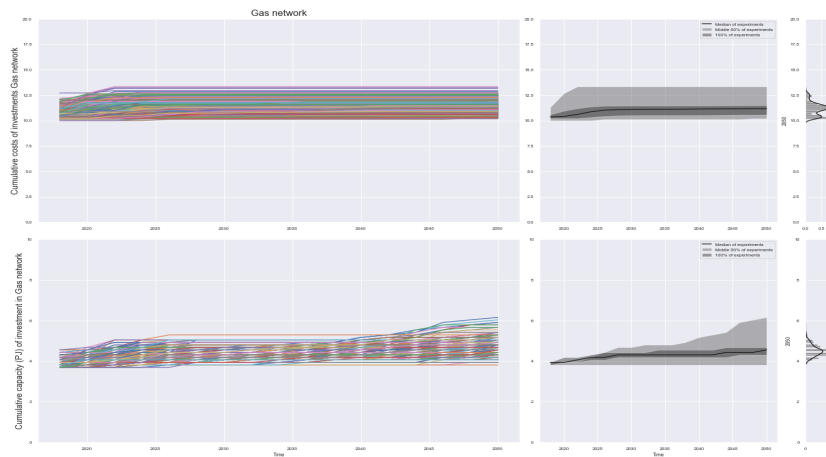


Figure 8.5: Lineplot & result density of the cumulative cost & capacity of all gas network investments made from 2018-2050 per experiment

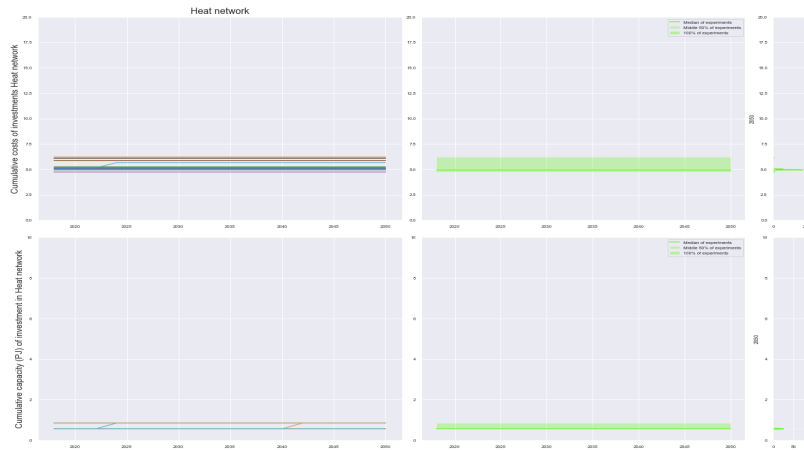


Figure 8.6: Lineplot & result density of the cumulative cost & capacity of all heat network investments made from 2018-2050 per experiment

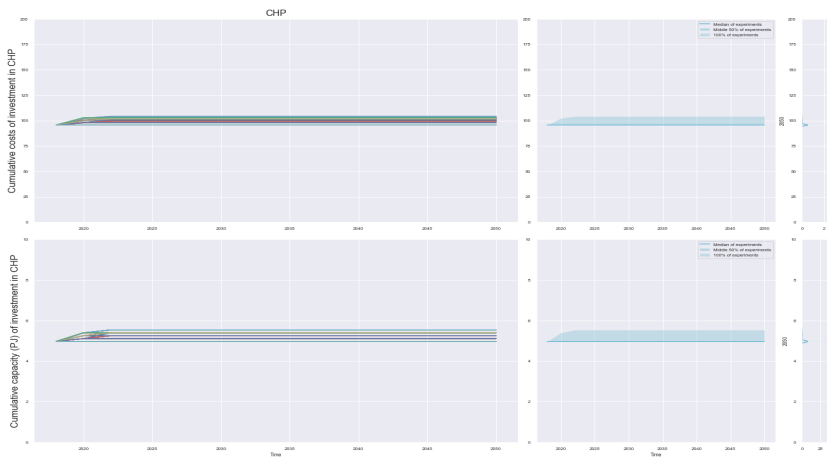


Figure 8.7: Lineplot & result density of the cumulative cost & capacity of all CHP conversion investments made from 2018-2050 per experiment

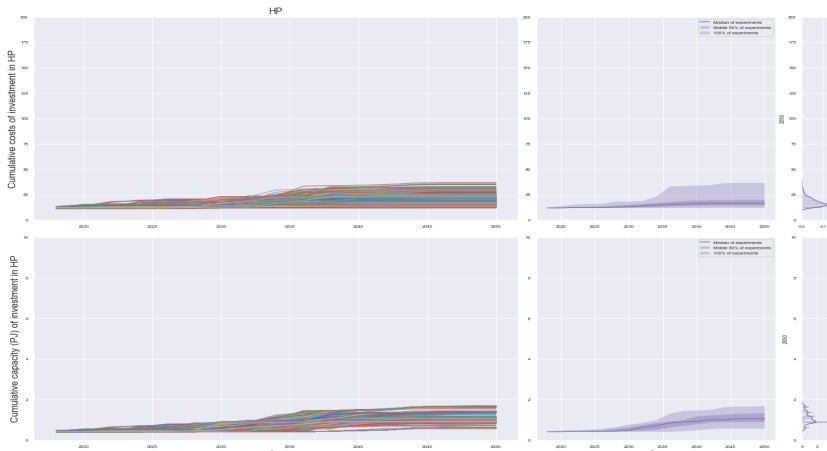


Figure 8.8: Lineplot & result density of the cumulative cost & capacity of all HP conversion investments made from 2018-2050 per experiment

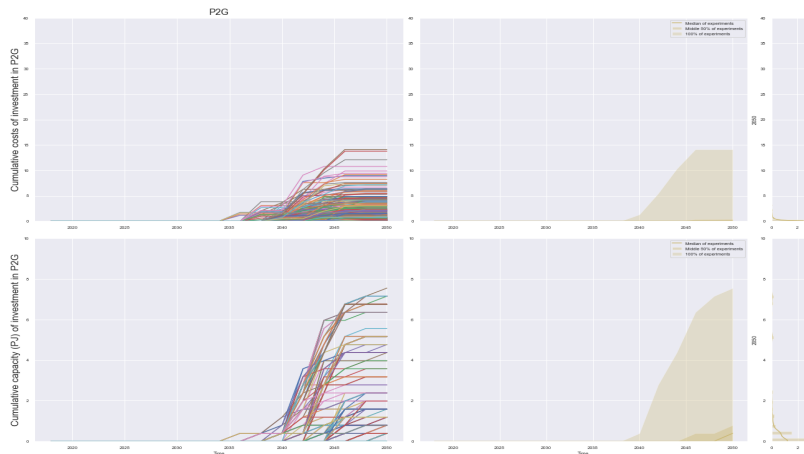


Figure 8.9: Lineplot & result density of the cumulative cost & capacity of all P2G conversion investments made from 2018-2050 per experiment

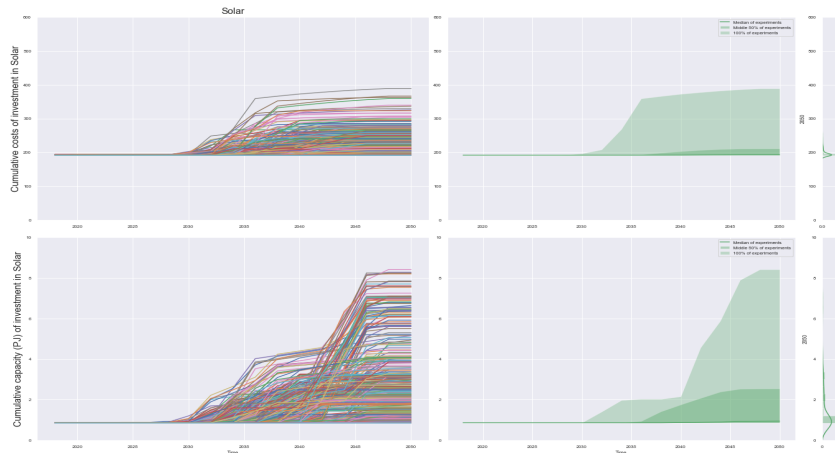


Figure 8.10: Lineplot & result density of the cumulative cost & capacity of all PV supply investments made from 2018-2050 per experiment

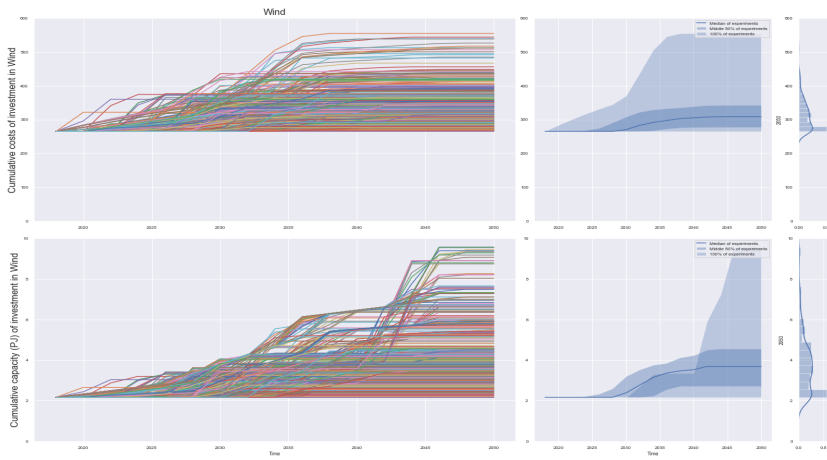


Figure 8.11: Lineplot & result density of the cumulative cost & capacity of all wind supply investments made from 2018-2050 per experiment

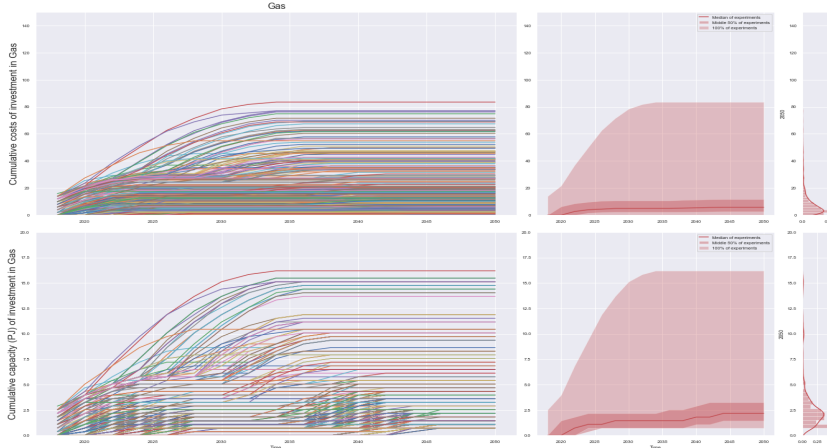


Figure 8.12: Lineplot & result density of the cumulative cost & capacity of all gas storage investments made from 2018-2050 per experiment

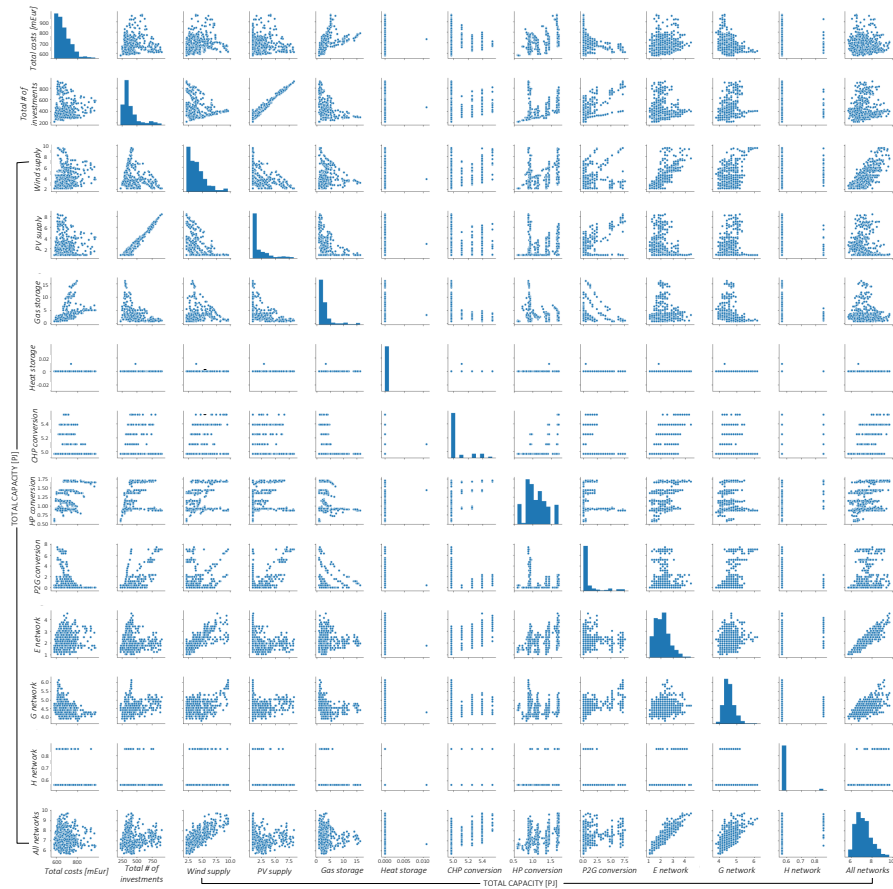


Figure 8.13: A combination of all pair plots between each outcome of interest showing the result values of all 800 experiments

8.3 Code

All of the code to run the entire multi-energy framework can be found on the author's Github [139]. The main code of the mathematical model is inserted here as reference.

```

1 # -*- coding: utf-8 -*-
"""
Created on Fri Nov 29 14:42:08 2019, updated Wed May 13, 2020

@author: IvB, latest update 6-8-2021
6 """
# Create mathematical model
from pyomo.environ import (ConcreteModel, Var, minimize, Objective
    , Constraint,
        Set, Param, NonNegativeIntegers,
        NonNegativeReals,
        Binary)
11

class Model:

    model = None
16
    def __init__(self):
        self.model = ConcreteModel()

    # Initialization of all the sets
21
    def InitializeSets(self, list_of_locations,
        list_of_energy_carriers,
            list_of_energy_converters,
                list_of_supply_types,
                    list_of_edges, list_of_arcs,
                        list_of_time_periods):
    # Set of all the locations (L)
    self.model.Locations = Set(initialize=list_of_locations)
    # Set of all the energy carriers (EC)
26
    self.model.EnergyCarriers = Set(initialize=
        list_of_energy_carriers)
    # Set of all energy converters (MT)
    self.model.EnergyConverters = Set(initialize=
        list_of_energy_converters)
    # Set of all the different supply types (Wind and solar,
        whch are used for electricity supply)
    self.model.SupplyTypes = Set(initialize=
        list_of_supply_types)
    # Set of edges (E), which define the possible link
        inewstments that can be made
31
    self.model.Edges = Set(initialize=list_of_edges)

```

```
# Set of arcs (A), which determine the between which
# locations there can be flow
36 self.model.Arcs = Set(initialize=list_of_arcs)
self.model.TimePeriods = Set(
    initialize=list_of_time_periods) # Set of time
    periods (T)

# Other parameters

41 def CreateParametersFromDictionaries(self, network_costs,
max_flow_line,
    supply_investment_costs, supply_external_factor,
    max_energy_supplied, converter_investment_costs,
    max_converted, conversion_efficiencies,
    storage_costs,
    storage_losses, min_stored,
    max_stored, loss_factor, demand, amount_given,
46 earlier_line_investment_made,
    earlier_supply_investment_made,
    earlier_converter_investment_made,
    earlier_storage_investment_made):
# Network Parameter
51 self.model.NetworkCosts = Param(self.model.EnergyCarriers,
    self.model.Locations, self.model.Locations,
    self.model.TimePeriods, initialize=network_costs) #
    Network Costs ( $\text{c}^F$ )
# Maximum flow over a line  $\Gamma^F$ , which depends on the
# energy carrier
self.model.MaxFlowLine = Param(
    self.model.EnergyCarriers, initialize=max_flow_line)
56 self.model.LossFactor = Param(
    self.model.EnergyCarriers, initialize=loss_factor)
# Supply Parameters
self.model.SupplyInvestmentCosts = Param(
    self.model.SupplyTypes, self.model.TimePeriods,
    initialize=supply_investment_costs) # Supply
    Investment Costs ( $\text{c}^S$ )
61 self.model.SupplyExternalFactor = Param(
    self.model.SupplyTypes, self.model.Locations, self.
    model.TimePeriods, initialize=
    supply_external_factor) # external factor for
    supply for e.g. weather scenarios
# Maximum amount of energy supplied ( $\Gamma^S$ )
self.model.MaxEnergySupplied = Param(
    self.model.EnergyCarriers, self.model.SupplyTypes,
    initialize=max_energy_supplied)
66 # Converter Parameters
self.model.ConverterInvestmentCosts = Param(
    self.model.EnergyConverters, self.model.TimePeriods,
    initialize=converter_investment_costs) #
```

```

    Converter Investment Costs ( $c^M$ )
# Maximum amount of energy that can be converted on the
# specific converter ( $\Gamma^M$ )
self.model.MaxConverted = Param(
    self.model.EnergyCarriers, self.model.EnergyConverters
    , initialize=max_converted)
self.model.ConversionEfficiencies = Param(self.model.
    EnergyCarriers, self.model.EnergyCarriers, self.model.
    EnergyConverters,
    initialize=conversion_efficiencies) # Energy efficiencies
    in conversion units ( $\eta^{MT_{\{E,V\}}}$ )
# Storage Parameters
self.model.StorageCosts = Param(
    self.model.EnergyCarriers, self.model.TimePeriods,
    initialize=storage_costs) # Storage Costs
self.model.StorageLosses = Param(
    self.model.EnergyCarriers, initialize=storage_losses)
    # Storage Losses
# Minimum amount of energy stored
self.model.MinStorage = Param(
    self.model.EnergyCarriers, initialize=min_stored)
# Maximum amount of energy stored ( $\Gamma^W$ )
self.model.MaxStorage = Param(
    self.model.EnergyCarriers, initialize=max_stored)
# Demand and amount of supply already existing
# Demand of every location and energy carrier (D)
self.model.Demand = Param(
    self.model.EnergyCarriers, self.model.Locations, self.
    model.TimePeriods, initialize=demand)
# Already existing supply (e.g. there is already some gas
# supply without any costs)
self.model.AmountGiven = Param(
    self.model.EnergyCarriers, self.model.Locations, self.
    model.TimePeriods, initialize=amount_given)
# Parameters for the amount of investments that are
# already made on the "existing" infrastructure.
self.model.EarlierLineInvestmentMade = Param(
    self.model.EnergyCarriers, self.model.Locations, self.
    model.Locations, initialize=
        earlier_line_investment_made, default=0)
self.model.EarlierSupplyInvestmentMade = Param(
    self.model.SupplyTypes, self.model.Locations,
    initialize=earlier_supply_investment_made, default
    =0)
self.model.EarlierConverterInvestmentMade = Param(
    self.model.EnergyConverters, self.model.Locations,
    initialize=earlier_converter_investment_made,
    default=0)
self.model.EarlierStorageInvestmentMade = Param(
    self.model.EnergyCarriers, self.model.Locations,
    initialize=earlier_storage_investment_made, default
    =0)

```

```
    initialize=earlier_storage_investment_made ,
    default=0)
101
# Variables Initialization
def InitializeVariables(self):
    # The (pipe)line investment variables, restricted to
    # integer number of investments ( $B^F$ )
    self.model.LineInvestmentMade = Var(self.model.
        EnergyCarriers, self.model.Locations,
        self.model.Locations,
        self.model.TimePeriods,
        within=
        NonNegativeIntegers
    )
    # The supply investment variables, restricted to integer
    # number of investments ( $B^S$ )
    self.model.SupplyInvestmentMade = Var(
        self.model.SupplyTypes, self.model.Locations, self.
        model.TimePeriods, within=NonNegativeIntegers)
    # The converter investment variables, restricted to
    # integer number of investments ( $B^M$ )
    self.model.ConverterInvestmentMade = Var(
        self.model.EnergyConverters, self.model.Locations,
        self.model.TimePeriods, within=NonNegativeIntegers
    )
    # The storage investment variables, restricted to the
    # maximum number of investments ( $B^W$ )
    self.model.StorageInvestmentMade = Var(
        self.model.EnergyCarriers, self.model.Locations, self.
        model.TimePeriods, within=NonNegativeIntegers)
111
    self.model.AmountSupplied = Var(self.model.EnergyCarriers,
        self.model.Locations,
        self.model.TimePeriods,
        within=
        NonNegativeReals) # amount of supply
        # inside a node (S)
    self.model.AmountFlow = Var(self.model.EnergyCarriers,
        self.model.Locations, self.model.Locations,
        self.model.TimePeriods, within
        =NonNegativeReals) # amount of flow to other
        # nodes (F)
    self.model.AmountConverted = Var(self.model.EnergyCarriers
        , self.model.EnergyConverters, self.model.Locations,
        self.model.TimePeriods,
        within=
        NonNegativeReals) # amount of energy
116
121
```

```

126                                     converted on
                                     particular conversion
                                     unit (M)
# amount of energy stored to a storage unit (Wstored)
self.model.AmountStored_In = Var(
    self.model.EnergyCarriers, self.model.Locations, self.
    model.TimePeriods, within=NonNegativeReals)
# amount of energy taken out of a storage unit (Wstored)
self.model.AmountStored_Out = Var(
    self.model.EnergyCarriers, self.model.Locations, self.
    model.TimePeriods, within=NonNegativeReals)
# self.model.StorageStartPeriod = Var(self.model.
EnergyCarriers, self.model.Locations, self.model.TimePeriods,
within = NonNegativeReals) #amount of energy in the storage at
the start of a period (Wstart)
# self.model.StorageEndPeriod = Var(self.model.
EnergyCarriers, self.model.Locations, self.model.TimePeriods,
within = NonNegativeReals) #amount of energy in the storage at
the end os a period (Wend)

131 # Objective function
def InitializeObjective(self):
    self.model.Cost = Objective(rule=ConstructionRules.
        totalCosts,
                               sense=minimize) # Constraint
                               (1)

136 # Constraints
def InitializeConstraints(self, with_or_without_storage):
    if(with_or_without_storage == "With"):
        self.model.MassBalanceConstraint = Constraint(
            self.model.EnergyCarriers, self.model.Locations,
            self.model.TimePeriods, rule=ConstructionRules.
            .balanceConstraint) # Constraint (2)
    self.model.StartStorageConstraint = Constraint(self.
model.EnergyCarriers, self.model.Locations, self.model.
TimePeriods, rule = ConstructionRules.startStorageConstraint)
#Constraint (6) + (8)
# self.model.EndStorageConstraint = Constraint(self.
model.EnergyCarriers, self.model.Locations, self.model.
TimePeriods, rule = ConstructionRules.endStorageConstraint) #
Constraint(7)
    self.model.MaxFlowConstraint = Constraint(
        self.model.EnergyCarriers, self.model.Edges, self.
        model.TimePeriods, rule=ConstructionRules.
        maxFlowConstraint) # Constraint(9-11)
    self.model.MaxConvertedConstraint = Constraint(self.
model.EnergyCarriers, self.model.Locations, self.
model.EnergyConverters,
        self.model.TimePeriods, rule=ConstructionRules.

```

```

        maxConvertedConstraint) # Constraint(12-14)
    #
    self.model.MinimumStoredConstraint = Constraint(self.
model.EnergyCarriers, self.model.Locations, self.model.
TimePeriods, rule = ConstructionRules.minimumStoredConstraint)
#Constraint(15-17)
#
    self.model.MaximumStoredConstraint = Constraint(self.
model.EnergyCarriers, self.model.Locations, self.model.
TimePeriods, rule = ConstructionRules.maximumStoredConstraint)
#Constraint(15,18,19)
    self.model.MaxSupplyConstraint = Constraint(
        self.model.EnergyCarriers, self.model.Locations,
        self.model.TimePeriods, rule=ConstructionRules.
        .maxSupplyConstraint) # Constraint(20-22)
151   self.model.MaxFlowInvestmentMade = Constraint(
        self.model.EnergyCarriers, self.model.Edges, self.
        model.TimePeriods, rule=ConstructionRules.
        maxFlowInvestmentMade) # Constraint(23)
    self.model.MaxSupplyInvestmentMade = Constraint(
        self.model.SupplyTypes, self.model.Locations, self.
        .model.TimePeriods, rule=ConstructionRules.
        maxSupplyInvestmentMade) # Constraint(24)
self.model.MaxStorageInvestmentMade = Constraint(
    self.model.EnergyCarriers, self.model.Locations,
    self.model.TimePeriods, rule=ConstructionRules.
    .maxStorageInvestmentMade) # Constraint(25)
self.model.MaxConverterInvestmentMade = Constraint(
    self.model.EnergyConverters, self.model.Locations,
    self.model.TimePeriods, rule=
    ConstructionRules.maxConverterInvestmentMade)
# Constraint(26)
# Additional constraint which states that there can be
# no link places between locations if there is no
# link between two locations. This is done such that
# there can only be links build between locations
# once ( for example: Link between Node_1 and Node_2
# is allowed, but a link between Node_2 and Node_1
# not. It is still alllowed to let flow go both ways
)
161   self.model.NoFlowInvestmentMade = Constraint(
        self.model.EnergyCarriers, self.model.Locations,
        self.model.Locations, self.model.TimePeriods,
        rule=ConstructionRules.noFlowInvestmentMade)
# Additional constraint. If there is not a possibility
# to place a link between two locations (so both
# ways not possible) there is no flow between these
# two locations. This only happens if the number of
# arcs is limited
self.model.NoAmountFlow = Constraint(self.model.
EnergyCarriers, self.model.Locations,
self.model.

```

```

    Locations ,
    self.model.
    TimePeriods ,
    rule=
    ConstructionRules
    .noAmountFlow
)
166   self.model.MaxAmountStoredOut = Constraint(
        self.model.EnergyCarriers , self.model.Locations ,
        self.model.TimePeriods , rule=ConstructionRules
        .maxAmountStoredOut)
    self.model.MaxAmountStoredIn = Constraint(
        self.model.EnergyCarriers , self.model.Locations ,
        self.model.TimePeriods , rule=ConstructionRules
        .maxAmountStoredIn)
#
    self.model.StartConstraint = Constraint(self.model.
EnergyCarriers , self.model.Locations , self.model.TimePeriods ,
rule = ConstructionRules.startConstraint)

171   else:
    self.model.MassBalanceConstraint = Constraint(
        self.model.EnergyCarriers , self.model.Locations ,
        self.model.TimePeriods , rule=ConstructionRules
        .balanceConstraint) # Constraint (2)
    self.model.MaxFlowConstraint = Constraint(
        self.model.EnergyCarriers , self.model.Edges , self.
model.TimePeriods , rule=ConstructionRules.
maxFlowConstraint) # Constraint(9-11)
176   self.model.MaxConvertedConstraint = Constraint(self.
model.EnergyCarriers , self.model.Locations , self.
model.EnergyConverters ,
self.model.TimePeriods , rule=ConstructionRules.
maxConvertedConstraint) # Constraint(12-14)
    self.model.MaxSupplyConstraint = Constraint(
        self.model.EnergyCarriers , self.model.Locations ,
        self.model.TimePeriods , rule=ConstructionRules
        .maxSupplyConstraint) # Constraint(20-22)
    self.model.MaxFlowInvestmentMade = Constraint(
        self.model.EnergyCarriers , self.model.Edges , self.
model.TimePeriods , rule=ConstructionRules.
maxFlowInvestmentMade) # Constraint(23)
    self.model.MaxSupplyInvestmentMade = Constraint(
        self.model.SupplyTypes , self.model.Locations , self
        .model.TimePeriods , rule=ConstructionRules.
maxSupplyInvestmentMade) # Constraint(24)
    self.model.MaxConverterInvestmentMade = Constraint(
        self.model.EnergyConverters , self.model.Locations ,
        self.model.TimePeriods , rule=
ConstructionRules.maxConverterInvestmentMade)
        # Constraint(26)

```

```

186
    self.model.NoFlowInvestmentMade = Constraint(
        self.model.EnergyCarriers, self.model.Locations,
        self.model.Locations, self.model.TimePeriods,
        rule=ConstructionRules.noFlowInvestmentMade)
    self.model.NoAmountFlow = Constraint(self.model.
        EnergyCarriers, self.model.Locations,
        self.model.
            Locations,
            self.model.
                TimePeriods,
                rule=
                    ConstructionRules.
                        .noAmountFlow
                )
191
    self.model.NoStorage = Constraint(
        self.model.EnergyCarriers, self.model.Locations,
        self.model.TimePeriods, rule=ConstructionRules
            .noStorage)

# _____
201
class ConstructionRules:
196
    # Minimize LineInvestmentCosts + SupplyInvestmentCosts +
        ConverterInvestmentCosts
    # Costs for the whole period
    @staticmethod
    def totalCosts(model):
        return \
            sum(sum(model.NetworkCosts[energy_type, edge[0],
                edge[1], time_period] * model.LineInvestmentMade[
                    energy_type, edge[0], edge[1], time_period]
                    for edge in model.Edges)
                for energy_type in model.EnergyCarriers)
                for time_period in model.TimePeriods) + \
            sum(sum(model.SupplyInvestmentCosts[supply_type,
                time_period] * model.SupplyInvestmentMade[
                    supply_type, location, time_period]
                    for supply_type in model.SupplyTypes)
                for location in model.Locations)
                for time_period in model.TimePeriods) + \
            sum(sum(model.ConverterInvestmentCosts[
                energy_converter, time_period] * model.
                    ConverterInvestmentMade[energy_converter, location
                    , time_period]
                    for location in model.Locations)
                for energy_converter in model.EnergyConverters
                )
211

```

```

        for time_period in model.TimePeriods) + \
    sum(sum(model.StorageInvestmentMade[energy_type,
        location, time_period]*model.StorageCosts[
        energy_type, time_period]
            for energy_type in model.EnergyCarriers)
        for location in model.Locations)
    for time_period in model.TimePeriods)

# removed from begin: model.AmountGiven[energy_type, location,
# time_period] + \
216
@staticmethod
def balanceConstraint(model, energy_type, location,
    time_period):
    return \
        model.Demand[energy_type, location, time_period] <=\
    model.AmountSupplied[energy_type, location,
        time_period] + \
    ((1-model.LossFactor[energy_type]) *
221
    sum(model.AmountFlow[energy_type, location_from,
        location, time_period]
        for location_from in model.Locations if((
            location_from, location) in model.Arcs)) - \
    sum(model.AmountFlow[energy_type, location,
        location_to, time_period]
        for location_to in model.Locations if((location,
            location_to) in model.Arcs)) + \
226
    sum(sum(model.AmountConverted[energy_type_2,
        energy_converter, location, time_period] * model.
        ConversionEfficiencies[energy_type, energy_type_2,
        energy_converter]
            for energy_converter in model.EnergyConverters
        )
        for energy_type_2 in model.EnergyCarriers) - \
    model.AmountStored_In[energy_type, location,
        time_period] + \
    model.AmountStored_Out[energy_type, location,
        time_period] #=
#model.Demand[energy_type, location, time_period] ==
# 0  #adjust equality/inequality
231

236
@staticmethod
def maxSupplyConstraint(model, energy_type, location,
    time_period):
    if(energy_type == 'Electricity'):
        return model.AmountSupplied[energy_type, location,
            time_period] <=\
    sum(sum(model.SupplyInvestmentMade[supply_type,
        location,
        time_period2]*model.MaxEnergySupplied[
        energy_type, supply_type] *
241

```

```
model.SupplyExternalFactor[supply_type ,  
    location , time_period] #add supply  
    external factor , for different (weather)  
    scenarios  
    for supply_type in model.SupplyTypes) for  
        time_period2 in  
model.TimePeriods if(int(time_period2) <= int(  
    time_period))) + \  
246    sum(model.EarlierSupplyInvestmentMade[supply_type ,  
        location] *  
        model.MaxEnergySupplied[energy_type ,  
            supply_type]  
        for supply_type in model.SupplyTypes)  
elif(energy_type == 'Gas'):  
    return model.AmountSupplied[energy_type , location ,  
        time_period] <=\  
251    model.AmountGiven[energy_type , location ,  
        time_period]  
elif(energy_type == 'Heat'):  
    return model.AmountSupplied[energy_type , location ,  
        time_period] == 0  
  
@staticmethod  
256 def maxFlowConstraint(model , energy_type , edge0 , edge1 ,  
    time_period):  
    return \  
        model.AmountFlow[energy_type , edge0 , edge1 ,  
            time_period] <= \  
        (sum(model.LineInvestmentMade[energy_type , edge0 ,  
            edge1 , time_period2] for time_period2 in model.  
                TimePeriods  
                if(int(time_period2) <= int(time_period))) +  
                model.EarlierLineInvestmentMade[energy_type ,  
                    edge0 , edge1])*model.MaxFlowLine[energy_type]  
261  
@staticmethod  
def maxConvertedConstraint(model , energy_type , location ,  
    energy_converter , time_period):  
    return \  
        (sum(model.ConverterInvestmentMade[energy_converter ,  
            location ,  
                time_period2] for  
                    time_period2 in  
                        model.  
                            TimePeriods  
                            if(int(time_period2) <= int(time_period))) +  
                            model.EarlierConverterInvestmentMade[energy_converter  
                                , location]) *\  
266    model.MaxConverted[energy_type , energy_converter] >= \  
        model.AmountConverted[energy_type ,
```

```

271                                         energy_converter , location ,
                                         time_period]

272
273     @staticmethod
274     def maxAmountStoredIn(model, energy_type , location ,
275                             time_period):
275         return model.AmountStored_In[energy_type , location ,
276                                     time_period] <= \
277             sum(model.StorageInvestmentMade[energy_type , location ,
278                             time_period2]*model.
279                             MaxStorage[
280                               energy_type]
281                         for time_period2 in model.TimePeriods
282                             if(int(time_period2) <= int(time_period))) - \
283                             sum(model.AmountStored_In[energy_type , location ,
284                                 time_period2] *
285                                 model.StorageLosses [energy_type]**(time_period-
286                                     time_period2)
287                         for time_period2 in model.TimePeriods
288                             if(int(time_period2) < int(time_period))) +\
289                             sum(model.AmountStored_Out[energy_type , location ,
290                                 time_period2]
291                             for time_period2 in model.TimePeriods
292                             if(int(time_period2) < int(time_period)))

293
294     @staticmethod
295     def maxAmountStoredOut(model, energy_type , location ,
296                             time_period):
297         return model.AmountStored_Out[energy_type , location ,
298                                     time_period] <= \
299             sum(model.AmountStored_In[energy_type , location ,
300                             time_period2] *
301                             model.StorageLosses [energy_type]**(time_period-
302                                 time_period2)
303                         for time_period2 in model.TimePeriods
304                             if(int(time_period2) < int(time_period))) - \
305                             sum(model.AmountStored_Out[energy_type , location ,
306                                 time_period2]
307                             for time_period2 in model.TimePeriods
308                             if(int(time_period2) < int(time_period)))

309
310     @staticmethod #adjusted slightly higher than with Julie ,
311                 originally 0, 0, 1, 2, 3, 4; first whole run:
312                 0,4,6,5,7,5,10
313     #20200825 scenario 5 is infeasible with 0,4,4,5,5,5. Doubling
314     solar? 20210804 SEE IF STILL WORKS?? NEW RES
315     def maxSupplyInvestmentMade(model, supply_type , location ,
316                                 time_period):
317         if((supply_type == 'Wind') and ((location == 'Node_1') or

```

```
(location == 'Node_2') or (location == 'Node_5'))):
    return model.SupplyInvestmentMade[supply_type ,
        location , time_period] == 0
elif((supply_type == 'Wind') and (int(time_period) ==
2018)):
    return model.SupplyInvestmentMade[supply_type ,
        location , time_period] <= 10 #original 10, for
        weather scenario 5 doubled
elif((supply_type == 'Solar') and (int(time_period) ==
2018)):
    return model.SupplyInvestmentMade[supply_type ,
        location , time_period] <= 20 #original 20, for
        weather scenario 5 doubled
elif((supply_type == 'Wind') and (int(time_period) ==
2020)):
    return model.SupplyInvestmentMade[supply_type ,
        location , time_period] <= 15 #original 15, for
        weather scenario 5 doubled
311 elif((supply_type == 'Solar') and (int(time_period) ==
2020)):
    return model.SupplyInvestmentMade[supply_type ,
        location , time_period] <= 30 #original 30, for
        weather scenario 5 doubled
#     elif((supply_type == 'Wind') and (time_period == '2022')
#           or
#           (time_period == '2024') or (time_period == '2026')
#           or
#           (time_period == '2028') or (time_period == '2030')):
316 #         return model.SupplyInvestmentMade[supply_type ,
#             location , time_period] <= 5
#         elif((supply_type == 'Solar') and (int(time_period) ==
#             2022) |
#             (int(time_period) == 2024) | (int(time_period) ==
#             2026) |
#             (int(time_period) == 2028) | (int(time_period) ==
#             2030)):
#             return model.SupplyInvestmentMade[supply_type ,
#                 location , time_period] <= 9
321     elif(supply_type == 'Wind'):
        return model.SupplyInvestmentMade[supply_type ,
            location , time_period] <= 15 #original 15, for
            weather scenario 5 doubled
# elif(supply_type == 'Solar'):
#     return model.SupplyInvestmentMade[supply_type ,
#         location , time_period] <= 10
else:
326     return model.SupplyInvestmentMade[supply_type ,
        location , time_period] <= 30 #original 30, for
        weather scenario 5 doubled
```



```
366     @staticmethod  
def noStorage(model, energy_carrier, location, time_period):  
    return model.AmountStored_In[energy_carrier, location,  
        time_period] == 0
```


Bibliography

- [1] United Nations Framework Convention on Climate Change, “Adoption of the Paris Agreement - Conference of the Parties COP 21”, United Nations, Tech. Rep., 2015. DOI: FCCC/CP/2015/L.9/Rev.1. [Online]. Available: <http://unfccc.int/resource/docs/2015/cop21/eng/109r01.pdf>.
- [2] “IPCC, 2022: Summary for Policymakers, Climate Change 2022: Mitigation of Climate Change, Contribution of working group iii to the sixth assessment report of the intergovernmental panel on climate change”, Cambridge, UK and New York, NY, USA, Tech. Rep. DOI: 10.1017/9781009157926.001.
- [3] M. Ge and J. Friedrich, *4 charts explain greenhouse gas emissions by countries and sectors*, 2020. [Online]. Available: <https://www.wri.org/blog/2020/02/greenhouse-gas-emissions-by-country-sector>.
- [4] International Energy Agency, “IEA Sankey Diagram - World Balance 2018”, International Energy Agency, Tech. Rep., 2018. [Online]. Available: <https://www.iea.org/sankey>.
- [5] W. Nijs, P. Castello, and I. Gonzalez, “Baseline scenario of the total energy system up to 2050”, Joint Research Center, Tech. Rep., 2017, Heat Roadmap Europe (HRE): Building the knowledge, skills, and capacity required to enable new policies and encourage new investments in the heating and cooling sector. This project has received funding from the European Union’s Horizon 2020 research and innovation

- programme under grant agreement No. 695989. [Online]. Available: www.heatroadmap.eu.
- [6] European Commission, “Going climate neutral by 2050”, European Commission, Luxembourg, Tech. Rep., 2019. [Online]. Available: <https://op.europa.eu/en/publication-detail/-/publication/92f6d5bc-76bc-11e9-9f05-01aa75ed71a1>.
 - [7] M. Ruth and B. Kroposki, “Energy systems integration: An evolving energy paradigm”, *The Electricity Journal*, vol. 27, no. 6, pp. 36–47, 2014. DOI: 10.1016/j.tej.2014.06.001.
 - [8] P. Mancarella, “Mes (multi-energy systems): An overview of concepts and evaluation models”, *Energy*, vol. 65, pp. 10–17, 2014. DOI: 10.1016/j.tej.2014.06.001.
 - [9] M. H. Shams, M. Shahabi, M. MansourLakouraj, M. Shafie-khah, and J. P. Catalão, “Adjustable robust optimization approach for two-stage operation of energy hub-based microgrids”, *Energy*, vol. 222, p. 119 894, 2021, ISSN: 0360-5442. DOI: <https://doi.org/10.1016/j.energy.2021.119894>. [Online]. Available: <https://www.sciencedirect.com/science/article/pii/S0360544221001432>.
 - [10] M. Craig, O. J. Guerra, C. Brancucci, K. A. Pambour, and B.-M. Hodge, “Valuing intra-day coordination of electric power and natural gas system operations”, *Energy Policy*, vol. 141, p. 111 470, 2020, ISSN: 0301-4215. DOI: <https://doi.org/10.1016/j.enpol.2020.111470>. [Online]. Available: <https://www.sciencedirect.com/science/article/pii/S0301421520302214>.
 - [11] I. van Beuzekom, M. Gibescu, and J. Slootweg, “A review of multi-energy system planning and optimization tools for sustainable urban development”, in *2015 IEEE Eindhoven PowerTech*, Eindhoven, the Netherlands, 2015, pp. 1–7.
 - [12] B. Hodge, H. Jain, C. Brancucci, *et al.*, “Addressing technical challenges in 100% variable inverter-based renewable energy power systems”, *WIREs Energy and Environment*, vol. 9, no. 5, e376, 2020. DOI: <https://doi.org/10.1002/wene.376>.
 - [13] Q. Wang, C. Zhang, Y. Ding, G. Xydis, J. Wang, and J. Ø stergaard, “Review of real-time electricity markets for integrating distributed energy resources and demand response”, *Applied Energy*, vol. 138, pp. 695–706, 2015. DOI: <https://doi.org/10.1016/j.apenergy.2014.10.048>.

- [14] J. Cochran, M. Miller, O. Zinaman, *et al.*, “Flexibility in 21st Century Power Systems”, National Renewable Energy Laboratory (NREL), Tech. Rep., May 2014.
- [15] D. Arent, J. Pless, T. Mai, *et al.*, “Implications of high renewable electricity penetration in the u.s. for water use, greenhouse gas emissions, land-use, and materials supply”, *Applied Energy*, vol. 123, pp. 368–377, 2014. DOI: <https://doi.org/10.1016/j.apenergy.2013.12.022>.
- [16] C. Müller, A. Hoffrichter, L. Wyrwoll, *et al.*, “Modeling framework for planning and operation of multi-modal energy systems in the case of germany”, *Applied Energy*, vol. 250, pp. 1132–1146, 2019. DOI: <https://doi.org/10.1016/j.apenergy.2019.05.094>.
- [17] C. Waibel, R. Evins, and R. Carmeliet, “Co-simulation and optimization of building geometry and multi-energy systems: Interdependencies in energy supply, energy demand and solar potentials”, *Applied Energy*, vol. 242, pp. 1661–1682, 2019. DOI: <https://doi.org/10.1016/j.apenergy.2019.03.177>.
- [18] D. Dodman, L. Diep, and S. Colenbrander, “Resilience and Resource Efficiency in Cities”, International Institute for Environment and Development for the United Nations Environment Programme, Tech. Rep., 2017.
- [19] C40 and AXA, “Understanding Infrastructure Interdependencies in Cities”, C40 Cities and Axa S.A., Tech. Rep., 2019.
- [20] IPCC, “Summary for Urban Policy Makers - What the IPCC Special Report on Global Warming of 1.5degC means for cities”, Intergovernmental Panel on Climate Change, Tech. Rep., 2018. DOI: 10.24943/SCPM.2018.
- [21] I. van Beuzekom, B.-M. Hodge, and H. Slootweg, “Framework for optimization of long-term, multi-period investment planning of integrated urban energy systems”, *Applied Energy*, vol. 292, p. 116880, 2021, ISSN: 0306-2619. DOI: <https://doi.org/10.1016/j.apenergy.2021.116880>. [Online]. Available: <https://www.sciencedirect.com/science/article/pii/S0306261921003664>.
- [22] I. van Beuzekom, B. Hodge, and J. Slootweg, “Exploring uncertainty in long-term, multi-stage investment planning of integrated urban energy systems”, *Energy Reports*, 2022, *Under review*. DOI: tbd.

- [23] World Energy Council, “World Energy Scenarios. Composing energy futures to 2050”, World Energy Council, Tech. Rep., 2013, Project Partner Paul Scherrer Institute (PSI), Switzerland. [Online]. Available: www.worldenergy.org/publications/2013/world-energy-scenarios-composing-energy-futures-to-2050.
- [24] S. Dumlao and K. Ishihara, “Dynamic Cost-Optimal Assessment of Complementary Diurnal Electricity Storage Capacity in High PV Penetration Grid”, *Energies*, vol. 14, p. 4496, 2021. DOI: <https://doi.org/10.3390/en14154496>.
- [25] R. Azizipanah-Abarghooee, F. Golestaneh, H. B. Gooi, J. Lin, F. Bavafa, and V. Terzija, “Corrective economic dispatch and operational cycles for probabilistic unit commitment with demand response and high wind power”, *Applied Energy*, vol. 182, pp. 634–651, 2016, ISSN: 0306-2619. DOI: <https://doi.org/10.1016/j.apenergy.2016.07.117>. [Online]. Available: <https://www.sciencedirect.com/science/article/pii/S0306261916310583>.
- [26] Y. Li, V. G. Agelidis, and Y. Shrivastava, “Wind-solar resource complementarity and its combined correlation with electricity load demand”, in *2009 4th IEEE Conference on Industrial Electronics and Applications*, 2009, pp. 3623–3628. DOI: 10.1109/ICIEA.2009.5138882.
- [27] Q. Chen, Z. Kuang, X. Liu, and T. Zhang, “Energy storage to solve the diurnal, weekly, and seasonal mismatch and achieve zero-carbon electricity consumption in buildings”, *Applied Energy*, vol. 312, p. 118744, 2022, ISSN: 0306-2619. DOI: <https://doi.org/10.1016/j.apenergy.2022.118744>. [Online]. Available: <https://www.sciencedirect.com/science/article/pii/S0306261922002008>.
- [28] J. Wohland, “Impacts of climate variability and climate change on renewable power generation”, Ph.D. dissertation, University of Cologne, Duisburg, Germany, 2019.
- [29] S. Collins, P. Deane, B. O Gallachoir, S. Pfenninger, and I. Staffell, “Impacts of Inter-annual Wind and Solar Variations on the European Power System”, *Joule*, vol. 2, pp. 2076–2090, 2018. DOI: 10.1016/j.joule.2018.06.020.
- [30] R. Wiser, Z. Yang, M. Hand, et al., “Wind Energy”, IPCC Special Report on Renewable Energy Sources and Climate Change Mitigation, Cambridge, UK, and New York, NY, USA, Tech. Rep., 2011, [O. Edenhofer, R. Pichs-Madruga, Y. Sokona, K. Seyboth, P. Matschoss, S. Kadner, T. Zwickel, P. Eickemeier, G. Hansen, S. Schlömer, C. von Stechow (eds)].

- [31] J. DeCarolis, H. Daly, P. Dodds, *et al.*, “Formalizing best practice for energy system optimization modelling”, *Applied Energy*, vol. 194, pp. 184–198, 2017, ISSN: 0306-2619. DOI: <https://doi.org/10.1016/j.apenergy.2017.03.001>. [Online]. Available: <https://www.sciencedirect.com/science/article/pii/S0306261917302192>.
- [32] T. Witt, M. Dumeier, and J. Geldermann, “Combining scenario planning, energy system analysis, and multi-criteria analysis to develop and evaluate energy scenarios”, *Journal of Cleaner Production*, vol. 242, p. 118414, 2020, ISSN: 0959-6526. DOI: <https://doi.org/10.1016/j.jclepro.2019.118414>. [Online]. Available: <https://www.sciencedirect.com/science/article/pii/S0959652619332846>.
- [33] C. Guiavarch, R. Lempert, and E. Trutnevyyte, “Scenario techniques for energy and environmental research: An overview of recent developments to broaden the capacity to deal with complexity and uncertainty”, *Environmental Modelling & Software*, vol. 97, pp. 201–210, 2017, ISSN: 1364-8152. DOI: <https://doi.org/10.1016/j.envsoft.2017.07.017>. [Online]. Available: <https://www.sciencedirect.com/science/article/pii/S1364815217303936>.
- [34] R. Lempert, S. Popper, and S. Bankes, *Shaping the next one hundred years: new methods for quantitative, long-term policy analysis*. Santa Monica, CA, USA: RAND, 2003, ISBN: 0-8330-3275-5. [Online]. Available: <https://citeseerx.ist.psu.edu/viewdoc/download?doi=10.1.1.446.7328&rep=rep1&type=pdf>.
- [35] S. Pfenninger, A. Hawkes, and J. Keirstead, “Energy systems modeling for twenty-first century energy challenges”, *Renewable and Sustainable Energy Reviews*, vol. 33, pp. 74–86, 2014, ISSN: 1364-0321. DOI: <https://doi.org/10.1016/j.rser.2014.02.003>. [Online]. Available: <https://www.sciencedirect.com/science/article/pii/S1364032114000872>.
- [36] I. van Beuzekom, M. Gibescu, P. Pinson, and J. Slootweg, “Optimal Planning of Integrated Multi-Energy Systems”, in *2017 IEEE Manchester PowerTech*, Manchester, UK, 2017, pp. 1–6.
- [37] T. Stant, “Decomposition Methods for the Design of an Integrated Energy Infrastructure”, M.S. thesis, Erasmus University Rotterdam, Rotterdam, Netherlands, 2019.

- [38] N. Bonenkamp, “Designing Multi-Energy Systems. Solution methods for a multi-period network design problem”, M.S. thesis, Delft University of Technology, Department of Applied Mathematics, Delft, Netherlands, 2020.
- [39] M. Geidl, G. Koeppel, P. Favre-Perrod, B. Klockl, and G. Andersson, “The Energy Hub, a powerful concept for future energy systems”, in *3rd Annual Carnegie Mellon Conf. on the Electricity Industry*, Pittsburgh, PA, USA, 2007, pp. 1–6.
- [40] G. Chicco and P. Mancarella, “Distributed multi-generation: A comprehensive view”, *Renewable & Sustainable Energy Reviews*, vol. 13, no. 3, pp. 535–551, 2009.
- [41] T. Krause, G. Andersson, K. Frohlich, and A. Vaccaro, “Multiple-Energy Carriers: Modeling of Production, Delivery, and Consumption”, *Proceedings of the IEEE*, vol. 99, no. 1, pp. 15–27, 2011.
- [42] M. R. Almassalkhi and A. Towle, “Enabling city-scale multi-energy optimal dispatch with energy hubs”, in *2016 Power Systems Computation Conference (PSCC)*, 2016, pp. 1–7. doi: 10.1109/PSCC.2016.7540981.
- [43] S. Bahrami and A. Sheikhi, “From Demand Response in Smart Grid Toward Integrated Demand Response in Smart Energy Hub”, *IEEE Transactions on Smart Grid*, vol. 7, no. 2, pp. 650–658, 2016.
- [44] Y. Wang, N. Zhang, C. Kang, D. Kirschen, J. Yang, and Q. Xia, “Standardized Matrix Modeling of Multiple Energy Systems”, *IEEE Transactions on Smart Grid*, vol. 7, no. 2, pp. 650–658, 2016. doi: 10.1109/TSG.2017.2737662.
- [45] S. Amiri, M. Honarvar, and A. sadegheih, “Providing an integrated Model for Planning and Scheduling Energy Hubs and preventive maintenance”, *Energy*, vol. 163, pp. 1093–1114, 2018, ISSN: 0360-5442. doi: <https://doi.org/10.1016/j.energy.2018.08.046>. [Online]. Available: <https://www.sciencedirect.com/science/article/pii/S0360544218315664>.
- [46] P. Gabrielli, M. Gazzani, E. Martelli, and M. Mazzotti, “Optimal design of multi-energy systems with seasonal storage”, *Applied Energy*, vol. 219, pp. 408–424, 2018, ISSN: 0306-2619. DOI: <https://doi.org/10.1016/j.apenergy.2017.07.142>. [Online]. Available: <https://www.sciencedirect.com/science/article/pii/S0306261917310139>.

- [47] S. Rahgozar, A. Zare Ghaleh Seyyedi, and P. Siano, “A resilience-oriented planning of energy hub by considering demand response program and energy storage systems”, *Journal of Energy Storage*, vol. 52, p. 104841, 2022, ISSN: 2352-152X. DOI: <https://doi.org/10.1016/j.est.2022.104841>. [Online]. Available: <https://www.sciencedirect.com/science/article/pii/S2352152X22008490>.
- [48] A. Gallo, J. Simoes-Moreira, H. Costa, M. Santos, and E. Moutinho dos Santos, “Energy storage in the energy transition context: A technology review”, *Renewable and Sustainable Energy Reviews*, vol. 65, pp. 800–822, 2016. DOI: 10.1016/j.rser.2016.07.028.
- [49] J. Xu, R. Wang, and Y. Li, “A review of available technologies for seasonal thermal energy storage”, *Solar Energy*, vol. 103, pp. 610–638, 2014, ISSN: 0038-092X. DOI: 10.1016/j.solener.2013.06.006.
- [50] CE-HEAT, “Low-grade waste heat utilization in the European Union”, Tech. Rep. [Online]. Available: <https://www.interreg-central.eu/Content.Node/CE-HEAT/Low-grade-waste-heat-utilization-in-the-European-Union.html>.
- [51] A. Härtel, M. Janssen, D. Weingarth, V. Presser, and R. van Roij, “Heat-to-current conversion of low-grade heat from a thermocapacitive cycle by supercapacitors”, *Energy Environ. Sci.*, vol. 8, pp. 2396–2401, 8 2015. DOI: 10.1039/C5EE01192B. [Online]. Available: <http://dx.doi.org/10.1039/C5EE01192B>.
- [52] B.-J. Lee, S.-M. Jung, J. Kwon, J. Lee, K.-S. Kim, and Y.-T. Kim, “Harvesting Low-Grade Waste Heat to Electrical Power Using a Thermo-electrochemical Cell Based on a Titanium Carbide Electrode”, *ACS Applied Energy Materials*, vol. 5, no. 2, pp. 2130–2137, 2022. DOI: 10.1021/acsaem.1c03683. eprint: <https://doi.org/10.1021/acsaem.1c03683>. [Online]. Available: <https://doi.org/10.1021/acsaem.1c03683>.
- [53] H. Blanco and A. Faaij, “A review at the role of storage in energy systems with a focus on power to gas and long-term storage”, *Renewable and Sustainable Energy Reviews*, vol. 81, pp. 1049–1086, 2018. DOI: <http://dx.doi.org/10.1016/j.rser.2017.07.062>.
- [54] M. Lehner, R. Tichler, H. Steinmüller, and M. Koppe, *Power-to-Gas: Technology and Business Models*. Springer, 2014. DOI: 10.1007/978-3-319-03995-4.

- [55] P. Liu, T. Ding, Z. Zou, and Y. Yang, “Integrated demand response for a load serving entity in multi-energy market considering network constraints”, *Applied Energy*, vol. 250, pp. 512–529, 2019, ISSN: 0306-2619. DOI: <https://doi.org/10.1016/j.apenergy.2019.05.003>. [Online]. Available: <https://www.sciencedirect.com/science/article/pii/S0306261919308578>.
- [56] S. Heinen, C. Hewicker, N. Jenkins, *et al.*, “Unleashing the Flexibility of Gas: Innovating Gas Systems to Meet the Electricity System’s Flexibility Requirements”, *IEEE Power and Energy Magazine*, vol. 15, no. 1, pp. 16–24, 2017.
- [57] L. Weimann, P. Gabrielli, A. Boldrini, G. J. Kramer, and M. Gazzani, “Optimal hydrogen production in a wind-dominated zero-emission energy system”, *Advances in Applied Energy*, vol. 3, p. 100032, 2021, ISSN: 2666-7924. DOI: <https://doi.org/10.1016/j.adapen.2021.100032>. [Online]. Available: <https://www.sciencedirect.com/science/article/pii/S2666792421000251>.
- [58] S. Long, O. Marjanovic, and A. Parisio, “Generalised control-oriented modelling framework for multi-energy systems”, *Applied Energy*, vol. 235, pp. 320–331, 2019, ISSN: 0306-2619. DOI: <https://doi.org/10.1016/j.apenergy.2018.10.074>. [Online]. Available: <https://www.sciencedirect.com/science/article/pii/S0306261918316428>.
- [59] I. van Beuzekom, L. Mazairac, M. Gibescu, and J. Slootweg, “Optimal Design and Operation of an Integrated Multi- Energy System for Smart Cities”, in *2016 IEEE International Energy Conference (ENERGY-CON 2016)*, Leuven, Belgium, Apr. 2016, pp. 949–955.
- [60] J. Qiu, H. Yang, Z. Dong, *et al.*, “A Linear Programming Approach to Expansion Co-Planning in Gas and Electricity Markets”, *IEEE Transactions on Power Systems*, vol. 31, no. 5, pp. 3594–3606, 2016.
- [61] S. Karamdel and M. Moghaddam, “Robust expansion co-planning of electricity and natural gas infrastructures for multi energy-hub systems with high penetration of renewable energy sources”, *IET Renewable Power Generation*, vol. 13, pp. 2287–2297, 2019. DOI: <10.1049/iet-rpg.2018.6005>.
- [62] A. Shabanzpour-Haghghi and A. Reza Seifi, “An Integrated Steady-State Operation Assessment of Electricity, Natural Gas, and Distributed Heating Networks”, *IEEE Transactions on Power Systems*, vol. 31, no. 5, pp. 3636–3647, 2016.

- [63] Q. Zeng, J. Fang, Z. Chen, and A. Conejo, “A Two-stage Stochastic Programming Approach for Operating Multi-energy Systems”, in *2017 IEEE Conference on Energy Internet and Energy System Integration (EI2)*, Beijing, China, 2017, pp. 1–6.
- [64] Viessmann, *Technology brochure - chp units for heat and power*, Allendorf, Germany, 2019.
- [65] J. Rissman, C. Bataille, E. Masanet, *et al.*, “Technologies and policies to decarbonize global industry: Review and assessment of mitigation drivers through 2070”, *Applied Energy*, vol. 266, 2020. DOI: <https://doi.org/10.1016/j.apenergy.2020.114848>.
- [66] S. J. Davis, N. S. Lewis, M. Shaner, *et al.*, “Net zero emission energy systems”, *Science*, vol. 360, no. 6396, 2018. DOI: <https://doi.org/10.1126/science.aas9793>.
- [67] A. Balakrishnan, G. Li, and P. Mirchandani, “Optimal network design with end-to-end service requirements”, *Operations Research*, vol. 65, no. 3, pp. 729–750, 2017.
- [68] Z. K. Pecenak, M. Stadler, and K. Fahy, “Efficient multi-year economic energy planning in microgrids”, *Applied Energy*, vol. 255, p. 113 771, 2019, ISSN: 0306-2619. DOI: <https://doi.org/10.1016/j.apenergy.2019.113771>. [Online]. Available: <https://www.sciencedirect.com/science/article/pii/S0306261919314588>.
- [69] M. Grond, “Computational Capacity Planning in Medium Voltage Distribution Networks”, Ph.D. dissertation, Eindhoven Univ. of Technology, Department of Electrical Engineering, Eindhoven, the Netherlands, 2016.
- [70] N. V. Emadi, T. Chaiechi, and A. R. Alam Beg, “A techno-economic and environmental assessment of long-term energy policies and climate variability impact on the energy system”, *Energy Policy*, vol. 128, pp. 329–346, 2019, ISSN: 0301-4215. DOI: <https://doi.org/10.1016/j.enpol.2019.01.011>. [Online]. Available: <https://www.sciencedirect.com/science/article/pii/S0301421519300114>.
- [71] R. Schmalensee, V. Bulovic, R. Armstrong, *et al.*, “The Future of Solar Energy: An Interdisciplinary MIT Study”, Massachusetts Institute of Technology, Tech. Rep., May 2015. [Online]. Available: <http://mitei.mit.edu/futureofsolar>.

- [72] V. Verter, “Uncapacitated and capacitated facility location problems”, in *Foundations of Location Analysis*, H. A. Eiselt and V. Marianov, Eds. New York, NY: Springer US, 2011, pp. 25–37, ISBN: 978-1-4419-7572-0. DOI: 10.1007/978-1-4419-7572-0_2. [Online]. Available: https://doi.org/10.1007/978-1-4419-7572-0_2.
- [73] H. W. H. Zvi Drezner, *Facility Location: Applications and Theory*. Springer Berlin, Heidelberg, 2004, ISBN: 978-3-540-42172-6.
- [74] D. B. Shmoys, “Approximation Algorithms for Facility Location Problems”, in *Approximation Algorithms for Combinatorial Optimization*, K. Jansen and S. Khuller, Eds., Berlin, Heidelberg: Springer, 2000, pp. 27–32, ISBN: 978-3-540-44436-7.
- [75] H. Hakli and Z. Ortacay, “An improved scatter search algorithm for the uncapacitated facility location problem”, *Computers & Industrial Engineering*, vol. 135, pp. 855–867, 2019, ISSN: 0360-8352. DOI: <https://doi.org/10.1016/j.cie.2019.06.060>. [Online]. Available: <https://www.sciencedirect.com/science/article/pii/S0360835219303900>.
- [76] D. S. Johnson, J. K. Lenstra, and A. H. G. R. Kan, “The complexity of the network design problem”, *Networks*, vol. 8, no. 4, pp. 279–285, 1978. DOI: <https://doi.org/10.1002/net.3230080402>. eprint: <https://onlinelibrary.wiley.com/doi/pdf/10.1002/net.3230080402>. [Online]. Available: <https://onlinelibrary.wiley.com/doi/abs/10.1002/net.3230080402>.
- [77] H. Lian, “Network Design Problems, Formulations and Solutions”, AAI3507762, Ph.D. dissertation, USA, 2012, ISBN: 9781267331922.
- [78] T. L. Magnanti, P. Mirchandani, and R. Vachini, “Modeling and solving the two-facility capacitated network loading problem”, *Operations Research*, vol. 43, no. 1, p. 142, 1995. DOI: [https://doi.org/10.1016/0966-8349\(95\)97847-D](https://doi.org/10.1016/0966-8349(95)97847-D).
- [79] Enexis, “Jaarverslag enexis holding n.v.”, Enexis, Tech. Rep., 2020. [Online]. Available: https://www.enexisgroep.nl/media/3100/jaarverslag_2020_enexis_holding_nv.pdf.
- [80] M. Daskin, A. Hurter, and M. Van Buer, “Toward an integrated model of facility location and transportation network design”, The Transportation Center, NorthWestern University, Evanston, IL, USA, Working Paper, 1993.

- [81] A. Ghaderi and M. Jabalameli, “Modeling the budget-constrained dynamic uncapacitated facility location–network design problem and solving it via two efficient heuristics: A case study of health care”, *Mathematical and Computer Modelling*, vol. 57, no. 3-4, pp. 382–400, 2013. DOI: <https://doi.org/10.1016/j.mcm.2012.06.017>.
- [82] I. Contreras, E. Fernández, and G. Reinelt, “Minimizing the maximum travel time in a combined model of facility location and network design”, *Omega*, vol. 40, no. 6, pp. 847–860, 2012.
- [83] R. Rahmaniani and A. Ghaderi, “A combined facility location and network design problem with multi-type of capacitated links”, *Applied Mathematical Modelling*, vol. 37, no. 9, pp. 6400–6414, 2013. DOI: [10.1016/j.apm.2013.01.001](https://doi.org/10.1016/j.apm.2013.01.001).
- [84] R. Ravi and A. Sinha, “Approximation Algorithms for Problems Combining Facility Location and Network Design”, *Operations Research*, vol. 54, no. 1, pp. 73–81, 2006. DOI: <https://doi.org/10.1287/opre.1050.0228>.
- [85] X. Chen and B. Chen, “Approximation Algorithms for Soft-Capacitated Facility Location in Capacitated Network Design”, *Algorithmica*, vol. 53, pp. 263–297, 2009. DOI: <https://doi.org/10.1007/s00453-007-9032-7>.
- [86] S. Melkote and M. S. Daskin, “Capacitated facility location/network design problems”, *European Journal of Operational Research*, vol. 129, no. 3, pp. 481–495, 2001, ISSN: 0377-2217. DOI: [https://doi.org/10.1016/S0377-2217\(99\)00464-6](https://doi.org/10.1016/S0377-2217(99)00464-6). [Online]. Available: <https://www.sciencedirect.com/science/article/pii/S0377221799004646>.
- [87] R. Rahmaniani and A. Ghaderi, “An algorithm with different exploration mechanisms: Experimental results to capacitated facility location/network design problem”, *Expert Systems with Applications*, vol. 42, no. 7, pp. 3790–3800, 2015.
- [88] G. Mavromatidis, K. Orehounig, and J. Carmeliet, “Design of distributed energy systems under uncertainty: A two-stage stochastic programming approach”, *Applied Energy*, vol. 222, pp. 932–950, 2018, ISSN: 0306-2619. DOI: [10.1016/j.apenergy.2018.04.019](https://doi.org/10.1016/j.apenergy.2018.04.019).
- [89] M. Bohlauer, A. Bürger, M. Fleschutz, M. Braun, and G. Zöttl, “Multi-period investment pathways - modeling approaches to design distributed energy systems under uncertainty”, *Applied Energy*, vol. 285, p. 116 368, 2021, ISSN: 0306-2619. DOI: <https://doi.org/10.1016/j.apenergy>.

- 2020 . 116368. [Online]. Available: <https://www.sciencedirect.com/science/article/pii/S0306261920317451>.
- [90] A. Ashouri, F. Petrini, R. Bornatico, and M. J. Benz, “Sensitivity analysis for robust design of building energy systems”, *Energy*, vol. 76, pp. 264–275, 2014, ISSN: 0360-5442. DOI: <https://doi.org/10.1016/j.energy.2014.07.095>. [Online]. Available: <https://www.sciencedirect.com/science/article/pii/S0360544214009359>.
- [91] Y. Liu, R. Sioshansi, and A. J. Conejo, “Multistage Stochastic Investment Planning With Multiscale Representation of Uncertainties and Decisions”, *IEEE Transactions on Power Systems*, vol. 33, no. 1, pp. 781–791, 2018. DOI: [10.1109/TPWRS.2017.2694612](https://doi.org/10.1109/TPWRS.2017.2694612).
- [92] K. Hunter, S. Sreepathi, and J. F. DeCarolis, “Modeling for insight using Tools for Energy Model Optimization and Analysis (Temoa)”, *Energy Economics*, vol. 40, pp. 339–349, 2013, ISSN: 0140-9883. DOI: <https://doi.org/10.1016/j.eneco.2013.07.014>. [Online]. Available: <https://www.sciencedirect.com/science/article/pii/S014098831300159X>.
- [93] E. Trutnevyyte, “Does cost optimization approximate the real-world energy transition?”, *Energy*, vol. 106, pp. 182–193, 2016, ISSN: 0360-5442. DOI: <https://doi.org/10.1016/j.energy.2016.03.038>. [Online]. Available: <https://www.sciencedirect.com/science/article/pii/S0360544216302821>.
- [94] J. Bollen and C. Brink, “Air pollution policy in Europe: Quantifying the interaction with greenhouse gases and climate change policies”, *Energy Economics*, vol. 46, pp. 202–215, 2014, ISSN: 0140-9883. DOI: <https://doi.org/10.1016/j.eneco.2014.08.028>. [Online]. Available: <https://www.sciencedirect.com/science/article/pii/S0140988314002126>.
- [95] J. Keirstead and C. Calderon, “Capturing spatial effects, technology interactions, and uncertainty in urban energy and carbon models: Retrofitting Newcastle as a case-study”, *Energy Policy*, vol. 46, pp. 253–267, 2012, ISSN: 0301-4215. DOI: <https://doi.org/10.1016/j.enpol.2012.03.058>. [Online]. Available: <https://www.sciencedirect.com/science/article/pii/S0301421512002637>.
- [96] H. Maier, J. Guillaume, H. van Delden, G. Riddell, M. Haasnoot, and J. Kwakkel, “An uncertain future, deep uncertainty, scenarios, robustness and adaptation: How do they fit together?”, *Environmental Modelling & Software*, vol. 81, pp. 154–164, 2016, ISSN: 1364-8152. DOI:

- <https://doi.org/10.1016/j.envsoft.2016.03.014>. [Online]. Available: <https://www.sciencedirect.com/science/article/pii/S1364815216300780>.
- [97] E. A. Moallemi and J. Köhler, “Coping with uncertainties of sustainability transitions using exploratory modelling: The case of the matisse model and the uk’s mobility sector”, *Environmental Innovation and Societal Transitions*, vol. 33, pp. 61–83, 2019, ISSN: 2210-4224. DOI: <https://doi.org/10.1016/j.eist.2019.03.005>. [Online]. Available: <https://www.sciencedirect.com/science/article/pii/S2210422418302594>.
- [98] S. Bankes, “Exploratory Modeling for Policy Analysis”, *Operations Research*, vol. 41, no. 3, pp. 435–449, 1993. DOI: 10.1287/opre.41.3.435.
- [99] M. D. McKay, R. J. Beckman, and W. J. Conover, “A Comparison of Three Methods for Selecting Values of Input Variables in the Analysis of Output from a Computer Code”, *Technometrics*, vol. 21, no. 2, pp. 239–245, 1979, ISSN: 00401706. [Online]. Available: <http://www.jstor.org/stable/1268522>.
- [100] T. A. Reddy, *Applied data analysis and modeling for energy engineers and scientists*. Springer Science & Business Media, 2011.
- [101] V. Krey, F. Guo, P. Kolp, et al., “Looking under the hood: A comparison of techno-economic assumptions across national and global integrated assessment models”, *Energy*, vol. 172, pp. 1254–1267, 2019, ISSN: 0360-5442. DOI: <https://doi.org/10.1016/j.energy.2018.12.131>. [Online]. Available: <https://www.sciencedirect.com/science/article/pii/S0360544218325039>.
- [102] G. Mavromatidis, K. Orehonig, and J. Carmeliet, “A review of uncertainty characterisation approaches for the optimal design of distributed energy systems”, *Renewable and Sustainable Energy Reviews*, vol. 88, pp. 258–277, 2018, ISSN: 1364-0321. DOI: 10.1016/j.rser.2018.02.021.
- [103] H. Kim, H. Cheon, Y.-H. Ahn, and D. G. Choi, “Uncertainty quantification and scenario generation of future solar photovoltaic price for use in energy system models”, *Energy*, vol. 168, pp. 370–379, 2019, ISSN: 0360-5442. DOI: <https://doi.org/10.1016/j.energy.2018.11.075>. [Online]. Available: <https://www.sciencedirect.com/science/article/pii/S0360544218322862>.

- [104] M. I. Radaideh and T. Kozlowski, “Combining simulations and data with deep learning and uncertainty quantification for advanced energy modeling”, *International Journal of Energy Research*, vol. 43, no. 14, pp. 7866–7890, 2019. DOI: <https://doi.org/10.1002/er.4698>. eprint: <https://onlinelibrary.wiley.com/doi/pdf/10.1002/er.4698>. [Online]. Available: <https://onlinelibrary.wiley.com/doi/abs/10.1002/er.4698>.
- [105] J. Zhang, H. Tang, and M. Chen, “Linear substitute model-based uncertainty analysis of complicated non-linear energy system performance (case study of an adaptive cycle engine)”, *Applied Energy*, vol. 249, pp. 87–108, 2019, ISSN: 0306-2619. DOI: <https://doi.org/10.1016/j.apenergy.2019.04.138>. [Online]. Available: <https://www.sciencedirect.com/science/article/pii/S0306261919307998>.
- [106] J. Fraiture, “The Robustness of Energy Systems: A novel method to explore the impact of uncertainties on Energy System Design Optimization Models”, M.S. thesis, Delft University of Technology, Delft, the Netherlands, 2020.
- [107] A. Chong, W. Xu, and L. Kheepoh, “Uncertainty analysis in building energy simulation: A practical approach”, in *14th conference of international building performance simulation association*, 2015, pp. 2796–2803.
- [108] J. H. Kwakkel and M. Jaxa-Rozen, “Improving scenario discovery for handling heterogeneous uncertainties and multinomial classified outcomes”, *Environmental Modelling & Software*, vol. 79, pp. 311–321, 2016, ISSN: 1364-8152. DOI: <https://doi.org/10.1016/j.envsoft.2015.11.020>. [Online]. Available: <https://www.sciencedirect.com/science/article/pii/S1364815215301092>.
- [109] J. H. Friedman and N. I. Fisher, “Bump hunting in high-dimensional data”, *Statistics and computing*, vol. 9, no. 2, pp. 123–143, 1999.
- [110] J. Kwakkel, “The Exploratory Modeling Workbench: An open source toolkit for exploratory modeling, scenario discovery, and (multi-objective) robust decision making”, *Environmental Modeling & Software*, vol. 96, pp. 239–250, 2017, ISSN: 1364-8152. DOI: <http://dx.doi.org/10.1016/j.envsoft.2017.06.054>.
- [111] R. Zadeh and A. Goel, “Dimension independent similarity computation”, *Journal of Machine Learning Research*, vol. 14, pp. 1605–1626, 2013.

- [112] J. Podani, “Net combinatorial clustering methods”, *Vegetatio*, vol. 81, pp. 61–77, 1989. DOI: <https://doi.org/10.1007/BF00045513>.
- [113] G. Shobha and S. Rangaswamy, “Chapter 8 - Machine Learning”, in *Computational Analysis and Understanding of Natural Languages: Principles, Methods and Applications*, ser. Handbook of Statistics, V. N. Gudivada and C. Rao, Eds., vol. 38, Elsevier, 2018, pp. 197–228. DOI: <https://doi.org/10.1016/bs.host.2018.07.004>. [Online]. Available: <https://www.sciencedirect.com/science/article/pii/S0169716118300191>.
- [114] Z. Li and M. de Rijke, “The Impact of Linkage Methods in Hierarchical Clustering for Active Learning to Rank”, in *Proceedings of the 40th International ACM SIGIR Conference on Research and Development in Information Retrieval*, ser. SIGIR ’17, New York, NY, USA: Association for Computing Machinery, 2017, 941–944, ISBN: 9781450350228. DOI: 10.1145/3077136.3080684. [Online]. Available: <https://doi.org/10.1145/3077136.3080684>.
- [115] L. Breiman, J. Friedman, R. Olshen, and C. Stone, *Classification and regression trees*. Monterey, CA: Wadsworth & Brooks/Cole Advanced Books & Software, 1984, ISBN: 9780412048418.
- [116] J. Fraiture and I. van Beuzekom, *Exploratory modelling optimization models*, 2020. [Online]. Available: <https://github.com>HelloYoulie/exploratory-modelling-optimization-models>.
- [117] J. Kwakkel, *Ema workbench*, Copyright 2011-2022, Revision f37cb269. [Online]. Available: <https://emaworkbench.readthedocs.io/en/latest/overview.html>.
- [118] M. Heder, “From NASA to EU: the evolution of the TRL scale in Public Sector Innovation”, *The Innovation Journal: The Public Sector Innovation Journal*, vol. 22, article 3, 2 2017.
- [119] M. Götz, J. Lefebvre, F. Mörs, et al., “Renewable Power-to-Gas: A technological and economic review”, *Renewable Energy*, vol. 85, pp. 1371–1390, 2016, ISSN: 0960-1481. DOI: <https://doi.org/10.1016/j.renene.2015.07.066>. [Online]. Available: <https://www.sciencedirect.com/science/article/pii/S0960148115301610>.
- [120] ETSAP, *Technology data*, Accessed 02.2021, Energy Technology Systems Analysis Program (ETSAP) of the International Energy Agency (IEA). [Online]. Available: <https://iea-etsap.org/index.php/energy-technology-data>.

- [121] M. Baran and F. Wu, “Network reconfiguration in distribution systems for loss reduction and load balancing”, *IEEE Trans. Power Del.*, vol. 4, 1401–1407, 2 1989.
- [122] Municipality of Eindhoven, *Eindhoven Klimaatplan 2016-2020*, In Dutch, Eindhoven, the Netherlands, 2016.
- [123] CBS, *Borough and neighborhood map*, Accessed 08.2019, Central Bureau for Statistics, 2016. [Online]. Available: <https://www.cbs.nl/nl-nl/dossier/nederland-regionaal/geografische\%20data/wijk-en-buurtkaart-2016>.
- [124] J. Steinbach and D. Stanaszek, “Discount rates in energy system analysis”, Buildings Performance Institute Europe (BPIE), Discussion Paper, May 2015, Collaboration with Fraunhofer ISI.
- [125] S. Kahouli-Brahmi, “Technological learning in energy–environment–economy modelling: A survey”, *Energy Policy*, vol. 36, pp. 138–162, 2008.
- [126] N. E. A. A. (PBL), *Model drivers image 3.0*, Netherlands Environmental Assessment Agency (PBL), 2020. [Online]. Available: https://models.pbl.nl/image/index.php/Drivers/Model_drivers#Table_of_drivers.
- [127] E3MLab/ICCS, “Prometheus Model - Model description”, Tech. Rep., 2017. [Online]. Available: http://www.e3mlab.eu/e3mlab/PROMETHEUSManual/ThePROMETHEUSMODEL_2017.pdf.
- [128] R. Loulou, G. Goldstein, A. Kanudia, A. Lettila, U. Remme, and K. Noble, “Documentation for the TIMES Model PART I - Concepts and Theory”, Tech. Rep., 2016. [Online]. Available: https://iea-etsap.org/docs/Documentation_for_the_TIMES_Model-Part-I_July-2016.pdf.
- [129] W. Cole, W. Frazier, P. Donohoo-Vallet, T. Mai, and P. Das, “2018 Standard Scenarios Report: A U.S. Electricity Sector Outlook”, Golden, CO, USA, Tech. Rep., 2018, NREL/TP-6A20-71913. [Online]. Available: <https://www.nrel.gov/docs/fy19osti/71913.pdf>.
- [130] W. McDowell, E. Trutnevyyte, J. Tomei, and I. Keppo, “Ukerc energy systems theme reflecting on scenarios working paper no. ukerc/wp/es/2014/002”, Tech. Rep., Jan. 2014.

- [131] D. P. van Vuuren, K. Riahi, R. Moss, *et al.*, “A proposal for a new scenario framework to support research and assessment in different climate research communities”, *Global Environmental Change*, vol. 22, no. 1, pp. 21–35, 2012, ISSN: 0959-3780. DOI: <https://doi.org/10.1016/j.gloenvcha.2011.08.002>. [Online]. Available: <https://www.sciencedirect.com/science/article/pii/S0959378011001191>.
- [132] C. Huber, T. Faber, R. Haas, *et al.*, “Deriving optimal promotion strategies for increasing the share of RES-E in a dynamic European electricity market”, Tech. Rep. [Online]. Available: {<https://green-x.at/downloads/FinalreportoftheprojectGreen-X.pdf>}.
- [133] P. Geurts, D. Ernst, and L. Wehenkel, “Extremely randomized trees”, *Machine learning*, vol. 63, no. 1, pp. 3–42, 2006.
- [134] B. P. Bryant and R. J. Lempert, “Thinking inside the box: A participatory, computer-assisted approach to scenario discovery”, *Technological Forecasting and Social Change*, vol. 77, no. 1, pp. 34–49, 2010.
- [135] Gurobi, *Mixed-integer programming (mip) – a primer on the basics*, 2022. [Online]. Available: <https://www.gurobi.com/resource/mip-basics/>.
- [136] J. Nash, “The (dantzig) simplex method for linear programming”, *Computing in Science & Engineering*, vol. 2, no. 1, pp. 29–31, 2000. DOI: 10.1109/5992.814654.
- [137] Gurobi, “Algorithms in Gurobi”, Tech. Rep., 2016. [Online]. Available: <https://assets.gurobi.com/pdfs/user-events/2016-frankfurt/Die-Algorithmen.pdf>.
- [138] Gurobi, *Choosing the right algorithm*, 2021. [Online]. Available: https://www.gurobi.com/documentation/9.5/refman/choosing_the_right_algorithm.html.
- [139] I. van Beuzekom, *Background data and code*, 2021. [Online]. Available: <https://github.com/ivbeuz/imes/>.
- [140] CBS, *Inwoners per gemeente*, In Dutch, Central Bureau for Statistics, 2021. [Online]. Available: <https://www.cbs.nl/nl-nl/visualisaties/dashboard-bevolking/regionaal/inwoners>.
- [141] Municipality of Eindhoven, “Klimaatplan 2021-2025 - Naar een klimaatneutraal Eindhoven”, Tech. Rep., 2020, In Dutch. [Online]. Available: https://www.eindhovenduurzaam.nl/sites/default/files/2021-01/WEBTX_Klimaatplan_0.pdf.

- [142] Enexis, *Open data*, Accessed 08.2019, Enexis, 2017. [Online]. Available: <https://www.enexis.nl/over-enexis/open-data>.
- [143] M. de Louw, “Future scenarios for an energy neutral Strijp”, M.S. thesis, Eindhoven University of Technology, Eindhoven, Netherlands, 2016.
- [144] Netherlands Ministry of Economic Affairs, “Energy report: Transition to sustainability”, Netherlands Ministry of Economic Affairs, The Hague, the Netherlands, Tech. Rep., 2016, In Dutch.
- [145] Netherlands Environmental Assessment Agency (PBL), *Energy transition scenarios*, Accessed 08.2019, Netherlands Environmental Assessment Agency (PBL), 2016. [Online]. Available: <http://themasites.pbl.nl/energietransitie/>.
- [146] Enexis, “Kwaliteits- en capaciteitsdocument - gas 2016-2025”, Enexis, Tech. Rep., 2016.
- [147] M. Liebreich, *State of the clean energy industry*, Accessed 02.2021, New York, NY, USA: Bloomberg New Energy Finance Global Summit, 2017. [Online]. Available: <https://about.bnef.com/blog/liebreich-state-industry-keynote-bnef-global-summit-2017/>.
- [148] ARUP, “Electricity Storage Technologies - Five minute guide”, ARUP, Tech. Rep. [Online]. Available: <https://www.arup.com/perspectives/publications/research/section/five-minute-guide-to-electricity-storage>.
- [149] S. Pfenninger and I. Staffell, “Long-term patterns of european pv output using 30 years of validated hourly reanalysis and satellite data”, *Energy*, vol. 114, pp. 1251–1265, 2016. DOI: 10.1016/j.energy.2016.08.060. [Online]. Available: renewables.ninja.
- [150] S. Pfenninger and I. Staffell, “Using Bias-Corrected Reanalysis to Simulate Current and Future Wind Power Output”, *Energy*, vol. 114, pp. 1224–1239, 2016. DOI: 10.1016/j.energy.2016.08.068.
- [151] BNEF, “Scale-up of Solar and Wind Puts Existing Coal, Gas at Risk”, Bloomberg New Energy Finance (BNEF), Tech. Rep., 2020. [Online]. Available: <https://about.bnef.com/blog/scale-up-of-solar-and-wind-puts-existing-coal-gas-at-risk/>.
- [152] M. S. Ziegler and J. E. Trancik, “Re-examining rates of lithium-ion battery technology improvement and cost decline”, *Energy Environ. Sci.*, vol. 14, pp. 1635–1651, 4 2021. DOI: 10.1039/D0EE02681F. [Online]. Available: <http://dx.doi.org/10.1039/D0EE02681F>.

- [153] National Renewable Energy Laboratory (NREL), "2017-NREL Annual Technology Baseline", NREL, Golden, CO, USA, Tech. Rep., 2017, http://www.nrel.gov/analysis/data_tech_baseline.html. [Online]. Available: <https://atb.nrel.gov/>.
- [154] TKF, *Middenspanningskabel ymekrvaslqwd 6/10 kv*, Online, in Dutch, 2017.
- [155] E. Koolwijk, P. Goudswaard, J. Grift, et al., *Heat and Power - Combined Heat and Power: An Overview and Guideline*, Groningen, the Netherlands: GasTerra, Castel International Publishers, 2010.
- [156] ETSAP, *Heat pumps*, Online, <https://iea-etsap.org/index.php/energy-technology-data>, Energy Technology Systems Analysis Program (ETSAP) of the International Energy Agency (IEA), 2013.
- [157] M. Thema, F. Bauer, and M. Sterner, "Power-to-Gas: Electrolysis and methanation status review", *Renewable and Sustainable Energy Reviews*, vol. 112, pp. 775–787, 2019, ISSN: 1364-0321. DOI: <https://doi.org/10.1016/j.rser.2019.06.030>. [Online]. Available: <https://www.sciencedirect.com/science/article/pii/S136403211930423X>.
- [158] S. Sabihuddin, A. Kiprakis, and M. Muellerr, "A Numerical and Graphical Review of Energy Storage Technologies", *Energies*, vol. 8, pp. 172–216, 2015, ISSN: 1996-1073. DOI: doi:10.3390/en8010172.
- [159] EBN, "Gasopslag Bergermeer officieel geopend", IEA, Taqa Energy BV, EBN BV, The Hague, the Netherlands, Tech. Rep., 2015, "In Dutch". [Online]. Available: <https://www.ebn.nl/nieuws/gasopslag-bergermeer-officieel-geopend/>.
- [160] S. van Gessel, J. Breunese, J. Juez Larré, T. Huijskes, and G. Remmelts, "Ondergrondse Opslag in Nederland - Technische Verkenning", Ministry of Economics and Climate, Utrecht, Netherlands, Tech. Rep., 2018, "In Dutch".
- [161] J. E. Smith, J. G. Erdman, and D. A. Morris, "Migration, Accumulation and Retention of Petroleum in the Earth", in *World Petroleum Congress (WPC)*, WPC-14102, vol. All Days, Jun. 1971. eprint: <https://onepetro.org/WPCONGRESS/proceedings-pdf/WPC08/A11-WPC08/WPC-14102/2079069/wpc-14102.pdf>.
- [162] S. Lochner, "The Economics of Natural Gas Infrastructure Investments - Theory and Model-based Analysis for Europe", Ph.D. dissertation, University of Cologne, Cologne, Germany, 2011.

- [163] T. van Wee and T. Witjes, “Masterplan Warmte-/Koudeopslag Goudse Poort Gouda”, Gouda Municipality, Almere, the Netherlands, Tech. Rep., 2008, In Dutch.
- [164] International Energy Agency, “IEA Sankey Diagram - Netherlands Balance 2018”, International Energy Agency, Tech. Rep., 2018. [Online]. Available: <https://www.iea.org/sankey/#?c=Netherlands&s=Balance>.
- [165] OECD, “Penergy: The next fifty years”, Tech. Rep.
- [166] P. Ravestein, G. van der Schrier, R. Haarsma, R. Scheele, and M. van den Broek, “Vulnerability of European intermittent renewable energy supply to climate change and climate variability”, *Renewable and Sustainable Energy Reviews*, vol. 97, pp. 497–508, 2018. DOI: 10.1016/j.rser.2018.08.057.
- [167] Dutch Ministry of Economic Affairs and Climate Policy, “Energy agenda: Towards a low carbon energy sector”, Dutch Ministry of Economic Affairs and Climate Policy, The Hague, NL, Tech. Rep., 2016.
- [168] N. Helistö, J. Kiviluoma, H. Holttinen, J. D. Lara, and B.-M. Hodge, “Including operational aspects in the planning of power systems with large amounts of variable generation: A review of modeling approaches”, *WIREs Energy and Environment*, vol. 8, no. 5, e341, 2019. DOI: <https://doi.org/10.1002/wene.341>. eprint: <https://wires.onlinelibrary.wiley.com/doi/pdf/10.1002/wene.341>. [Online]. Available: <https://wires.onlinelibrary.wiley.com/doi/abs/10.1002/wene.341>.
- [169] T. Bruckner, I. Bashmakov, Y. Mulugetta, et al., “2014: Energy Systems. In: Climate Change 2014: Mitigation of Climate Change. Contribution of Working Group III to the Fifth Assessment Report of the Intergovernmental Panel on Climate Change”, Intergovernmental Panel on Climate Change (IPCC), Cambridge, UK and New York, NY, USA, Tech. Rep., 2014.
- [170] WindStats, *Dutch wind statistics*, In Dutch, Bosch & van Rijn, 2021. [Online]. Available: <https://windstats.nl/statistieken>.
- [171] Nationaal Programma Regionale Energie Strategie, *Regionale Energie Strategie - Waarom zijn wind en zon op land nodig?*, In Dutch, Ministry of Economics and Climate, 2021. [Online]. Available: <https://www.regionale-energiestrategie.nl/energiesysteem/elektriciteit/1989424.aspx>.

- [172] R. Bryce, I. Losada Carreño, A. Kumler, B.-M. Hodge, B. Roberts, and C. Brancucci Martinez-Anido, “Consequences of neglecting the inter-annual variability of the solar resource: A case study of photovoltaic power among the hawaiian islands”, *Solar Energy*, vol. 167, pp. 61–75, 2018, ISSN: 0038-092X. DOI: <https://doi.org/10.1016/j.solener.2018.03.085>. [Online]. Available: <https://www.sciencedirect.com/science/article/pii/S0038092X18303414>.
- [173] C. Jung and D. Schindler, “On the inter-annual variability of wind energy generation – a case study from germany”, *Applied Energy*, vol. 230, pp. 845–854, 2018, ISSN: 0306-2619. DOI: <https://doi.org/10.1016/j.apenergy.2018.09.019>. [Online]. Available: <https://www.sciencedirect.com/science/article/pii/S0306261918313278>.
- [174] P. McCallum, D. P. Jenkins, A. D. Peacock, *et al.*, “A multi-sectoral approach to modelling community energy demand of the built environment”, *Energy Policy*, vol. 132, pp. 865–875, 2019, ISSN: 0301-4215. DOI: <https://doi.org/10.1016/j.enpol.2019.06.041>. [Online]. Available: <https://www.sciencedirect.com/science/article/pii/S0301421519304112>.
- [175] A. Hermelink and D. de Jager, “Evaluating our future - the crucial role of discount rates in european commission energy system modelling”, The European Council for an Energy Efficient Economy (eceee) and Ecofys, Sveavagen 98, Stockholm, Sweden, Tech. Rep., 2015. [Online]. Available: <https://www.researchgate.net/publication/324170334>.
- [176] T. Wright, “Factors Affecting the Cost of Airplanes”, *Journal of the Aeronautical Sciences*, vol. 3, pp. 122–128, DOI: 10.2514/8.155.
- [177] A. Held, M. Ragwitz, W. Eichhammer, *et al.*, “Estimating energy system costs of sectoral res and ee targets in the context of energy and climate targets for 2030”, Fraunhofer ISI, TU Vienna, IIT Comillas, Fraunhofer ISE, Prognos, ECN, Germany, Tech. Rep., 2014.
- [178] E. A. Moallemi, F. de Haan, J. Kwakkel, and L. Aye, “Narrative-informed exploratory analysis of energy transition pathways: A case study of India’s electricity sector”, *Energy Policy*, vol. 110, pp. 271–287, 2017, ISSN: 0301-4215. DOI: <https://doi.org/10.1016/j.enpol.2017.08.019>. [Online]. Available: <https://www.sciencedirect.com/science/article/pii/S030142151730513X>.

- [179] I. van Beuzekom, B. Hodge, and J. Slootweg, “Projecting solar photovoltaic efficiencies from lab to market”, in *IEEE ENERGYCON 2018*, Limmasol, Cyprus, 2018, pp. 1–6.
- [180] G. Box, “Robustness in the Strategy of Scientific Model Building”, in *Robustness in Statistics*, R. L. LAUNER and G. N. WILKINSON, Eds., Academic Press, 1979, pp. 201–236, ISBN: 978-0-12-438150-6. DOI: <https://doi.org/10.1016/B978-0-12-438150-6.50018-2>. [Online]. Available: <https://www.sciencedirect.com/science/article/pii/B9780124381506500182>.

Acknowledgments

Thank you for reading my thesis, or at least part of it. Or perhaps only these acknowledgements.. If you belong in the latter group, I do recommend the summary! Anyway, it has been quite the journey these past eight years, unfortunately with many more challenges besides 'just' doing a PhD in part-time. Fortunately also including some wonderful extras along the way! (some of which are still in the making :)) Many different people were part of this journey, and I'd like to specifically thank some of them here.

First of all, I want to thank two people who are unfortunately no longer with us, but were both instrumental to the start of my PhD. First is Albert Bogaard, friend and colleague at ORTEC. Albert, thank you for always inspiring and supporting me, and after listening to my frustrations on the progress in the energy transition, saying the words "Why don't you do a PhD in that area?" Great idea! Most of the time, anyway ;). Then, of course, there was professor Wil Kling. You immediately understood my vision of incorporating multiple (energy) networks to find practical solutions and convinced me to join the Electrical Energy Systems (EES) group in Eindhoven. In those short few months, you were an invaluable sounding board and connected me to some great pioneering researchers discovering the value of multi-energy systems. Thanks, Wil. I still miss both of you and am grateful for having had you around in my life, however shortly. I hope I've made both of you proud.

Next, I'd like to thank my (previous) supervisors: Madeleine Gibescu, Han Slootweg, and Bri-Mathias Hodge. Madeleine, although you couldn't be around the entire time, I am very glad we met and still meet from time to time to discuss research, kids, and life in general. Han, thanks for all your down-to-earth input and finishing this journey with me. I'm sure it was challenging to have a first non-Enexis PhD-student, let alone a non-electrical engineer who even wanted to include water and waste water networks. We found common ground in the systematic approach to energy networks and I'm glad I

was able to connect more personally when times got tough. Last, but definitely not least, Bri, thank you for all your support since my stay at NREL. I have loved all our discussions about my research, the academic world, dealing with publications, raising kids, politics, climate change, renting houses in the Netherlands, and everything else. I am very grateful to have met you and your family and I hope we can meet again someday, preferably on some mountain while wearing skis.

To the rest of my committee, professors Floor Alkemade, Zofia Lukszo, Pierre Pinson, and Joaquim dos Santos Gromicho, thank you for being a part of the final leg of my PhD. Thank you for your feedback and insightful discussions on a broad range of subjects, befitting the multi-disciplinary nature of my thesis. Pierre, thanks as well of course for hosting me in Denmark, for always being honest, and for showing me the ropes. Joaquim, thank you for your incredible enthusiasm and kindness, also outside the realm of academia. I'm glad we're still working together on such wonderful causes; on to many more!

Of course, I also met many people in the EES group, at the KIC InnoEnergy PhD School, as well as both research groups I visited: at the Elektro group at DTU in Lyngby, Denmark, and at the Energy Systems Integration Facility at NREL in Golden, Colorado, USA. A few people stand out. Among them are Elke, Michiel, Mana, Raoul and Samina in my first few years in Eindhoven, with whom I had some wonderful times. At DTU, the whole group was incredibly welcoming, both at Lyngby and at Risø. At the former with a memorable, Danish Christmas dinner (*skål!*) and at the latter with what was apparently my first, real Italian pasta carbonara. I'd like to particularly thank Leyla and Lesia for quickly becoming great friends. At NREL, I'd first and foremost like to thank Bethany for being my host and turning into a wonderful friend. You taught me many things about growing food, making it last throughout the winter (to make the best peach mimosas when the time called for it) and of course how to navigate NREL. Tien Tien, I'm so happy that I ran into you and loved our conversations, hikes, climbing, and shopping sessions. Finally, Tarek, thanks for all your positivity and activity! Beautiful hikes, amazing Red Rocks concerts, and especially our skiing day trips. Although I still thoroughly dislike getting up so early, you were right that those mountains are worth it!

In addition to these academics, I want to specifically thank the many students that I worked with throughout the years. First is Milou. Thank you for your enthusiasm and all your great work at the municipality of Eindhoven; providing me the foundation of data for my case. Then there were Safee, Sergio, and Suzy. Although you didn't work on my project, it was great fun to see how I could guide each of you to a successful end of your masters degrees at the TU Eindhoven. Besides the students at Eindhoven, I also had many stu-

dents at ORTEC in the last few years. Tim, Julie, Noortje, Leonie, Gijs, and Maaike, thanks for all your enthusiasm and efforts to work with me and my CFLNDP! For pulling me from AIMMS to Python (thank god!), for spreading the word of sustainable energy developments at ORTEC, for all your comments on the mathematics (I wish you all agreed, though), and for helping me rediscover my enthusiasm for energy transition research.

Besides all the people I met in academia, of course I also kept working throughout my time as PhD-student. Mainly at ORTEC, but also at different start-ups, for the Big Data Alliance, at SET Ventures, and finally at Analytics for a Better World. I'd like to thank my managers, first Patrick, then Frans, for always supporting me and my research. Karin for becoming my friend, sounding board, and road trip partner from Chicago to Colorado. Adriaan and Wouter for helping me formulate my very first mathematical optimization model and translating it into AIMMS. Jeroen, first for assisting me at the Sustainability Office, and later to further shape my multi-energy model and work out some more programming kinks. Levi, Dasha, Bart, Lianne, Guusje, Jelke, Manon, Robert, Rianne, Frank, Ronald, and many others: thanks for always making me feel at home at ORTEC. And finally, Dorine, thank you for being my (and our) friend all these years and for being someone who always manages to make me smile, no matter how tough the times.

Talking about friends, there are quite a number who -fortunately- had nothing to do with my research or my work, and who have been a great help for me along the way. First of all, Jessie, thanks for all the laughs, borrels, trips, concerts, climbing dates, party ideas, belgolympics, and whatever else you organized; you always helped remind everyone that we work to live, not the other way around. I'm so glad to have you as friend. All the other Haagies, thanks for all the fun we've had over the years, on to more adventures! Krisz, thanks for being my friend and confidante, and amazing lunch partner, of course. Thanks to the rest of the Waddinxveen, the Rotterdam crew and the handful of special cases who insist on living in our capital city.. ;) We've had such great times together in Belgium, at Lowlands, New Year's, and all those birthday parties (especially the themed ones, looking at you, Icara!). And still going strong, even with this new, great bunch of kids that we seem to have made (so far anyway). Thanks for all the love!

Besides friends who are nearly family, there are also those that actually are family. Part of them are the ones I (almost) married into: the Wijnsmas. I'm glad Taco came attached to all of you and that you were there to share this journey with me. Thanks for all your support and of course the occasional *mon chou-bastogne* pie. On my side of the family, opa (or opie), Anita, and Frank, thanks for your steady presence and love throughout the years. Bart, thanks

for all your enthusiasm and pride in my work. It means a lot! Finally, mom, dad, you mean the world. Without the tenacity and curiosity you always fed and encouraged, I don't think I would have even started this PhD. Dad, thanks for always believing in me and supporting all my ideas, and feeding me with mathematical theories that first confused, but later always helped me move forward. Mom, thanks for everything. Without your help to pull me through after all the physical challenges, I don't think I could have finished this. It has been wonderful to share my work with you and to get your invaluable feedback. And both of you, thanks for being such wonderful grandparents to Emily. I love you.

Finally, and most importantly: Taco & Emily. Emily, you are the light of my life. An amazing present that ended a very challenging time and promised hope for recovery. Even though that hasn't been easy either, what with the season ticket we seemed to have to the hospital at some point.. you were and are always a trooper and such a happy, curious, loving ray of sunshine for both of us. I love being your mom. Taco, my love, thank you for everything. For being there with me through all the ups and downs, through all the (long) distances I managed to find, discovering new places together, and encouraging my adventuring. For being my biggest cheerleader, the best sparring partner in all the subjects I managed to put together, maths, programming, energy modeling, economics, and of course for being the softest, yet sturdiest shoulder to cry on. I am so grateful to have you there with me through all of it. I love you to the moon and back, and I can't wait to go on our next adventure together as a family <3.

Iris van Beuzekom
Eindhoven, December 2022

Curriculum Vitae

Iris van Beuzekom received the joint BSc degree in Sustainable Molecular Science & Technology from the Delft University of Technology and the University of Leiden, both in the Netherlands, in 2008, and the MSc degree in Civil and Environmental Engineering from Stanford University, Palo Alto, CA, USA, in 2010. She is currently pursuing a PhD in the Electrical Energy Systems group at the Eindhoven University of Technology. She is also a self-employed senior (research) consultant on energy innovations and sustainable development for different companies. Her latest assignments have been for ORTEC, a mathematical optimization software and advanced analytics company, SET Ventures, an independent, sustainable energy venture capital investor, and Analytics for a Better World, specifically helping The Ocean Cleanup amplify their impact.

List of Publications

Journals

- I. van Beuzekom, B.-M. Hodge, J.G. Slootweg, Exploring uncertainty in long-term, multi-stage investment planning of integrated urban energy systems, *Energy Reports - Under review*, 2022
- I. van Beuzekom, B.-M. Hodge, and H. Slootweg, “Framework for optimization of long-term, multi-period investment planning of integrated urban energy systems”, *Applied Energy*, vol. 292, p. 116 880, 2021, ISSN: 0306-2619. DOI: <https://doi.org/10.1016/j.apenergy.2021.116880>. [Online]. Available: <https://www.sciencedirect.com/science/article/pii/S0306261921003664>

Proceedings and Congress Contributions

- I. van Beuzekom, B. Hodge, and J. Slootweg, “Projecting solar photovoltaic efficiencies from lab to market”, in *IEEE ENERGYCON 2018*, Limassol, Cyprus, 2018, pp. 1–6
- I. van Beuzekom, M. Gibescu, P. Pinson, et al., “Optimal Planning of Integrated Multi-Energy Systems”, in *2017 IEEE Manchester PowerTech*, Manchester, UK, 2017, pp. 1–6
- I. van Beuzekom, L. Mazairac, M. Gibescu, et al., “Optimal Design and Operation of an Integrated Multi- Energy System for Smart Cities”, in *2016 IEEE International Energy Conference (ENERGYCON 2016)*, Leuven, Belgium, Apr. 2016, pp. 949–955
- I. van Beuzekom, M. Gibescu, and J. Slootweg, “A review of multi-energy system planning and optimization tools for sustainable urban development”, in *2015 IEEE Eindhoven PowerTech*, Eindhoven, the Netherlands, 2015, pp. 1–7

Technical Reports (Non-Refereed)

- J.G. Slootweg, I. van Beuzekom, S. Schouwenaar, J. Peters, Decentraal beleid voor versnelling energietransitie, *Energie+*, vol. 2, June, 2017, pp. 7-9
- I. van Beuzekom, M. van Dam, J.G. Slootweg, Verduurzaming van verwarming vereist integrale aanpak, *Energie+*, vol. 4, December 16, 2016, pp. 14-17

In order to remain below 1.5°C global warming, nearly all carbon dioxide emissions need to be reduced to zero by 2050. Most of these emissions originate in the energy system, which contains a myriad of existing infrastructure, with a diverse mix of multiple energy carriers and a largely fossil energy supply. An energy transition towards solely zero carbon, or renewable energy sources is required. This transition is complex and uncertain, influenced by all sorts of social, technological, political, and environmental pathway effects. To implement stringent climate actions, cities play a large role given their increasing population density and resource intensity. Furthermore, many cities are already dealing with the effects of climate change, leading to a strong motivation to act. At the same time this scale of energy systems has been surprisingly understudied in the literature and is thus ripe for developing actionable policies that can have a clear impact.

In this thesis three specific challenges were examined at an urban scale: the carrier mismatch, the temporal mismatch, and the deep uncertainty present in long-term energy models. To tackle these challenges, this thesis proposed a multi-energy optimization framework for long-term, multi-period investment planning of integrated urban energy systems, including an exploratory modeling methodology to incorporate uncertainty. It aims to help urban decision makers design a pathway for their energy transition such that climate goals are reached, and large-scale implementation of zero-carbon energy sources is achieved in the most cost-efficient manner, all while assuring a safe and reliable energy system. The framework allows for a fully coupled network planning, including investments in conversion, supply, and storage assets for each energy carrier considered. It incorporates both relevant physical constraints as well as techno-economic effects for each of these assets. It is formulated as a mixed integer linear program and translates to a novel application of the combined facility location network design problem.